Technical Report

4th May 2010

Warwick Mobile Robotics
International Manufacturing Centre
University of Warwick
Coventry
CV4 7AL

Telephone: +44 (0) 2476 574 306

Web: www.mobilerobotics.warwick.ac.uk

Email: mobilerobotics@eng.warwick.ac.uk

Table of Contents

Figures

Tables

Equations

1. Introduction

1.1. Motivation for project

The US Geological Survey National Earthquake Information Center records the number of earthquakes and their effects worldwide. In the last decade an estimated 690,000 deaths have been caused by earthquakes worldwide with an estimated 240,000 in 2010 alone. The development of technology for the purpose of saving lives must be a priority in the field of engineering and this project aims to advance technology in this area. By developing a highly mobile robot the project aims to be able to reach hard to get to areas which may be deemed unsafe for a human rescue attempt.

1.1.1. European open and world competition

The RoboCup Rescue competition was initiated after the Great Hanshin earthquake, which hit Kobe (Japan) on the 17th January 1995, with a magnitude of 7.2 on the Richter scale. As a result over 6,400 people lost their lives, 300,000 were left homeless and damage was estimated at £68 billion. The lessons learnt highlighted the need for robust and reliable technologies that can acquire, process and relay necessary information. Robots can be used in areas which may be unsafe for humans, do not suffer from fatigue and can access deep voids where oxygen levels are low. Their sensing capabilities are versatile and relevant information can be relayed back to the user remotely.

The RoboCup world competition hosts various regional competitions around the world and world finals to bring all the best teams together in one location. Some of the main benefits of this kind of competition are to provide a suitable platform for testing and a motivation to encourage research institutions to be innovative. Competing in the RoboCup European Open was a target for the project and helped the team to focus their efforts, providing them with a standardised testing platform for their robots.

1.1.2. Arena and scoring

The RoboCup arena is comprised of three distinct sections which aim to challenge different aspects of mobile robotics in order to assess robots' durability in the field.

Figure 1 – RoboCup competition arena

Detailed below (Figure 2) is a description of each of the three areas of the arena and some of the challenges involved in the navigation of each.

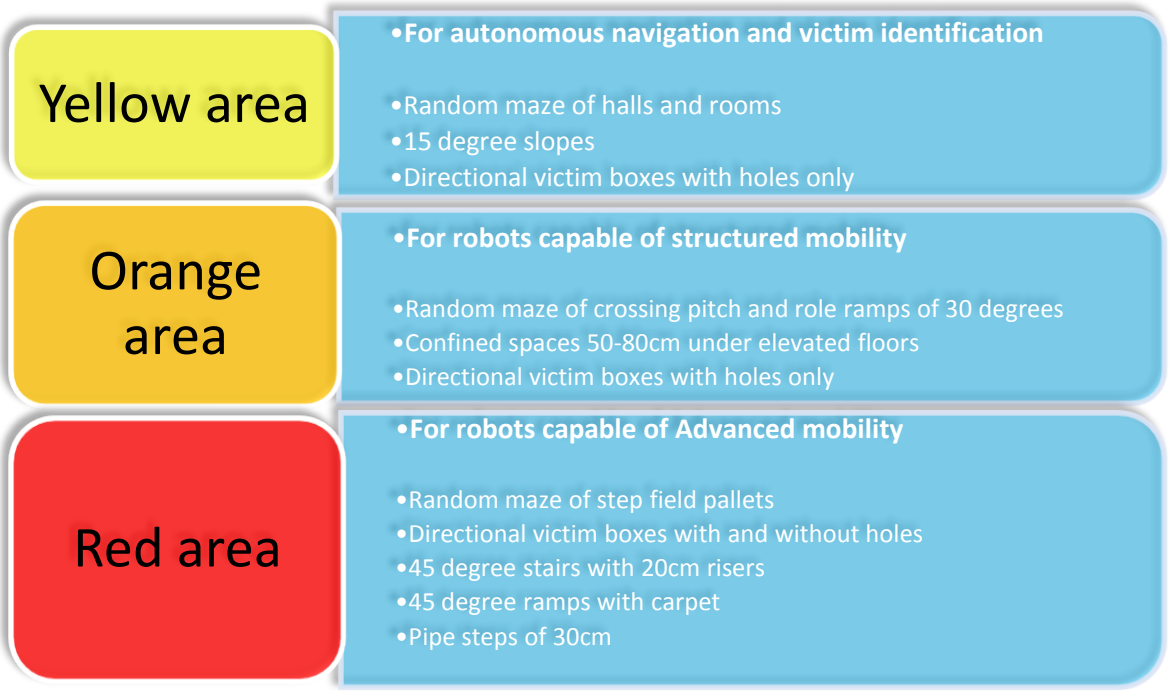

Figure 2 – Arena breakdown

The scoring system involved with victim identification rates each discovery on a number of levels. The score available for each victim is broken down in a number of different categories adding up to a maximum available score for each victim.

Visual recognition (15)	Signs of life (15)	Mapping (40)	Total score
Finding the victim box (5)	Body heat (5)	Map quality of walls (20)	(70)
Hazard warning sign (5)	CO2 (5)	Map location of victim (20)	
Reading victim card (5)	Communications (5)		

Table 1 - Competition scoring system

The scoring system detailed in Table 1 encourages teams to showcase an array of different victim detection techniques including Visual, heat and CO2 sensing as well as mapping.

1.2. This year's team aims and objectives

The Team's main aim is to develop and advance its mobile robotics capability in time for the 2010 RoboCup Rescue League with the ultimate goal of winning the competition. The competition requires tele-operated and autonomous robots to navigate simulated disaster zones. They are required to overcome challenging terrains, identify victims and produce a map of the environment. We aim to achieve this by meeting the objectives listed below:

- Redesign robot chassis with possible use of composite materials.
- Design and manufacture new robot solely for autonomous section.
    - Use of laser cutting and folding technology.
    - Work with computer science team for development of A.I. software.
- Improve reliability of software and controls of robot.
- Develop mapping for both robots through the use of LiDAR (Light Detection And Ranging)
- Acquisition of new motor for front flippers and servicing of others.
- New method of battery connection and installation.
- Design of new arm for inclusion of more sensors and possible gripper.
    - More sensors to identify victims such as CO2 and development of a two-way communication capability.
- Improve cooling of robot.
- Overall weight reduction for better power to weight ratio with improved range.
- Add new connectors to electronics (Harwin connectors sponsorship)

- Ensure adequate funding for the project through company sponsorship.
    - Produce and distribute quarterly newsletter

1.2.1. Tele-operated robot

1.2.1.1. Chassis

One of the main focuses of this year's Mobile Robotics team is to reduce the weight of the chassis and create more space inside the robot. This would involve moving away from the bulky aluminium modular panels towards a mixture of carbon fibre and 0.9mm stainless steel panels. The reason for doing this is to prolong the battery life of the robot when subject to heavy loads such as ascending stair sets and steep slopes where it had shown fatigue in earlier years. Another advantage of the re-design is to re-arrange the interior and create a larger, less cluttered space for maintenance and assembly. The whole chassis is to be overhauled creating a new simple modular structure made up of panels which span the length of the robot. These will be assembled using folded tabs and riv-nuts for ease of manufacture and assembly.

1.2.1.2. Electronics

The electronics stack is to be re-evaluated to provide a neat and intuitive solution which is both easy to access and well cooled. With the new larger space inside the robot there is room to consolidate all the circuit boards into one stack where cooling will be optimized and maintenance will be easier. In order to simplify the amount of cables and connectors needed to supply power and data to the entire robot a form of composite connector is to be used to consolidate several systems into one connector. This kind of arrangement makes testing of individual components much simpler. It will also be much easier to remove and replace electronics in the robot which was a major problem in previous years.

1.2.1.3. Robot arm

In order to make better use of the sensors for navigation and victim identification a stable and diverse platform is necessary. Since the victims are sometimes placed in directional boxes which may be located in areas of difficult terrain it is essential that this platform be mobile and flexible to allow viewing of the victims. Another of the main aims of this year's project it to create a 5 degree of freedom robot arm capable of holding all the sensors at a reasonably long extension. In order to achieve the required loading of the robot arm powerful motors are to be housed inside carbon fibre tubes which are connected by sturdy aluminium joints. This will make a highly robust and flexible arm capable of taking heavy loads at long distances.

1.2.2. Autonomous

1.2.2.1. Simplified robot platform

It was decided that a separate robot be built for tackling the autonomous section of the arena as this offered many benefits for both the Engineering and Computer science teams. First of all the competition rules state that multiple robots of the same team are allowed in the arena at any one time as long as there is only one operator**.** For this reason alone having a separate platform which could work simultaneously alongside the main robot without the need for a second operator would ultimately score more points per run. As the yellow section of the arena presents less challenging terrain only a simple platform is needed and so mechanical work on this project is easier. Another main reason for building the second robot is to allow software testing to be conducted throughout the year when the team's main platform would otherwise be unavailable due to the constant implementation of new mechanical features. This presents a valuable opportunity for the computer science team as testing is very extensive and each new test improves the accuracy of the simulation.

The autonomous chassis is based on a design from the 07-08 Mobile Robotics team which was a simpler design and used many components already available in the lab, saving much time and money. Using the same laser cutting technique planned for the tele-operated chassis will offer speed of manufacture and simplicity of design.

1.2.2.2. Autonomous navigation and Mapping

The main aim of the computer science team is to create a Simultaneous Localisation And Mapping (SLAM) system which uses a laser range finder (LiDAR) to extract wall features, creating a map of the environment. It then uses these images to navigate through the environment. This system is to be fully autonomous and can be activated at the start of a run without needing to be monitored by a separate operator.

1.3. Stakeholder analysis

Warwick Mobile Robotics has always taken care to consider all parties involved and their interest with its development (Figure 3).

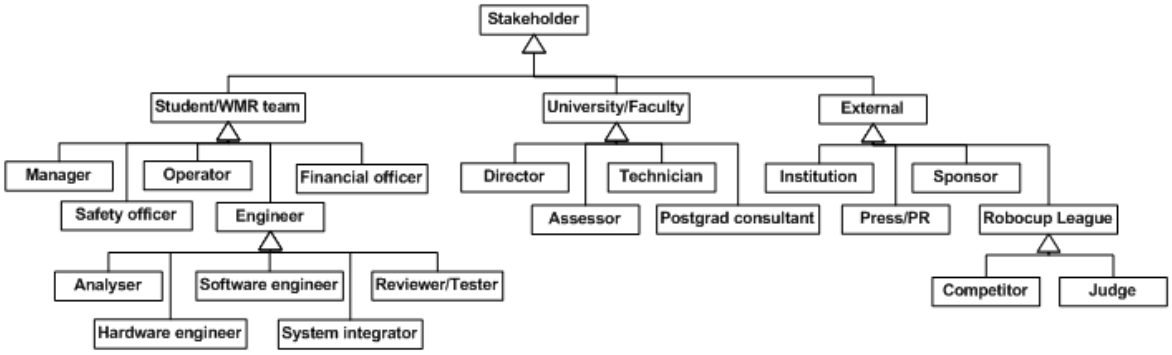

Figure 3 – Stakeholder diagram (WMR systems design report 08/09)

The WMR team is concerned with personal development as well as the project aims with regards to the RoboCup competition. The University on the other hand is also interested in exposure and publicity. Sponsors invest in the project because of their interest in graduates and advertising.

2. Design methodology

2.1. Required Capabilities

In order to plan and execute a successful project a detailed analysis of the needs of the project and the required capabilities from the end user should be taken into account.

2.1.1. Manoeuvrability

Earthquake and other disaster scenarios often leave terrain and buildings in an unsafe and erratic rubble which can be difficult to negotiate safely. There may also be cramped spaces caused by collapsed ceilings and the general disarray of the incident. For these reasons any rescue robot would need to be able to cover a wide variety of different terrain. The manoeuvrability of any mobile robot would need to include:

- Steep slope climbing
- Stair navigation
- Advanced movement over unstable and unpredictable rubble
- The ability to fit in tight spaces

For the success of the project it would be vitally important to include all these features.

2.1.2. Motor and power systems

In order to negotiate highly uneven terrain and steep slopes and to allow for prolonged use in extended missions, power systems and motor sizing is an important issue. In order to negotiate steep slopes a powerful motor system and good grip is necessary; however such strenuous work requires a large internal power supply. A good balance between weight, power and battery life is vital for the extended operation of such a vehicle in the specified environment.

2.1.3. Tele-operation

The basic interface between any mobile robot and the user would take the form of a tele-operated control system to manipulate the motion of the robot. All the various motion systems would need to be controlled by a simple interface which could be modified and upgraded to suit new features as they are developed. In such an environment as to be explored by this area of mobile robotics many feedback mechanisms would need to be employed to provide the user with the required data to navigate through the terrain. Some such features might include cameras, position feedback, and independent motor control centralised into one location for easy access and interpretation.

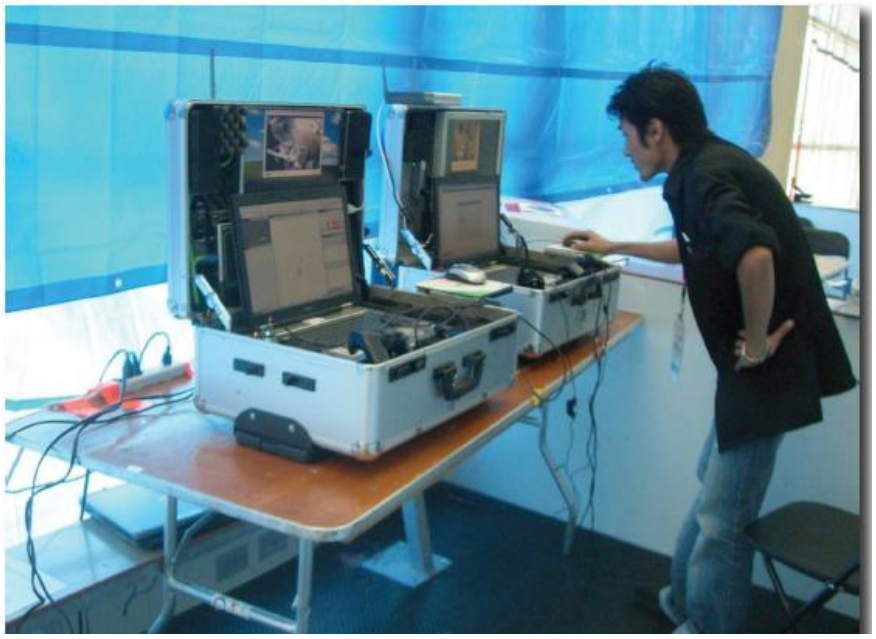

Figure 4 – An example of a tele-operated control system using laptops and hand held controllers

2.1.4. Autonomous control and mapping

A more advanced control system could be implemented where radio drop-out occurs in situations such as deep rescue missions or areas of interference. For these kinds of operations an autonomous control logic would need to be implemented to allow user-independent navigation and mapping of the area. Advanced systems such as these would need to be able to locate itself in an environment and be able to recognise features such as walls and obstacles in its projected path. In addition to this it would need to make decisions about where to go, how to get there and be able to map a safe path through the landscape to its chosen destination. This requires internal processing, advanced algorithms and intelligent motor control and feedback systems. In addition to this the user may require a detailed map

of the area to plan further rescue attempts or to asses the situation from a safe location. One of the most successful methods of this is Simultaneous Localisation and Mapping (SLAM) which generally uses laser range finding and filter systems to create a 2D or even 3D map of an area.

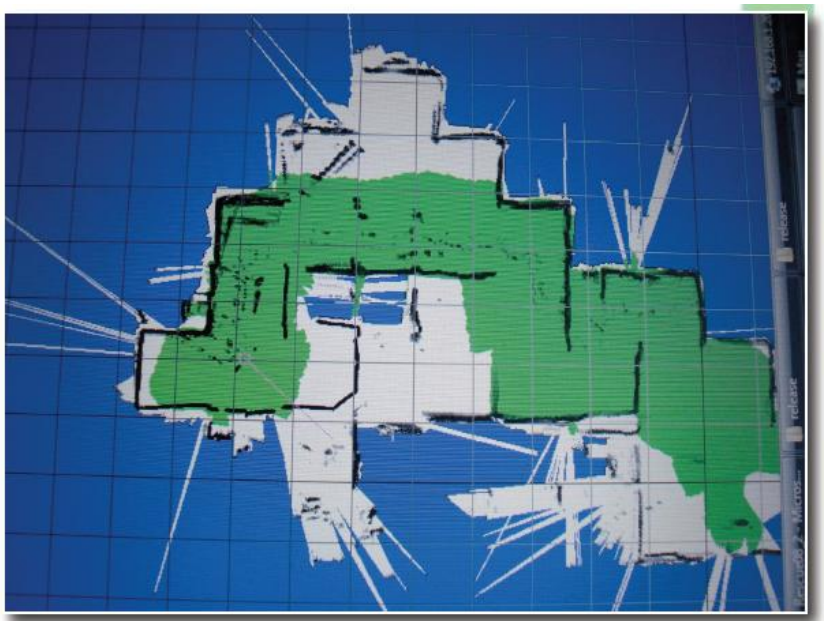

Figure 5 - An example of a GeoTiff map produced by SLAM autonomous mapping using LiDAR

2.1.5. Victim sensing

The main purpose of any rescue operation would be to find and identify victims' locations and situations in order to plan a successful rescue attempt or to deliver much needed survival supplies. Any rescue robot would need to be able to identify victims in a number of different ways so as to maximise the chances of rescue. Some of these methods could include: visual, heat, CO2, audio or movement sensors to allow for a full range of victim identification. In order to optimise such equipment some kind of manipulation system could be implemented to scan local areas for victims. This could take the form of a robot arm or other elevated platform to allow looking into holes, tight spaces, or to simply get a better view of an area.

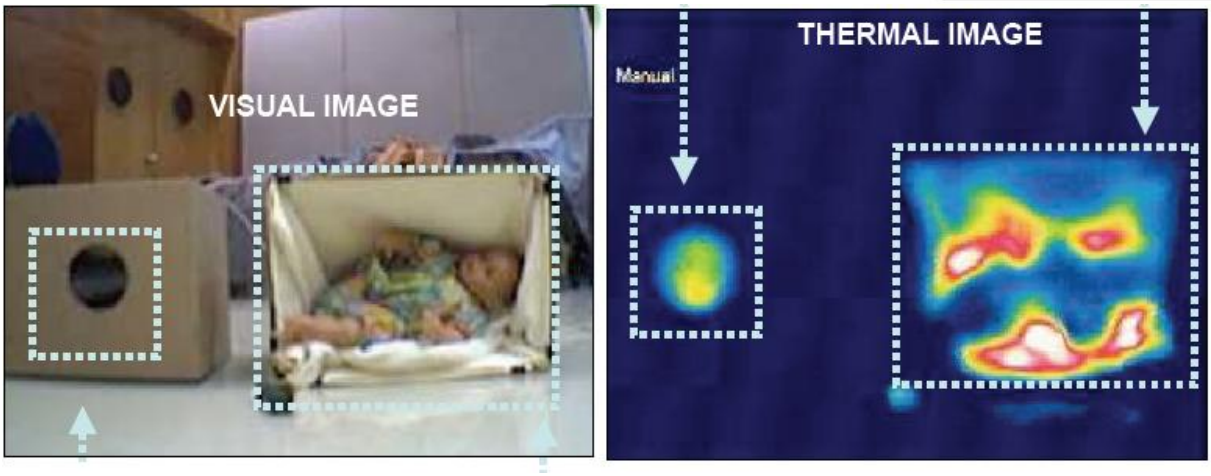

Figure 6 - An example of different imaging techniques used to identify victims in a simulated environment

2.1.6. Testing

In order to ensure optimum operation of all internal sub-systems, it should be possible to test each individual component separately from the assembly. In order to solicit this process a modular design approach should be implemented throughout the design process, and testing should be performed at regular intervals. In addition to this, full systems testing should be performed regularly and to detail to ensure that all components are designed in synergy and to their optimal configuration.

2.1.7. Safety

Due to the unpredictable nature of power electronics and control logic, unexpected errors or human mistakes can cause robots to perform in a way not previously anticipated. For this reason various safety measures must be executed when and where appropriate. Features such as emergency stop mechanisms and hardware redundancy should be able to prevent the propagation of unsafe activities. Over and above this, normal operation should not pose threat or harm to any human being or property.

2.2. Handover capabilities

At the time of handover of the project two years of previous work had been put into designing and building a mobile rescue robot in order to meet the growing demands of the competition, and the

outside world. Many good features were developed which could be used in future projects; however much room for improvement was evident in some areas. With more time and money the current group hopes to improve on the previous work and leave a better end product for future groups.

2.2.1. Manoeuvrability

In the previous years competition the WMR group received best in class for mobility at the RoboCup European Open with their advanced track robot. This robot saw the implementation of a double flipper system which had independent motor control and allowed easy manoeuvrability amongst difficult terrain. They successfully navigated the red step field, an area of challenging ground and steep slopes to identify victims in more advanced areas. One of the main problems with this however was that the battery life was significantly drained by attempting the steep inclines and stair sets. This was due to the hefty weight of the robot and power losses in the circuitry. Another issue was the centre of gravity of the robot. When attempting slopes it was difficult to tip the robot over the top edge because of the weight distribution issues. This made traversing of these slopes increasingly difficult and was a constant drain on the batteries.

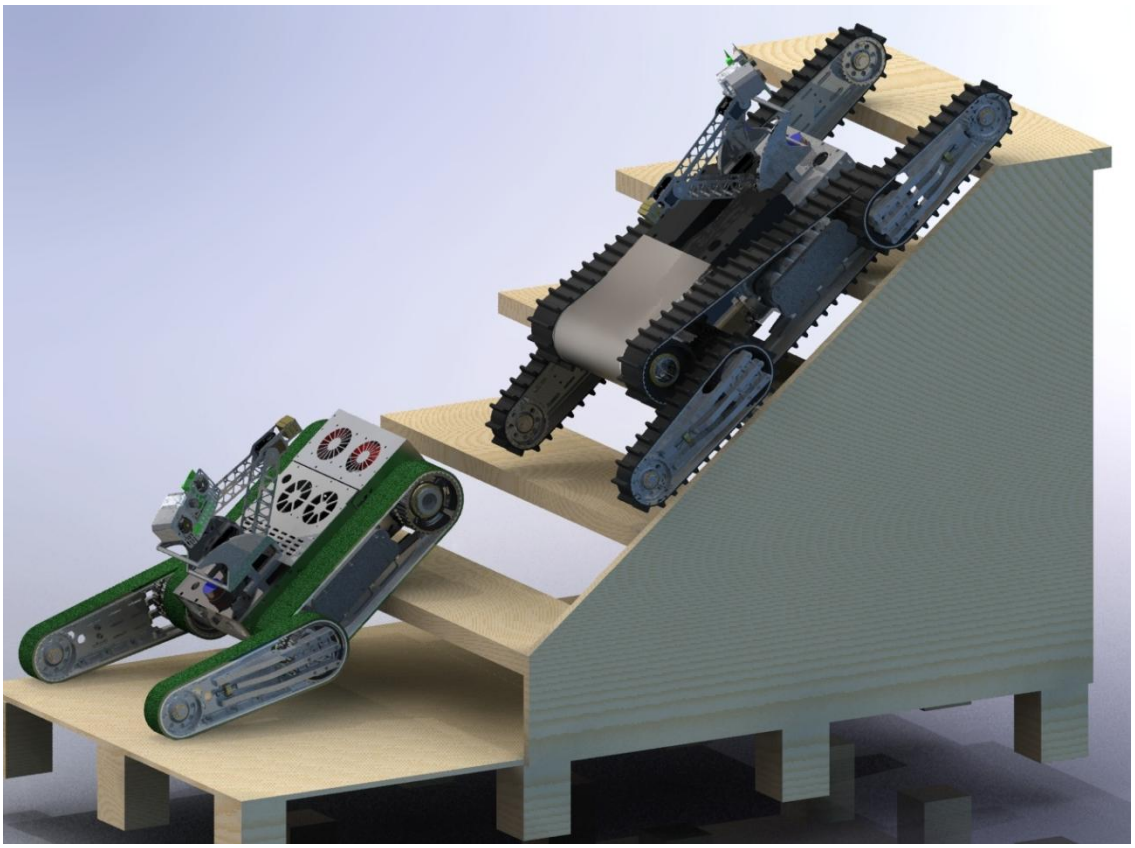

Figure 7 - Evolution of design for manoeuvrability showing dual flipper system

2.2.2. Motor, power systems and electronics

The previous year's mobile robot utilised a pair of large Lithium Polymer (LiPo) batteries which provided power to the electronics and motors of the robot. A power board was used to supply the relevant voltages for each of the systems on board. The motors used were a combination of Digital and analogue for the flippers and drive, respectively, which required a series of motor control boards. The use of the older heavier analogue motor meant that a separate motor control board needed to be used which wasted space and weight in the robot. The way the batteries were connected and their casings made changing them a very difficult process. The weight and inconvenience of these holders were cumbersome, wasting vital competition time and weight. There was also a problem with the sharp drop off of voltage as the batteries began to reach a low level of charge as their monitoring systems did not run accurately. This led to it becoming increasingly difficult to negotiate the steep slope climbing as the motors would lose voltage fast at repeated attempts. The design of the onboard circuitry was a very cramped and inefficient stack of boards with loose connectors. This led to it being incredibly difficult to remove the electronics for maintenance or repair.

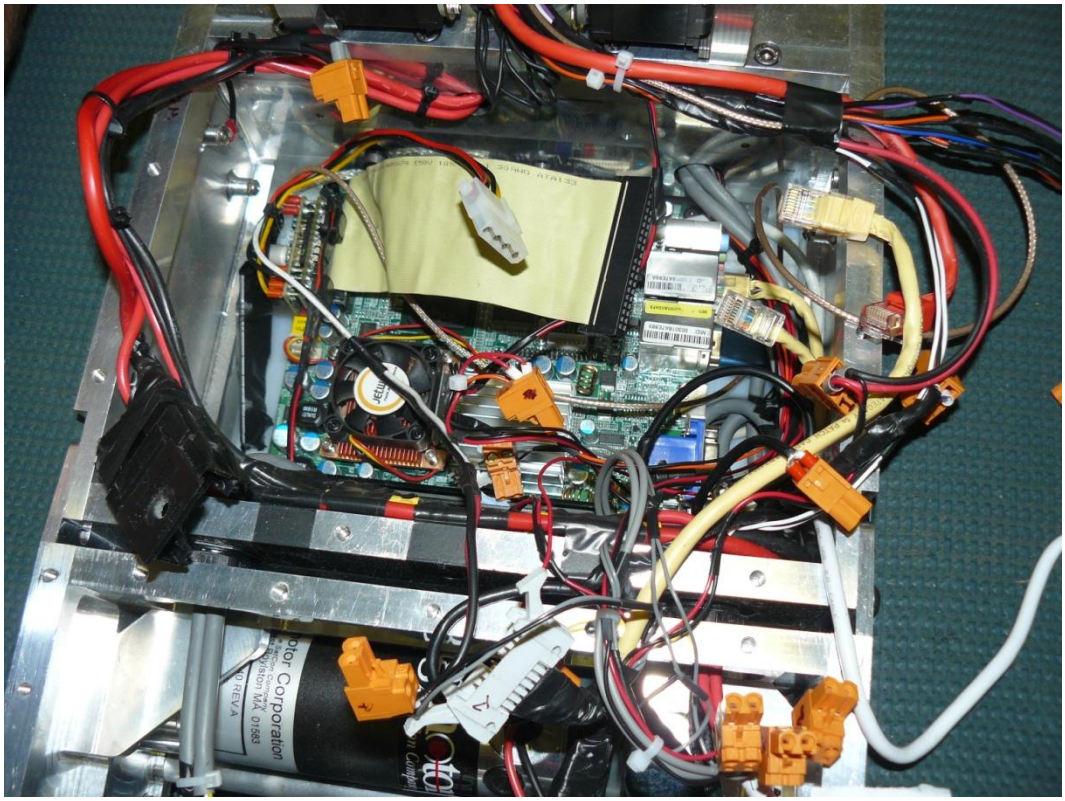

Figure 8 – Cramped electronics configuration

2.2.3. Tele-operation

At the point of handover test runs were carried out to assess the systems in place. The method of tele-operated control consisted of a dual analogue controller which provided independent track manipulation and front and back flipper movement using other buttons on the controller. A GUI system which displayed the orientation of the robot flippers and the video feedback from the two onboard cameras provided the user with visual feedback and allowed navigation through the arena. One of the main problems with this system was the lag in the video feedback which meant that fluent movement was very difficult because camera feedback had significant delay. Also the flipper position shown on the GUI was not always accurate as when the system was reset the flippers became out of sync with the data. The dual analogue manipulation of the tracks was also over complicated making intuitive movement difficult at times.

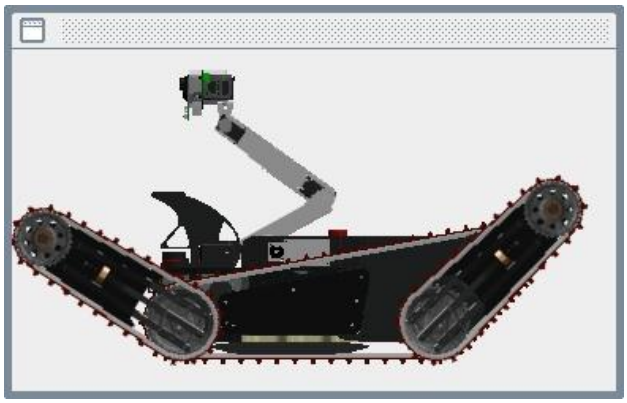

Figure 9 – Examples of images from the GUI controller

2.2.4. Autonomous control and mapping

The previous year's team had many problems implementing their Autonomous Mapping and Control systems. The main reason for this was the lack of available time and programming experience on the team. They did however manage to create an autonomous control system loosely based on collision avoidance. The system used a Laser range finder (LiDAR) to measure the distance from approaching objects and change course into more open areas. Unfortunately they did not end up utilising this in the competition. Using LiDAR range finding they were able to create a 2D map using partial (SLAM) with

some success. Unfortunately they were not able to implement this feature in the competition because of compatibility issues.

2.2.5. Victim sensing

The two main victim sensing techniques employed by the previous team were the web-cameras and the IR camera which provided them with visual and heat data on the victim. The IR camera and one of the visual cameras were situated in the head with one additional camera on the rear of the robot. The IR camera identifies victims via measuring the Infra-red radiation emitted form the victim and using blob detection to differentiate the image from the background radiation. Also included on the robot were a CO2 sensor and two way audio communication but these were not in use during the competition. This allowed the user to remotely identify the victim using heat and visual stimulus which included reading victim data from 0.6m away.

2.2.6. Testing

The robot was fully tested during the 2009 RoboCup European Open competition as well as subsystems being tested throughout the design and implementation phase. Most of the systems were pre-tested including:

- Power systems
- Motor systems
- Flipper systems
- Central computer
- Software systems
- Robot arm
- Victim identification

The full system was run and tested using a small scale arena much like the competition terrain. This enabled important practice using the tele-operated controller and learning how to negotiate the terrain. Several systems were also de-bugged in this way.

Figure 10 – Miniature arena

2.2.7. Safety

The 08/09 robot made use of an emergency stop button on the actual robot which could be triggered physically, cutting power to the motors at any time. Also included was a software emergency stop system which could be triggered at the control station. A Failure Modes and Effects Analysis (FMEA) was carried out to asses the most likely causes of failure and the appropriate responses which aided in the safety process .

2.3. Capabilities capture

With a detailed analysis of the previous years work the objectives of this year's project were to improve on the design of the previous year's robot, and implement a new autonomous robot which would be programmed by an associate computer science team for autonomous mapping and navigation. To accomplish this, the following sections were considered in the design process.

2.3.1. Manoeuvrability

In light of the success of the previous year's robot in the mobility section (best in class) at the European Open, much of the manoeuvrability of the robot is to remain the same. The same dual flipper system and independent track control is to be kept, with more focus put on the chassis design. With the aim of reducing weight and better weight distribution a new design for the tele-operated chassis is to be introduced. Made of modular panels using 0.9mm stainless steel and carbon fibre this should significantly reduce the weight of the chassis which accounted for 40% of the total weight of the robot. With the reduced weight of the robot, slope climbing, one of the most difficult aspects of the mobility section of the competition should be easier. In addition to weight saving it is also proposed to re-distribute the weight of the motors further back in the chassis to make it back heavy. This will aid in tipping the robot over the top of the steep slopes and stair sets which has been a big challenge in previous years.

The new autonomous chassis is intended to have basic mobility as this is all that is required of it during the competition. To do this it will be simply constructed using designs from previous years and a 0.9mm stainless steel box like modular chassis. It is to be given tracks much like those on the tele-operated chassis but without flippers as these are not required to overcome the obstacles of the autonomous section.

2.3.2. Motor and power systems

One of the main aims of this year's project is to make better use of the power systems and provide the robot with new motors which are all digital. This setup would include new drive motors and a new flipper motor for the front flipper. This will reduce the need for the analogue motor and its separate control board and provide more consistent performance from the batteries. The batteries themselves are to remain the same on the tele-operated robot with new similar LiPo batteries for the autonomous robot which should provide good performance. The autonomous robot is to utilise the old drive motors from last year's robot as these meet the requirements. It will also be equipped with the same motor control boards and power boards in an act to facilitate easy software sharing between the two robots.

2.3.3. Tele-operation

Some of the new features planned for this year's team include resolving the lag issues from the previous year and re-forming some of the GUI features to make them clearer for the user. In terms of the lag

issues it is planned to separate the channels, sending the camera data separate from that of the motor controls. To more accurately display the robots orientation a new 3D java program is to be compiled to display the positions of the robot arm and flippers in 3-dimenesions. This also makes controlling the different joints more intuitive. The dual analogue track control from the previous year is to be replaced by a single analogue control.

2.3.4. Autonomous control and mapping

One of the main advantages of this year's robotics team is its collaboration with the Computer Science department and their autonomous control, mapping and victim identification project. At the beginning of the year a specification was submitted to a team of computer scientists who are undertaking a master's project in autonomous robotics. The aim of their group is to be able to fully implement SLAM mapping and control logic into this year's autonomous robot and also to be able to identify victims autonomously using a rating system. The SLAM system uses the teams LiDAR, tilt sensor and compass data to navigate intelligently through the surrounding terrain, mapping wall features and recording its path. Although this software is using this year's autonomous robot as a testing platform, software sharing between robots is the desired end result of this departmental collaboration.

2.3.5. Robot arm

One of the main focusing areas of this year's mobile robotics project is the design and implementation of a 5-DOF robot arm which would be used to house many of the robots victim sensing and navigational cameras. This would be a re-design from the previous year's robot arm which had some shortcomings in the testing phase of operation. One of the main setbacks of the previous year's design was its lack of robustness. Its basic construction was a thin steel frame linked together with servo-motors. The problem with this design was that the thin frame produced shaking during operation which made navigating using the mounted cameras more difficult. In addition to this the servo-motors although rated at higher loads failed and needed to be replaced quite regularly incurring additional cost and reducing usability. The aim of this year's robot arm was to provide a strong stable platform using robust materials and high powered reliable mechanical motor systems. Providing the extra degree of freedom from a rotating base joint would allow the whole arm to rotate to objects aligned perpendicular to the robot. This overcomes the problem of positioning the robot directly in front of hard to reach victims in difficult terrain. This new design will see the integration of a new larger robot head which will house more equipment and be carried at increasing distances from the robots position providing better fields of view.

2.3.6. Victim sensing

In terms of victim identification this year's team will utilise two approaches on the two different robots. The autonomous robot requires full automation in terms of victim identification and will utilise the Infra-red camera to locate hotspots associated with victims and move towards them using the SLAM control system. Once in close proximity to the suspected victim it will use still images from a webcam to identify the victims face and information provided on victim cards. In addition to this it will sample the CO2 concentration in the air and use all of these factors to calculate the probability of this being identified as a victim. It will then log the victim's location on the map and continue to navigate into new areas of the arena. In contrast to this the teleoperated robot operator will be able to navigate towards victims using a webcam. Once aligned with the victim the operator can make use of the robot arm to position the victim identification sensors into a more favourable position. Both robots make use of the same sensors to identify victims, these being:

- Webcam
- Infra-red camera
- CO2 sensor

These are the qualifying systems required for victim identification in the RoboCup competition.

2.3.7. Testing

As well as testing each individual component in turn and software testing a new scale arena has become available for the testing of this year's robots in a simulated environment. This new larger scale arena is housed in the International Digital Laboratory and includes many of the features that will be present at the competition. Having additional space in which to practise with the tele-operated controls and de-bug the autonomous software will provide the much needed opportunities to gain experience and insight into working the systems of each robot.

2.3.8. Safety

In addition to the emergency stop features in the previous years robots this year's design will implement collision detection in the arm control software which will limit damage done to the arm by unforeseen errors. This is extremely important as the new high powered arm will need very careful manipulation to make sure it does not impact with the robot flippers. A software e-stop will also be implemented into the control of both robots allowing remote shutdown of the motors. This is vital in the autonomous

robot as physically touching the robot during an autonomous run would lead to a penalty in which the robot is required to be replaced at the start of the run and the run restarted.

3. Core systems design

3.1. Chassis

3.1.1. Tele-operated robot

3.1.1.1. Weight reduction to improve slope climbing and battery life

A major issue with the robot inherited by the 2009/10 WMR team was the limited range on the robot as a result of low battery life. A large contributing factor to the problem of low battery life was the weight of the robot. One of the team's first objectives was to improve the range of the robot to increase the amount of time the robot was actively locating and identifying victims. It was reasoned that any time and effort put into the sensing hardware, software and programming would be largely wasted if the robot could not reach a competitive number of victims.

In terms of strategies for increasing the range of the robot, two options were available. The first was to increase the capacity of the batteries being used. However, the batteries used by the inherited robot were bespoke Lithium Polymer (LiPo) with a capacity of 5300mAh which was found to be at the high end of affordable battery capabilities and therefore difficult to improve upon. The remaining option was to reduce the weight of the robot.

3.1.1.2. Weight Profiling and New Chassis Concepts

The team created a weight profile of the robot in order to ascertain areas in which weight reduction would be possible. One area in particular which was identified as being especially disproportionate in terms of its contribution to the total robot weight was the chassis. The chassis of the inherited robot was built from 12mm plate aluminium using five-axis computer numerically controlled (CNC) machines. Consequently, the chassis was responsible for approximately 40% of the total robot weight. Additionally, the chassis of the inherited robot had been designed to allow for adjustments of the tension in the driving tracks. As a result, the chassis had elements of its design which compromised the abundance of space within the robot. For example, the chassis had been divided into two sections with adjustable tensioning bolts between the adjoining plates. Without this horizontal partition, the available space

within the robot would have been much more flexible and allow for more innovative and efficient design of mechanical systems and electronics hardware. It was clear that a entirely new chassis, based on the original elements, but designed with weight reduction and efficient utilisation of space, was necessary.

3.1.1.3. Materials Selection

The WMR team had access to Warwick Manufacturing Group's machining facilities and so had a wide range of materials and machining methods available for the new chassis design. The team had a strong ambition to strive for contemporary methods and materials both through personal interest and enjoyment and in order to establish the WMR brand as innovative and pioneering. Because of this, carbon fibre arose as a first choice for the material of the chassis since it has an excellent strength to weight ratio (see section 3.1.1.7). However, carbon fibre cannot be bent and formed after curing and so for any panels requiring angled bends or curved surfaces, for functional or aesthetic reasons, a foam plug would have to be made in order to produce the required shapes. This would be extremely time consuming since the foam plug may have to be CNC machined and the fibre laying process is arduous and requires high levels of care and precision. However, a number of flat carbon fibre panels were laid by members of the WMR team which had the potential to be used for any flat panels of the chassis.

Unfortunately, carbon fibre is potentially hazardous when being cut by machine tools due to the minute fibre fragments that occur which can irritate the skin and airways. In order to overcome this, the team performed tests utilising WMG's laser cutting facilities to cut the carbon fibre. The laser cutting was tests were performed using a 6000W *Trumpf TLF6000* mounted on an Aerotech XYZ CNC controlled table. The laser cutting produced reasonable quality cut edges which would have required little to no post processing. However, the laser cutting process produced potentially hazardous smoke as a result of burning the carbon. The extraction facilities available were not significant enough to ensure the safety of the technicians and subsequently it was decided that laser cutting of carbon fibre was not a safe and viable option.

3.1.1.4. Selection of Chassis Manufacturing Method

Laser cutting, as a manufacturing method, was seen by the team as an extremely advantageous one for a number of reasons.

Firstly, within the International Manufacturing Centre (IMC), where the team were based, there was access to advanced laser cutting machinery and a skilled laser cutting technician in Neil Timms. The advantage of this was that designs for components which the team envisaged to be laser cut could be

reviewed by Mr. Timms so that his expert knowledge could be applied to ascertain their suitability and viability for the intended purpose. Although this level of technical support may have been available from exterior manufacturing sources, the speed of feedback and ease of communication from such establishments cannot match that of an in-house provider. Additionally, such valuable support from a third party is unlikely to be imparted at no cost.

Figure 11 - *Trumpf TFL6000 Laser Cutter*

The second major advantage of laser cutting is the speed of the manufacturing process itself. The Warwick Mobile Robotics team has the privilege of access to a number of skilled technicians whose manufacturing knowledge extends beyond laser cutting to a vast number of techniques. Previous teams have put to great use the access to WMG's high class five-axis CNC machinery and in addition expertise of technician Adam Land. Mr Land's proficiency was once again available to the 2009/10 WMR team and so the unparalleled level of the design consultation provided by Mr Timms for laser cutting was also available for CNC machining via Mr Land. However, the differentiating factor for the choice the team faced between manufacturing methods for the main chassis of the robot was speed of the two processes. CNC machining processes have a much longer lead time than laser cutting processes largely due to the long set-up times, both in terms of physical set-up and data input set-up. The physical set up time for a CNC is much longer than that of a laser cut machine due to the tool adjustments required for each part to be made. The laser specification for a particular material and form are largely computerised in the form of presets whereas whilst the same may be true for CNC machining (tool selection, coolant flood rates etc. may be incorporated into the machining code) the CNC machine must be set to an initial state compliant with the CAM data inputted. For example the zero datum faces (for the y-direction this

is almost always the upper face of the material to be machined) must by identified by use of a probe. Producing the CAM (Computer Aided Manufacture) data forms the other main component of the CNC machine set-up time. Both CNC machining and laser cutting require some form of CAM data to instruct the machine tool (metal cutting tool or laser) as to the path it must take when cutting. Since the laser has only two degrees of freedom, whereas the CNC machine tool has five, it is far easier to describe the path for the laser in terms of code. All Computer Aided Design (CAD) for the robot was performed using the software package *Solidworks 2009 since a*lmost every member of the 2009/10 WMR team was highly proficient with this CAD software. *Solidworks 2009* enables users to produce highly accurate three-dimensional models which are used to check assembly fits and as visual aids for demonstrations and in conveying concepts, but primarily these models form the basis of the CAM code used to produce precise replicas of what is drawn. The most challenging part of producing a component using CAD/CAM software is expressing what the designer draws in a form which is understood by the machinery. This challenge is not helped by the vast range of CAD/CAM coding languages available today.

As previously mentioned, CNC machinery can cut with five degrees of freedom and so a large amount of information must be conveyed within the CAM code in order to assure the cuts are made in the correct orientation, using the correct size tool, at the correct tool speed, with the correct feed rate of material and with the correct coolant etc applied. Although the base coding for all this is obtained through CAM software, the software itself requires a highly skilled operator especially when the cost of errors is considered. The CNC machine most frequently used within the IMC costs approximately £250,000. That being the case, use of CAM software to generate appropriate tool-paths and operation of CNC machinery had to be done by Adam Land.

Since the laser cutter machine has only two degrees of freedom, it is only capable of cutting “two dimensional” (ignoring sheet material thickness) forms in sheet metal. Thus, any component designed for laser cutting but intended to have form in three dimensions will require bending, subsequently, designs must allow for this. That is, the WMR team were required to produce three-dimensional parts within *Solidworks 2009* so that the chassis (and moreover the entire robot) could be assembled and checked for errors before manufacture, but then reproduce those three-dimensional parts as “two-dimensional” forms which could later be cut in sheet metal and folded to the correct form. Due to the nature of three-dimensional models in *Solidworks 2009* this became an extremely arduous task. Put simply, *Solidworks 2009* represents three-dimensional models as series of extrudes from sketches on the x, y and z planes. Therefore, in order to “flatten” such a model, each sketch has to be transferred from its original plane to a single 'master' plane whilst maintaining the correct orientation and dimensions. To compound the difficulty of this task, it is necessary to adjust the dimensions of the sketches on the master plane to compensate for the bend radiuses which occur as a result of folding sheet metal. However, it was discovered by the WMR team that within *Solidworks 2009* there is a tool which allows designers to alter the nature of three-dimensional models so that they are represented by a flat sketch pattern on a single plane, folded into a three-dimensional form with automatic allowance for and representation of bend radiuses. The part can then be saved within *Solidworks 2009* in the .DXF file format which is required for use on the *Trumpf TLF6000* laser cutting machine. This tool became

invaluable for producing and subsequent components through laser cutting and folding. Unfortunately this tool was discovered after the vast majority of chassis design had been completed.

Due to the high volume of complex components required for the chassis it was decided that since the component designs for laser cutting could be completed to a near machine-ready state by the WMR team without the need for technician assistance (other than as expert consultants) and that the process itself is faster than CNC machining, a chassis comprising components manufactured by laser cutting was the best option.

3.1.1.5. New chassis design

Once the manufacturing method had been decided, the details of the chassis could be determined.

First, the material from which the chassis was to be produced had to be established. The main reason for the decision to redesign the entire robot chassis was weight reduction. Therefore it was important to use a material which is both lightweight and strong. However, the WMR project had a budget which did not allow for large amounts of money to be spend on materials, and therefore the chosen material needed to be low cost. Additionally, laser cutting is limited by the range of material which it can cut (especially with regards to material thickness) and as had been demonstrated by the attempts to cut carbon fibre, certain materials can be hazardous to laser cut. As a result, it was decided that the chassis would be made from 0.9mm stainless steel, largely due to the fact that Mr Timms had had a large amount of experience cutting this material and that it was readily available, but also because of its good strength and weight properties.

Second, considerations as to form the chassis would take were made. One factor of major importance which hindered the ease of assembly and disassembly of the inherited robot, was the arrangement of the chassis components. Access to the vast number of bolts needed to remove the excessive number of chassis panels was identified as a clear problem early on in the project. In addition, it was sometimes necessary to remove two or more panels to properly access single mechanical or electrical components, which further increased the time and complexity of disassembly. In order to address these issues, it was decided that the new chassis be built with accessibility, robustness and minimalism in mind. The chassis first needed to be capable of withstanding the hardships of the test arenas which simulate an earthquake scenario. However, this should be achieved without the use of surplus panels and hardware. It was decided that the number of panels should be kept to the bare minimum without compromising accessibility and similarly the number of bolts fixing those panels should be minimised. The team also noted that where 0.9mm sheet stainless steel had been employed in past WMR robots it had suffered a large amount of damage in the form of dents and scratches. In the interests of aesthetics and in order to prevent continual damage from negatively impacting the functioning of the robot, it was decided that it should be possible to easily replace the panels most vulnerable to damage, namely the front, rear and base panels. Due to the fact that laser cutting had been used as the manufacturing technique, spare

panels could easily and quickly be made in preparation for the competition or earlier if testing rigours demanded it. In order to increase the ease of assembling the chassis from its discrete panels, the two side panels were fitted with M5 stainless steel rivnuts. This allowed the two chassis side panels to form a natural basis for assembly and the remaining five panels could be removed individually without the need for a large disassembly, as intended. Due to the fact that the team had decided to maintain the inherited track and pulley system, the major dimensions of the chassis were predetermined. However, it was an aim of the team's to utilise the space within the chassis with maximum efficiency.

With all these considerations in mind, it became clear that the chassis for the tele-operated robot would require a careful, considerate and importantly, clever design. Since it had been decided that the side panels of the robots were to form the basis for assembly, leaving the remaining panels to be largely non-functional other than for rigidity and protection, their design became increasingly complex. The side panels were the main point of fixation for the drive motors, pulley stub shafts, battery holders and flipper motor mounts. The position of each of these components (excluding the battery holders) had to be extremely precise in order to achieve the correct tension in the drive tracks and flipper motor chains and thus ensure efficient drive of the robot and precise articulation of the flippers respectively. The track and flipper arrangement and the tracks themselves were inherited from the previous robot. It was decided that since the preceding team had achieved the 'Best in Class for Mobility' award that there was little need for improvements to the mechanical system responsible.

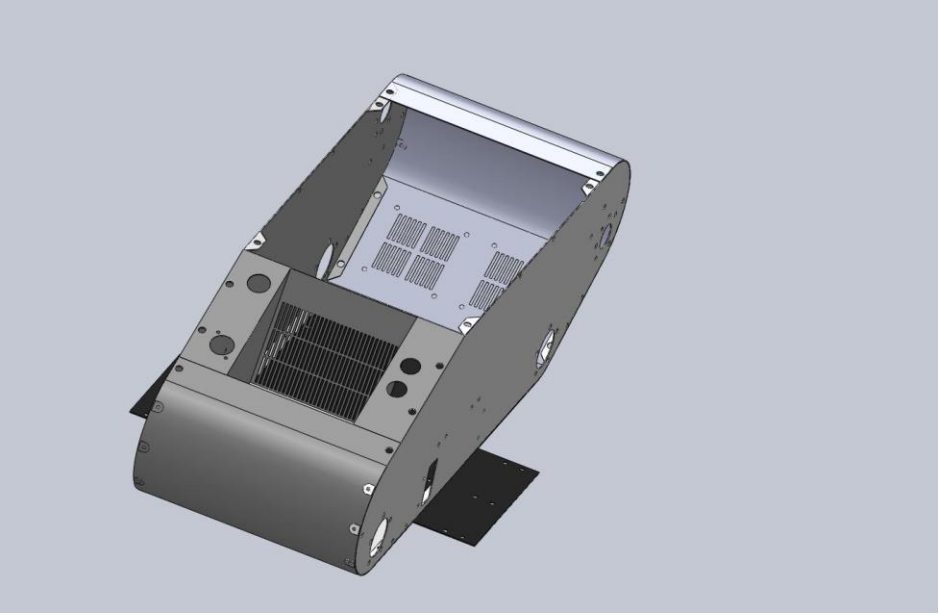

Figure 12 - New Chassis Assembly (without lid panel)

Accurate positioning of components within the robot chassis to ensure efficient use of space proved itself to be a major difficulty. It was somewhat of a dichotomy that the chassis designed needed to accommodate several components when the position of some (particularly electronics and wiring) which could not be decided until the chassis itself was built. This was due to the fact that it was a goal of the electronic engineers within the team to minimise wiring within the robot, and thus the position of many components (fuses, for example) was dependant upon the position of several others. This complex 'chain of wiring' made it extremely difficult to visualise or model the location of electronics. The position of the mechanical components, such as motors and mounting brackets, could be modelled relatively easily in *Solidworks 2009* and was used to great effect, whereas the modelling of wiring and electronics components is extremely difficult and not worth the proportion of time required to perform it.

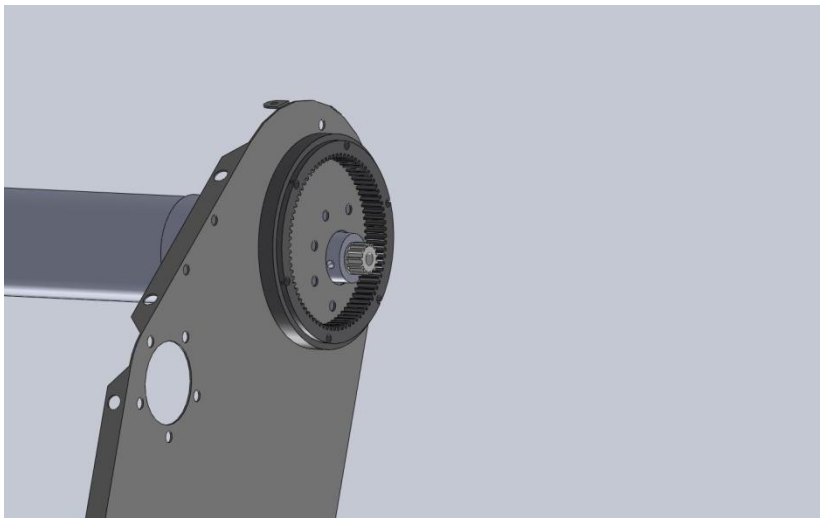

Figure 13 - Gear-Mesh test modelled in *Solidworks 2009*

In scenarios such as these it became more apparent how advantageous the decision to use 0.9mm laser cut stainless steel was. Any additional holes for the attachment of components whose location had not been predetermined could quickly and easily be added at almost any point in the construction phase by use of a hand drill. Although this was only necessary a small number of times due to the careful design of the chassis, the tight time constraints to which the team was working meant that any time lost to redesigning and/or reworking CNC machined chassis panels could have jeopardised entry to the competition.

One particular area which proved difficult to design correctly, and which subsequently required a number of redesigns, was the positioning of the flipper motor mounts in order to achieve good chain tension. As with the inherited robot, the front and rear flippers were each on a single shaft rotating

driven by a motor-gear-chain arrangement. It was imperative to have the correct tension within the chain to ensure accurate flipper control. If the chain were too slack, the flippers would have a range of movement possible in the flipper which was not controlled and regulated by the motors. A small amount of movement is practically unavoidable due to backlash occurring between the gears and chain. This phenomenon makes the need to minimise all other contributing factors all the more important. Conversely, if there were no slack at all in the chains, the loading on the motor shaft and gearbox would constantly be at a high level leading to rapid wear. With the entirely redesigned chassis, the flipper motor mountings also required a new design. The flipper motor mounts (required to accurately position the motors to achieve the required chain tension) were designed to be bolted to the two chassis side panels and be positioned above the motors themselves. They required the ability to withstand the high loads generated when moving the flippers (especially when the flippers would be used to raise the main body of the robot) and it was decided that they should be CNC machined from aluminium.

3.1.1.6. CNC Machining of Other Components

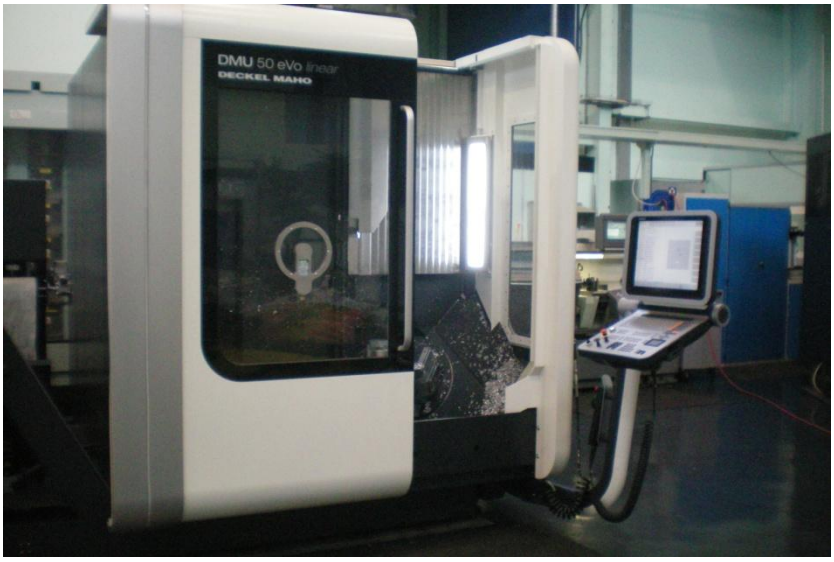

Figure 14 – 5-axis CNC machine

Despite the fact that it was not chosen as the primary manufacturing method for the chassis of the tele-operated robot, CNC machining was used for a number of other vital components within. Due to the change in chassis thickness as a result of using 0.9mm stainless steel sheet in place of 10mm aluminium plate, a number of components involved in the drive and mobility system required redesign. It was decided that it was preferable to maintain the inside dimensions of the chassis to reduce the amount of rework machining required. A number of corrective adjustments were unavoidable however, such as the

reduction in length of the flipper shafts and pulley stub shafts in order to keep the tracks close to the robot chassis. As a consequence of these reductions, equivalent extensions to the drive motor mounts and spur gear collars (required to attach the spur gear to the drive motor shaft) were required to maintain the correct meshing between the spur gear attached to the drive motor and the annulus gear within the drive pulleys. Due to the complexity of the drive motor mounts (a collar which was ensured strong point of fixation between the drive motor and chassis), it was decided that these too would be CNC machined from aluminium. Another component which was CNC machined was the arm mount which provided a firm base to deal with the large and varying loads of the robot arm.

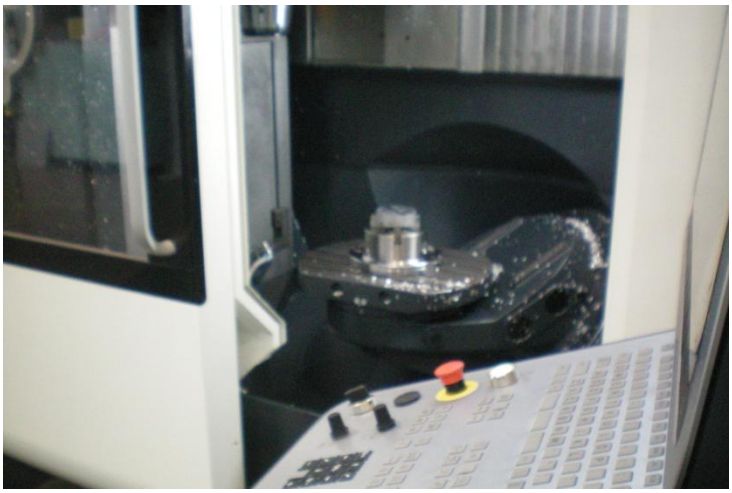

Figure 15 – 5-axis CNC machine close-up

A further component of the chassis which required a complete redesign from what was present on the inherited robot was the packs for holding the batteries. The lithium polymer batteries used on the tele-operated robot were highly volatile and susceptible to exploding when subjected to heavy impacts. As a result the team had a duty of care to ensure safe housing of these batteries within the robot to prevent such occurrences. Like the chassis, the battery packs were laser cut from 0.9mm stainless steel sheet and bent into shape.

Figure 16 - Closed Battery Pack

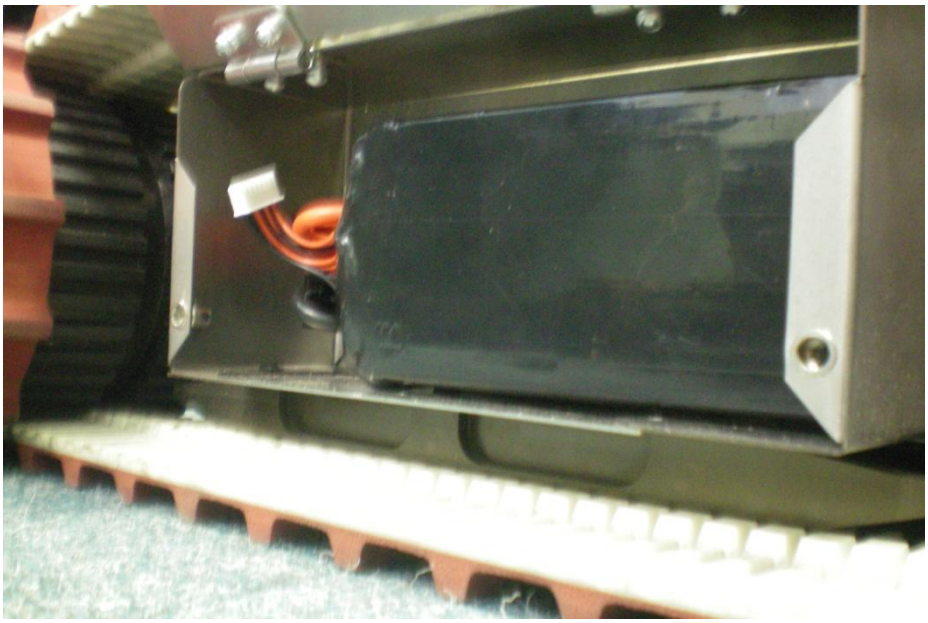

Figure 17 - Open Battery Pack with Battery

3.1.1.7. Carbon Fibre Manufacture

One of the main aims for the 2009-10 WMR team was to reduce the weight of the chassis of last year's robot by 10kg. The 2008-09 robot is made of 12mm thick aluminium plate and comprises the majority (40%) of the robot's total weight. For this reason the chassis was selected as the primary area to focus on for weight reduction. The use of sheet steel or composite materials, such as carbon fibre, was identified as a key enabler for weight reduction without negating structural integrity. Sheet steel was selected for ease of manufacture, low cost and production time, as outlined in section 3.1.2.2. Conversely, carbon fibre is an extremely versatile material offering a high strength to weight ratio. The facilities and equipment necessary for making carbon fibre panels is available in the WMG Composites Laboratory workshop. Considering the WMR team has had no experience with carbon fibre production, this was seen as a side project learning experience with the potential to replace the sheet steel on both robots for even lower weight. An image of the final carbon fibre panel is shown in Figure 18.

Figure 18 - Carbon fibre panel

We used the vacuum bagging method to produce carbon fibre panels with a 200g/cm^2 carbon fibre twill weave fabric, giving an aesthetic checkered pattern upon hardening. The first trial we completed was a test to get acquainted with the process and health and safety precautions. These included wearing gloves when handling hardened carbon fibre, epoxy resin and hardener, and ensuring adequate ventilation of the working area. A cross section diagram of the vacuum bagging technique layers is shown in Figure 19.

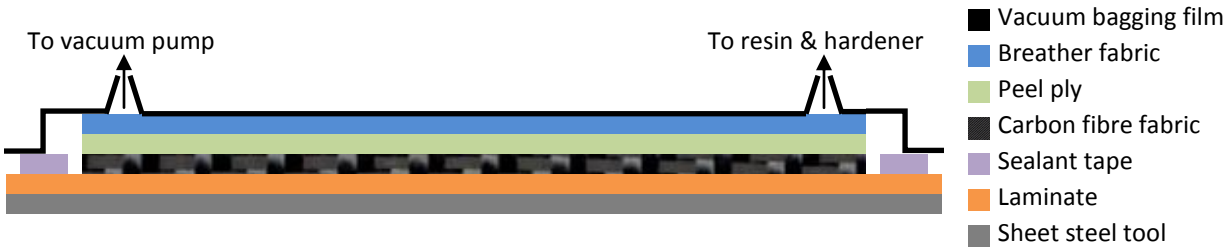

Figure 19 - Cross section carbon fibre layup

The vacuum bagging method is outlined in a step by step approach:

- Cut laminate to size of tool (Figure 20): laminate is used to provide a smooth surface for the carbon fibre to be laid up on, producing a smooth shiny surface also known as the *A-surface*.

Figure 20 - Cutting laminate

- Stick laminate onto tool: this is done by peeling the white sheet off the laminate and sticking this side onto the tool carefully. It is important to ensure as little air bubbles are captured between the laminate and the tool as possible. Any imperfections on the laminated tool will be seen on the cured carbon fibre A-surface. A flat sheet steel panel was used as the tool.

- Cut carbon fibre fabric to desired size (Figure 21): carbon fibre is best cut with scissors by taking out one strand and following this to get a straight edge. The fabric must be smaller than the tool so the sealant tape can fit around the edges.

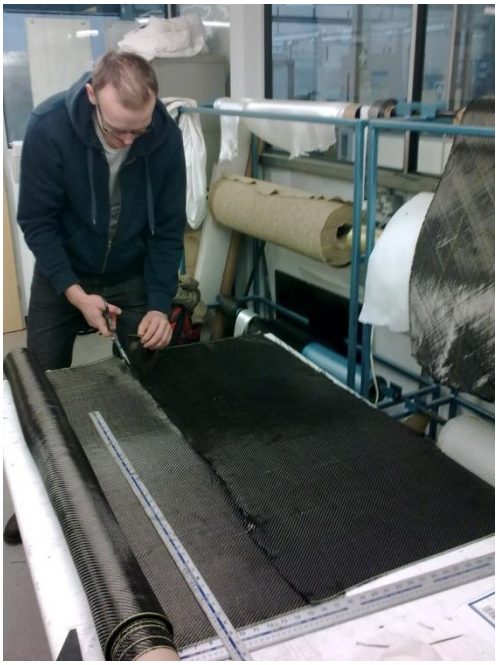

Figure 21 - Cutting carbon fibre fabric

- Lay carbon fibre sheets on laminate (Figure 22): one must ensure the sheets are aligned to give a uniform panel when hardened and remove as much fray on the sides as possible.

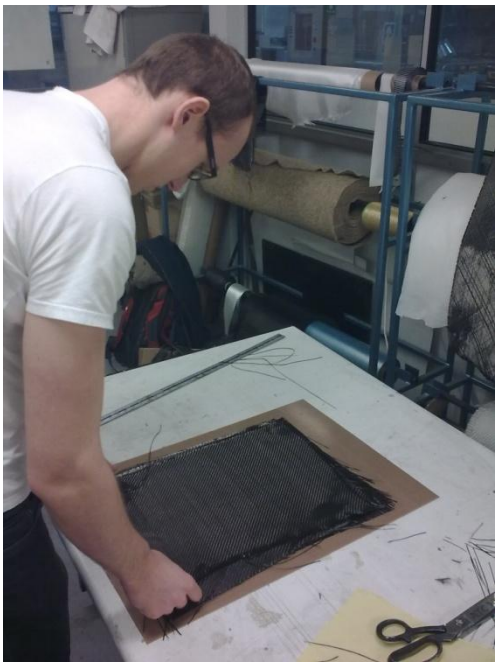

Figure 22 - Placing carbon fibre fabric on tool

- Cut a single sheet of breather fabric and peel ply (Figure 23): these should be the same size as the carbon fibre sheets and placed directly above. The peel ply is placed on the carbon fibre first and can be peeled off the cured carbon fibre. Peel ply is an open weave material made of fibreglass. The breather fabric is a loosely woven glass fabric and provides a continuous vacuum path over the part for improved distribution of the epoxy resin and hardener. Small squares of breather fabric are placed at the inlet port to aid in the ingestion of epoxy resin and hardener. Small squares of felt are placed at the outlet port to ensure as little as possible epoxy resin and hardener are ingested into the outlet port which leads to the vacuum pump.

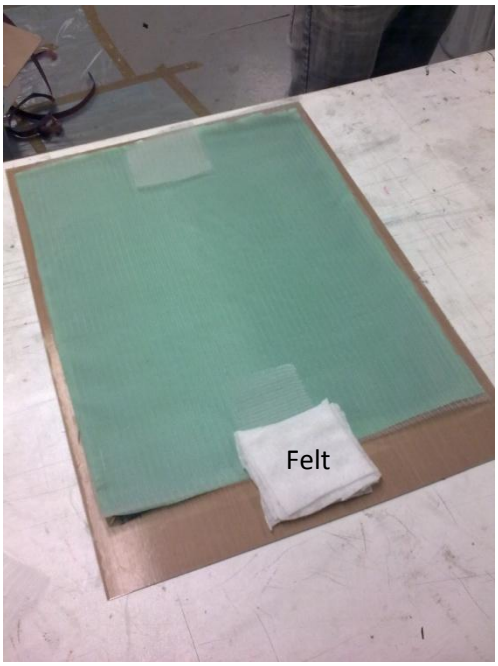

Figure 23 - Tool, laminate, carbon fibre sheets, peel ply, breather fabric and felt (in order)

- Place the inlet and outlet male vacuum ports in the appropriate places and fixate the vacuum bagging film with the sealant tape (Figure 24): the vacuum ports should be placed at the ends to minimize the size of their imprint on the cured carbon fibre part. The vacuum bag must be pressed down hard on the tape to seal the entire *sandwich*.

Figure 24 - Sealant tape being placed around the edges of the tool

- Screw in the female inlet and outlet ports from outside the vacuum bag (Figure 25): the ports cut a small hole into the vacuum bag and are self sealing once screwed down tightly. It is important to remove the waste plastic from the small cut-out, which could block the inlet and outlet ports.

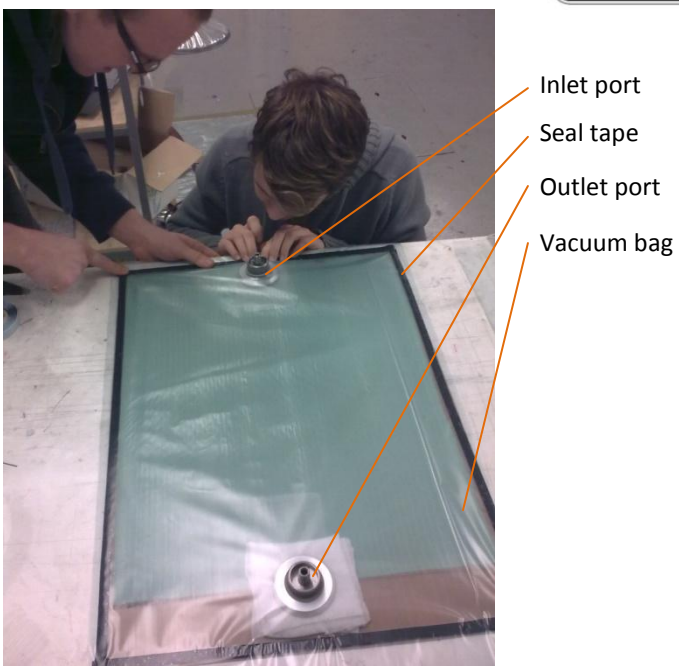

Figure 25 - Complete vacuum bag

- Ensure the bag is sealed (Figure 26): this is achieved by attaching a hose to the outlet port which lead to the vacuum pump and switching this on while the inlet port hose is blocked. Jubilee clips are used to fixate the inlet and outlet hose to the inlet and outlet ports, respectively. If the bag is properly sealed a vacuum will be achieved in the bag with no visible air bubbles.

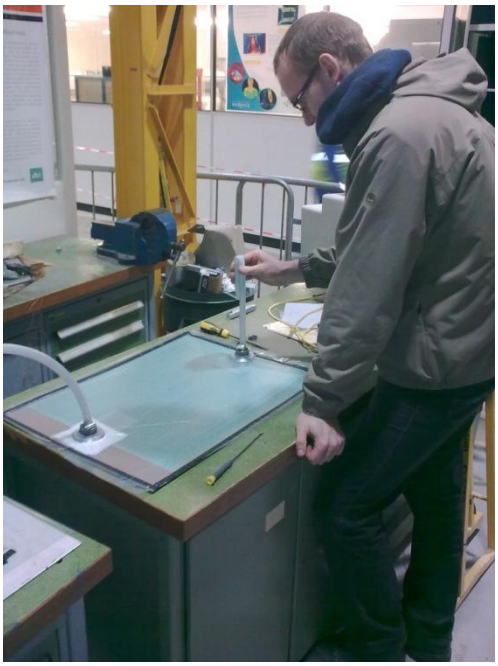

Figure 26 - Vacuum check

- Mix the epoxy resin and hardener (Figure 27): we used the *EP522* epoxy resin and *H522* hardener mixed with a 22 unit epoxy resin to 1 unit hardener ratio. It is important to get a homogenous mixture between the two as well as exact measures to achieve a high-quality carbon fibre panel. The mixture will heat up after a certain amount of time therefore it is important to minimise mixture quantities. The equation for determining the amount of mixture necessary is,

$$Mixture\ Mass = \underbrace{Mass\ Per\ Unit\ Area \times Area\ Of\ One\ Sheet \times Number\ Of\ Layers}_{Of\ Carbon\ Fibre}$$

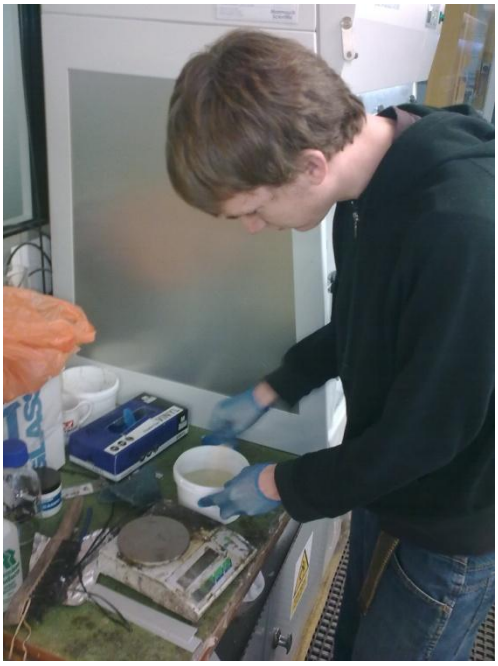

Figure 27 - Mixing of EP522 and H522

- Infusing epoxy resin and hardener mixture into vacuum bag (Figure 28): the inlet hose is submerged into the container with the epoxy resin and hardener mix. The pump is then switched on to suck through the mixture and is switched off when three quarters of the carbon fibre sandwich has been infused with the mixture, as shown in Figure 28.

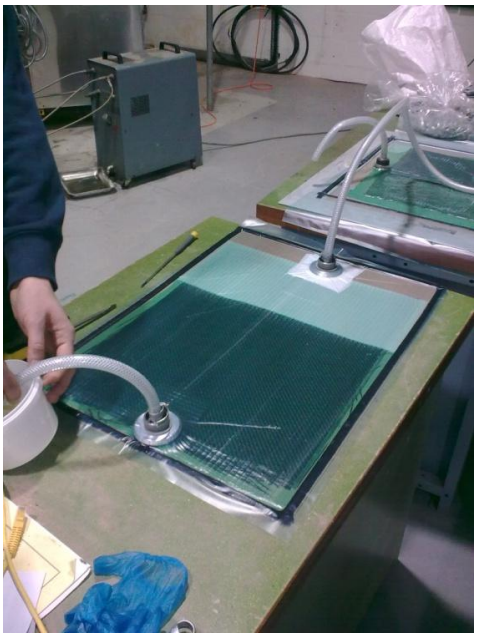

Figure 28 - Sucking mixture into carbon fibre sandwich

- Stop infusing epoxy resin and hardener mixture into vacuum bag (Figure 29): use another jubilee clip to close off the inlet hose, making sure no more mixture or air is being sucked in. If the amount of mixture is insufficient to cover the entire sandwich, the inlet hose can be re-submersed into the container and the jubilee clip loosened. It is essential that the outlet port hose is closely observed to ensure that no mixture is ingested into the vacuum pump. This is best avoided by putting loops into the hose and having a long hose.

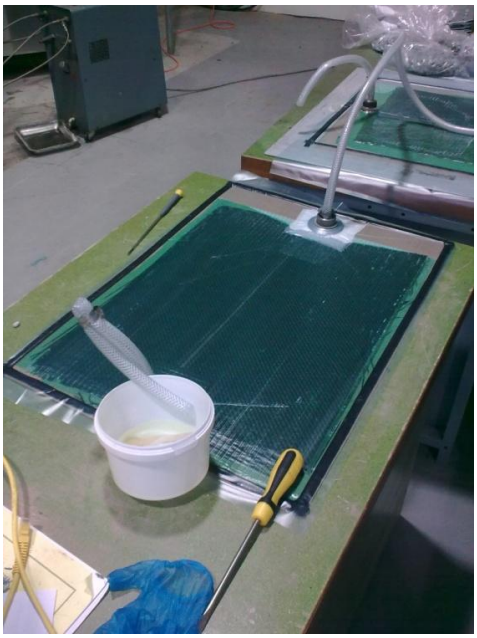

Figure 29 - Preparations for curing stage

- Cure carbon fibre sandwich (Figure 30): the carbon fibre should be left to cure with for approximately 12 hours with the inlet hose fully closed and the vacuum pump on.

Figure 30 - Curing stage

- Peel off all layers above carbon fibre part (Figure 31Figure 31 - Cured part): it is important to use a glove when handling cured fibre glass.

Figure 31 - Cured part

This process was repeated twice to produce two additional carbon fibre panels with the correct thickness and dimensions. It was anticipated that these panels would be cut into the desired shape using the laser cutting method outlined in section 3.1.2.2 of the report. It was found that there was insufficient ventilation on the laser cutting setup while cutting the carbon fibre, resulting in smoke and fumes during cutting which is undesirable for health and safety reasons. Nonetheless laser cutting of carbon fibre has proven itself as an effective, cheap and quick method as shown with a partly cut panel in Figure 32.

Figure 32 - Uncompleted laser cut carbon fibre panel

The carbon fibre panels could therefore not be utilised on this year's teleoperated robot however could be used for future chassis designs. If adequate ventilation for laser cutting carbon fibre is still not available by then, external companies for water jet cutting should be looked into.

3.1.2. Autonomous robot

3.1.2.1. New prototype autonomous chassis uses similar design to 07/08 team

During the initial stages of the project a team decision was made to work on two robots concurrently: the "main" tele-operated robot and a simplified robot for the autonomous section of the competition. The aim of the autonomous robot was to enable the computer science team to develop their mapping capabilities on a simple robot while the tele-operated robot would undergo major design changes. This enabled the mobile robotics and computer science teams to work on two separate robots concurrently, therefore working more efficiently together. A box shaped chassis made of sheet steel was a quick and easy way to establish the basic structure of the robot and start with hardware implementation. The autonomous robot is made of 0.9mm thick stainless steel flat sheet, which is cut using a laser cutter based on a SolidWorks (2009 SP2.1) CAD model. The *sheet metal* tool is used in SolidWorks to enable components to be designed in 3D and subsequently flattened, with automatic compensation for bend radius' and notches for highly stressed regions. The infrared camera mount in the robot head is shown in Figure 33 as an example of a sheet metal part in its actual form and as a flattened shape.

(a) 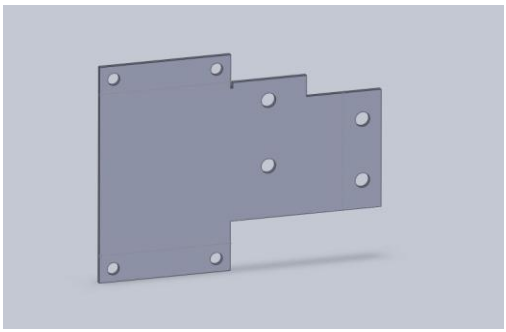 (b) 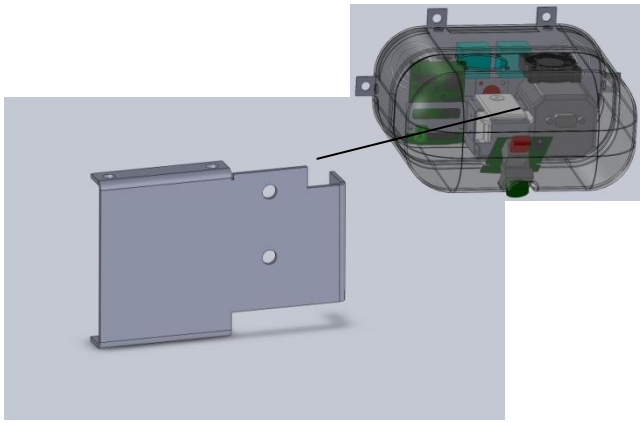

Figure 33 - Infrared camera mount in (a) flattened and (b) non-flattened state

3.1.2.2. Laser Cutting

Laser cutting or Laser-Beam Machining (LBM) is a manufacturing technology by which laser light is focused on a workpiece for cutting, as illustrated in Figure 34.

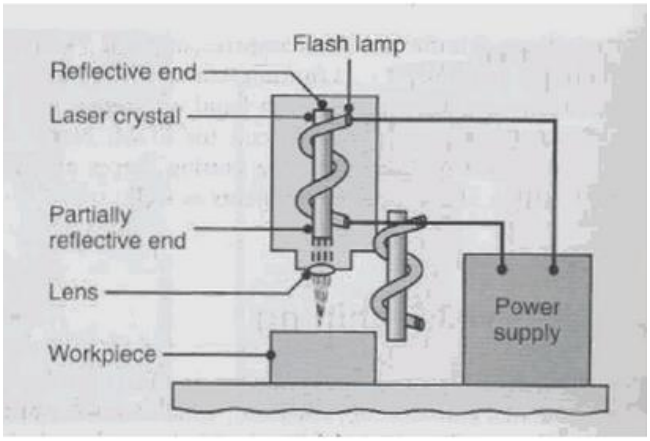

Figure 34 - Laser cutting[1]

Components can be made within minutes at low cost, there is no wear of the cutting tool, surface finish is excellent, there is a narrow heat effected zone and high accuracies are possible (Kalpakjian & Schmid 2006). The main disadvantage is the high energy required. As described in Kalpakjian & Schmid (2006), the highly focused and high energy source melts and evapourates sections of the workpiece in a controlled manner. Work pieces can be metallic and non-metallic. The governing physical parameters of the workpiece are reflectivity, thermal conductivity, specific heat and latent heats of melting and evapouration. The lower these parameters are the less energy will be required for cutting. The cutting depth is given by

$$t = \frac{CP}{vd},$$

where C: constant; P: power input; v: cutting speed; d: laser spot diameter.

Two different types of laser are used based on the type of components being manufactured. For smaller parts a *Lumonics JK 701 Nd:YAG (Neodymium: Yttrium-Aluminium-Garnet)* (Figure 35) laser is used with

[1] KALPAKJIAN, S. & SCHMID, S. R. 2006 Manufacturing engineering and technology. Fifth edition. Prentice Hall.

a maximum average power rating of 400W, 0.3mm beam diameter and 0.05mm accuracy. This laser operates in combination with an oxygen gas stream to increase energy absorption when cutting sheet steel. The laser is mounted on an *Aerotech* XYZ CNC controlled table, has a feed rate of 300mm/min and is more accurate than the laser described next.

Figure 35 - Lumonics JK 701 Yag Laser

For larger parts a *Trumpf TLF6000* laser (Figure 11) with a maximum power rating of 6000W, 0.015mm beam diameter and 0.025mm accuracy is used. Similar to the Lumonics laser, the Trumpf laser is mounted on an Aerotech XYZ CNC controlled table however the feed rate is increased to 2m/min. This laser uses high pressure nitrogen gas, leaving a polished oxide free edge with no burrs that can improve weldability. The high pressure gas also aids in blowing away molten and vapourised material from the workpiece surface.

The aluminium is formed into the desired shape using a sheet metal hand brake and fixated using rivets. The simple robot design gives the computer science team flexibility to implement various hardware components necessary for autonomous operation, and is sufficient to master the flat terrain during competition.

3.1.2.3. Single track design

The single track design is sufficient to climb 15 degree slopes and navigate through the rest of the terrain without the need for flippers. This drastically saved space and time making this new robot very spacious and allowed for significant cooling of the more powerful CPU.

3.2. Power systems

3.2.1. Tele-operated

3.2.1.1. AX500 motor control boards

The configuration of the AX500 motor control boards is shown below in Figure 36.

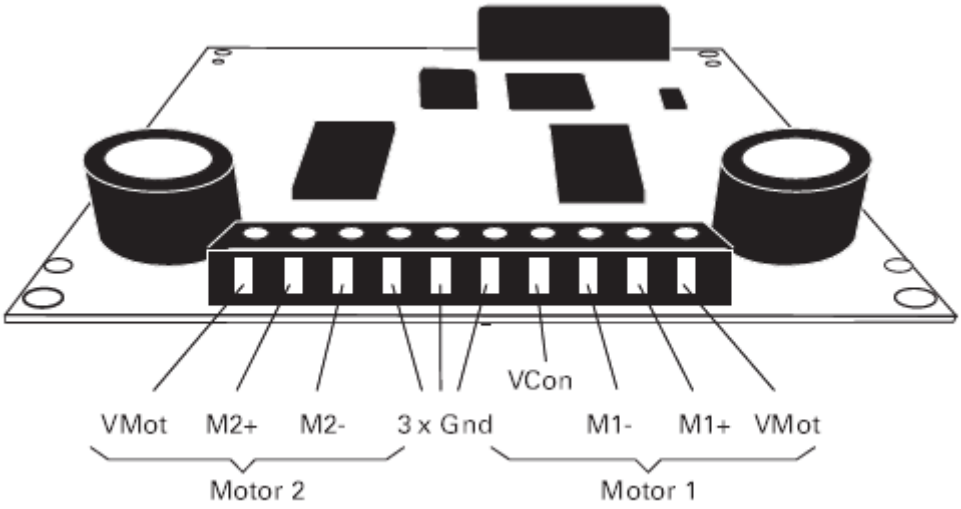

Figure 36 - AX500 motor control boards rear view (AX500 Roboteq technical manual)

The AX500 motor control boards are used to control the arm motors. The motor control boards provide power from the batteries to the motors and data from the motors to the software for feedback.

The connection of power and data to and from the motors is detailed in Figure 37.

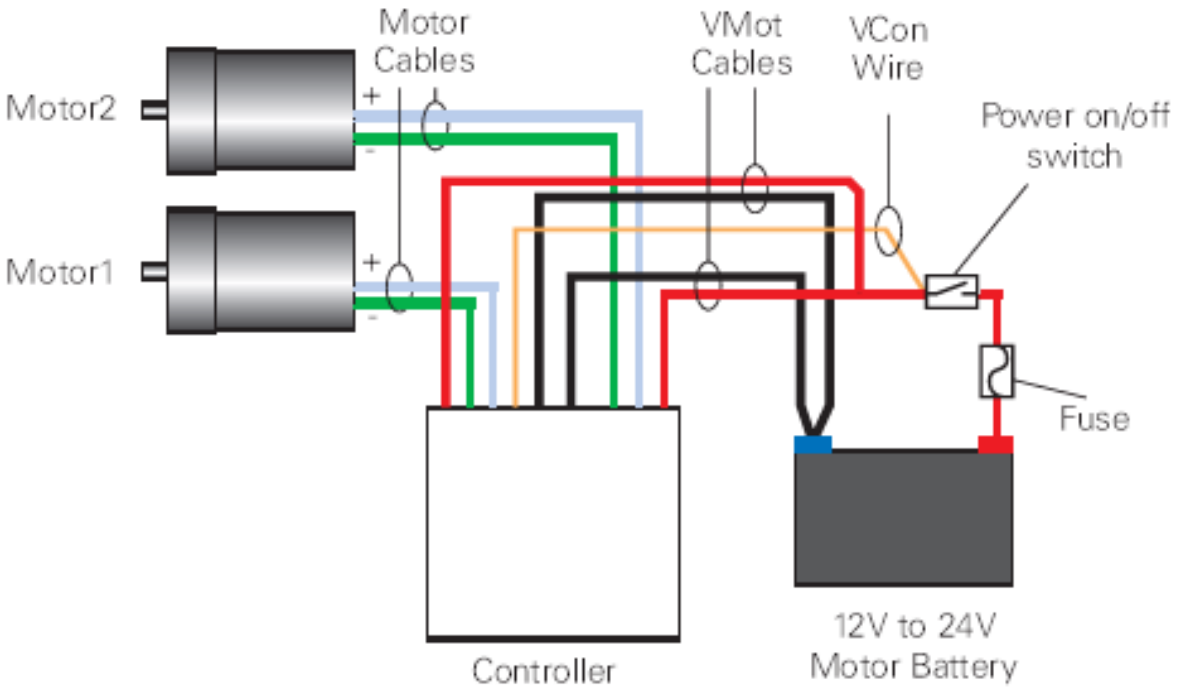

Figure 37 Connecting the batteries and motors to the control board (AX500 Roboteq technical manual)

In order to control the motors and use the feedback from the encoders a software called RoboteQ which is provided with the motor control boards is used. This software can be used to manually enter positional data to drive the motors or integrated into other software used for overall control of the robot via a controller. Figure 38 shows an example fo the software package being used to gain feedback from the encoders and driving the motors to specific positions. This software is used for controlling both the AX500 and AX3500 motor control boards.

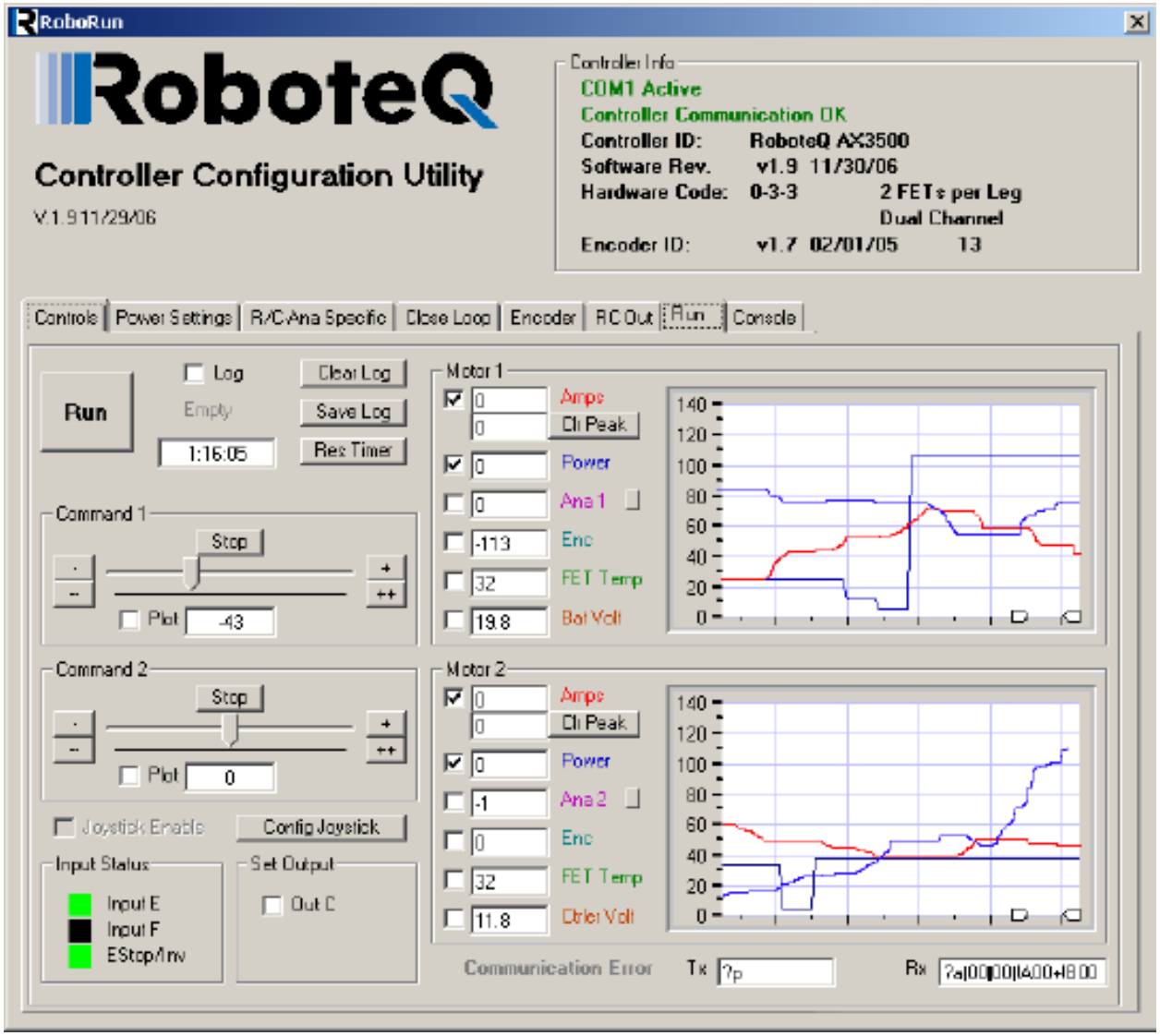

Figure 38 roboteQ software window

3.2.1.2. AX3500 motor control boards

These boards are used to control the two drive motors and the flippers on the tele-operated robot. The control boards are located in the central electronics stack.

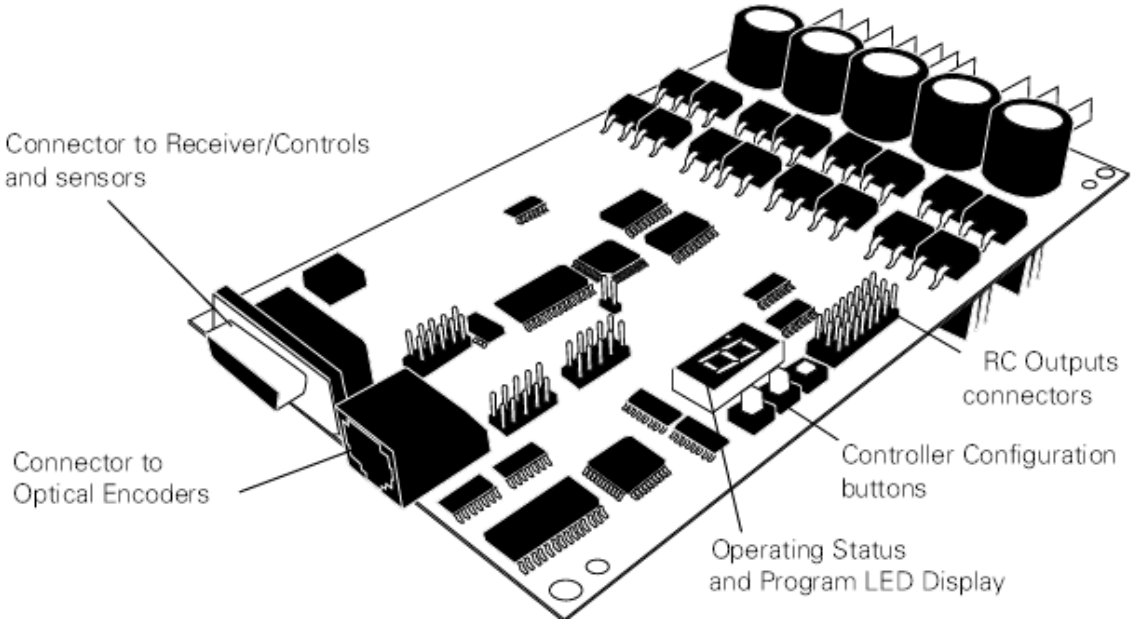

Figure 39 - AX3500 motor control boards (AX3500 Roboteq technical manual)

Similar in configuration to the AX500 control boards connectors for optical encoders and control commands are relayed here.

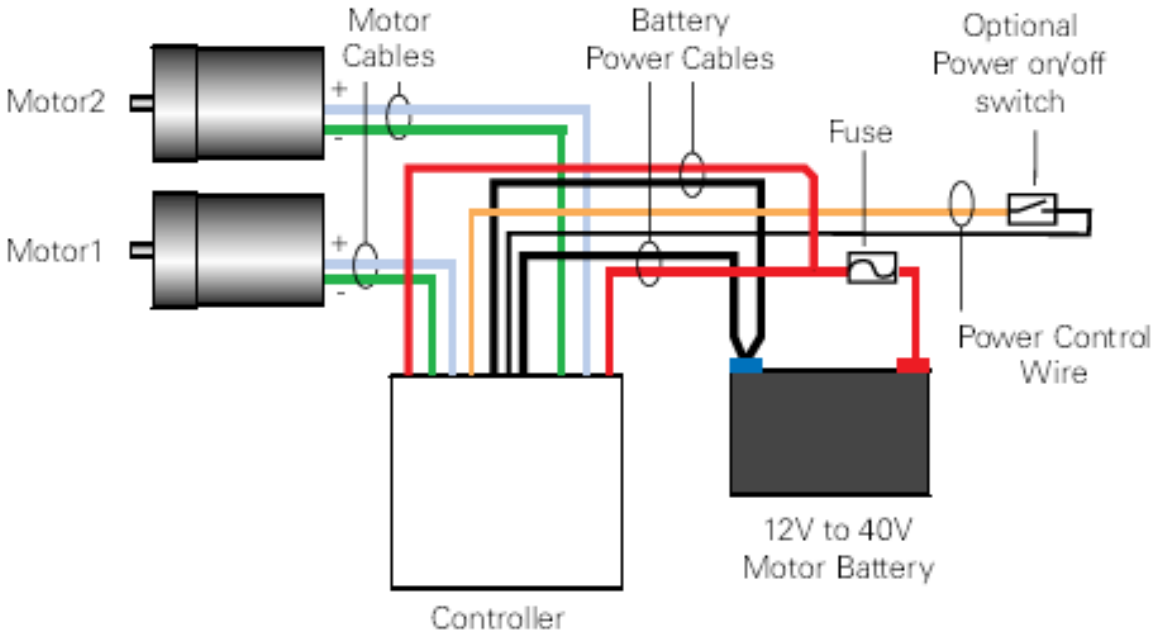

Figure 40 - Connections for the AX3500 motor control boards (AX3500 Roboteq technical manual)

These boards feature and optional on/off power switch which is useful for isolating motors during testing. Most commonly the flipper motors were disabled during testing when the robot was positioned on a low clearance block so as not to accidently topple the robot during testing.

3.2.1.3. Power board

The power board was custom made in the previous year specifically for the tele-operated robot. Its function is to convert the battery current and voltage into the various different currents and voltages required by all the component in the robot.

Outputs		
24V	3.5A	Computer
12V	1A	IR camera, fans, flipper controllers
5V	4A	LiDAR, webcams, router
24V	0.25A	fans
24V	64A	(typical)Motors

Figure 41 outputs from the power board

3.2.2. Batteries

The batteries were the of the most performance-critical aspects of the design. Carried over from last year were:

- 1.2V, 10,000mAh NiMHcells connected in series to make a 12V pack (x4)

Figure 42 – Old 12V battery packs

- FlightPower EVO LITE 22.2V, 5350mAh Lithium Polymer batteries (x4)

Figure 43 – Old 24V LiPo Batteries

To supplement these, four more Lithium Polymer batteries were purchased:

- RapidCharge 22.2V, 5200mAh (x2)

Figure 44 – New 24V LiPo Batteries (1)

- FlightTech EON 22.2V, 5000mAh (x2)
-

Figure 45 – New 24V LiPo Batteries (2)

In addition to those, a second charger was purchased (RobbePowerPeak Infinity 3), to ensure that the batteries would always be available for a run during the competition.

Before the competition, all the original batteries were tested for capacity, by running them through a charge/discharge cycle on the charger (Table 2). From the 5350mAh specification, the batteries had indeed lost capacity, by different amounts. The new batteries, it was decided, would be used for competition runs, while the old batteries would be useful for testing.

Battery	Discharge Time (hh:mm:ss)	Capacity (mAh)
A	2:15:16	5069
B	2:15:36	4955
C	2:17:43	5146
D	2:10:45	4860

Table 2 - Battery Capacity Testing

3.2.3. Autonomous

3.2.3.1. NiMH batteries from 07/08 team

It was decided early on to use the existing 12 volt NiMH battery packs from the previous year. Each pack consisted of 10 small 1.2V batteries, wired together in series to give the required 12 volts. Each battery offered 10,000mAh at this voltage. This decision had several implications for the robot:

- The two battery packs would need to be connected in series to power the robot, in order to provide the required 24 volts.
- The lower capacity compared to the Lithium Polymer batteries meant that the robot would need to be lighter and slower than the teleoperated platform to achieve the same running time.
- It would be possible to run the robot on one 24 volt LiPo battery, but every precaution would need to be taken to ensure that two of these batteries were not connected, as this would provide 48 volts to the components connected to the main rail, likely damaging components.

3.2.3.2. Power control

Rather than using a bespoke power control board, the robot used commercial DC-DC converters for any components that required lower than the 24 volt battery supply rail. The advantage of this was that it could easily be modified. A preliminary list of the voltages required was created:

- 5V: router, LiDar, Phidgets Interface Kit, servo controller, tilt sensor.
    - This would be supplied by a SunPower SD-15B-05 DC-DC Converter.
- 12V: CO2 sensor, power LEDs
    - Again, using a Sunpower converter, but model SD-25B-05.
- 24V: PC supply – specialist voltages required
    - The PC was supplied with a miniITX switch mode power supply, providing the various voltages required by the motherboard.

As long as the current rating of each converter was sufficient, any component subsequently added could be easily powered. Additionally, if a different voltage level was required, it would be easy to include another converter in the chassis.

3.2.3.3. AX3500 induced PC crash issue

Following the preliminary build of the autonomous robot it was discovered that un-e-stopping the robot seemed to cause the PC inside to turn off. To further investigate this problem the battery voltage was measured using an oscilloscope to aid faultfinding. During normal conditions with the PC turned on, the following data was collected (Figure 46).

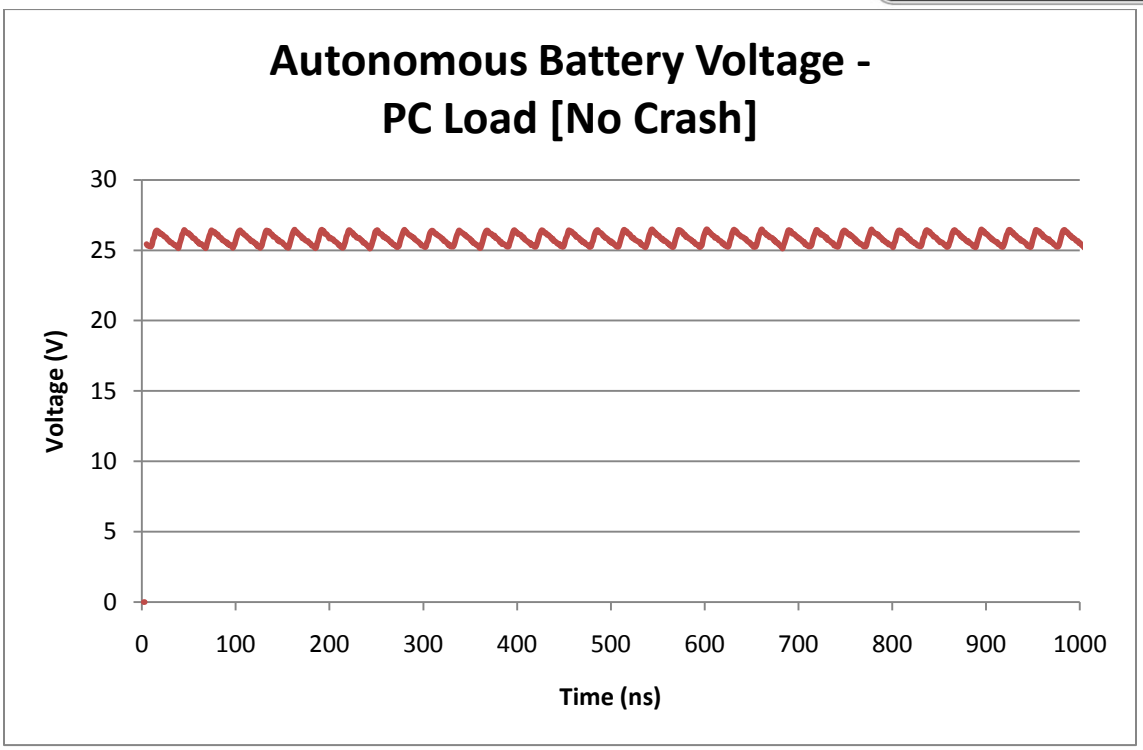

Figure 46 - PC on, steady average voltage

This graph clearly show a stable average voltage – the ripple present is likely to be caused by the switch mode power supply of the computer.

Then, data was collected for the battery voltage when the E-stop was reset, shown in Figure 47.

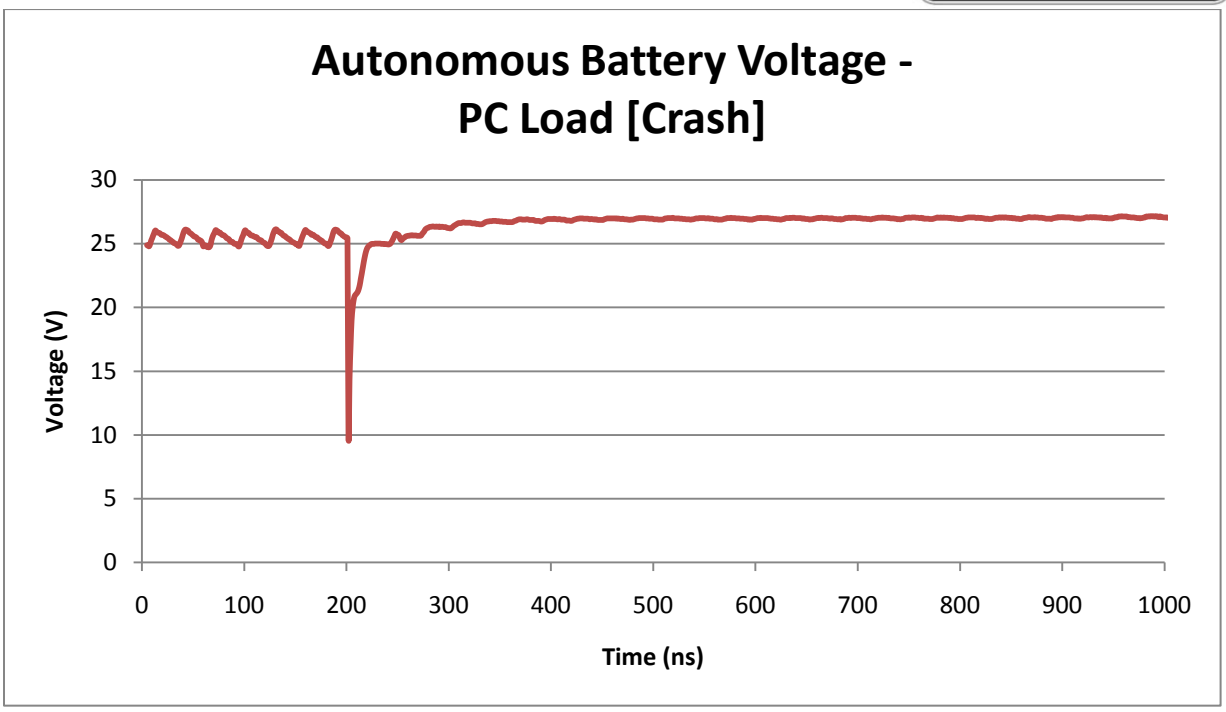

Figure 47 - PC crashed, 15 volt drop

It was clear from this test that the cause of the PC crashes was the massive, 15 volt drop when the E-stop was reset. It was proposed that this drop was caused by the large capacitors on the AX3500 motor control board, which drew large currents to charge when initially connected to the supply. To avoid this problem, a resistor was connected across the relay, in effect short-circuiting the switch in its open state. The value of the resistor chosen (6K8Ω) was such that the capacitors were allowed to charge, but the voltage was not enough to power the control board itself.

$$Current\ through\ resistor\ I = \frac{V}{R} = \frac{25}{6800} = 3.6mA$$

$$P = I^2R = (3.6mA)^2 \times 6800 = 88mW$$

This calculated wattage was well within the rating for the resistor used, so there was no safety hazard involved.

To avoid this problem on the teleoperated robot, the decision was taken to introduce this modification across the robot fleet.

3.3. Electronic systems

3.3.1. Tele-operated robot

3.3.1.1. Re-design of electronics stack for better space and easier maintenance

Easy access to the electronic boards in the robot was deemed to be vital for two reasons. Firstly, since the robot was being designed to operate under harsh conditions the potential for electronic hardware failure would be higher than if it were working under normal conditions. To ensure minimal disruption to the possibly life-saving operation of the robot, it was decided that all electronic circuit boards should be mounted in such a way that removal would be expedited when necessary.

Secondly, during the testing phase of the robot build, access to the electronic circuit boards was expected to be vital and speedy access would enable quick problem solving and allow for improvements to be made.

3.3.1.1.1. Blade mounting concept

An initial concept was based on a server-style set up that allowed boards to be slotted into the top of the robot. Should one board fail, the problematic board could then easily be removed. See Figure 48 for a diagrammatic explanation.

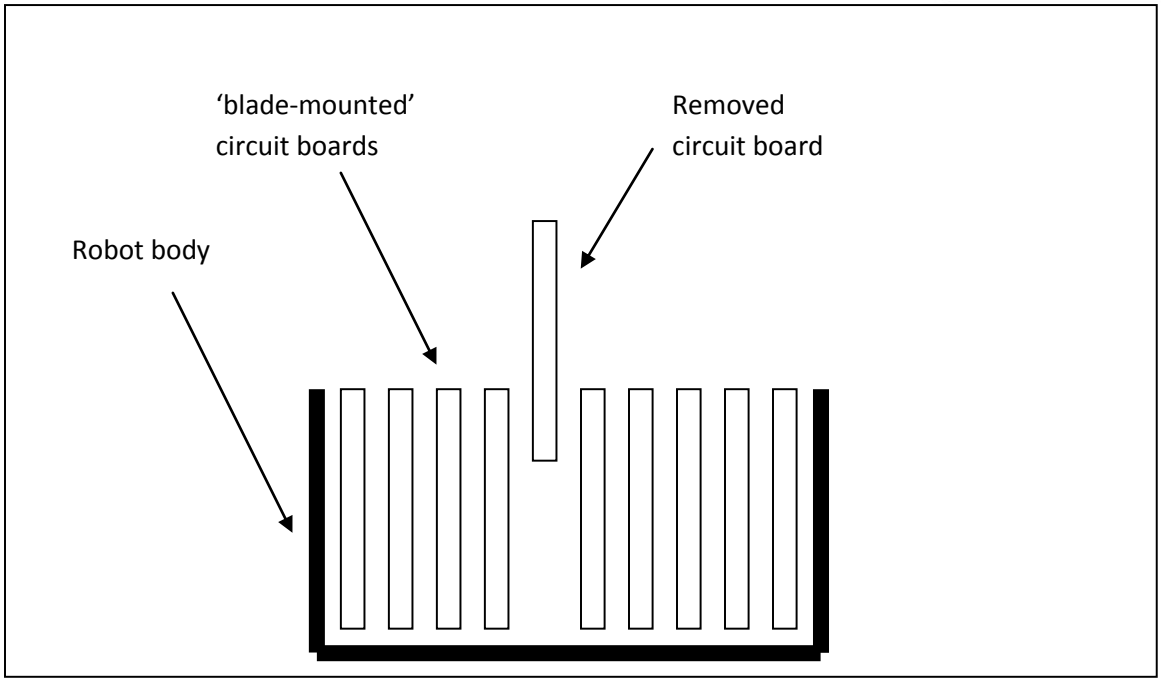

Figure 48 - Blade-mounted server style mounting of all circuit boards (prelim. idea)

This 'rack-mounting' system idea was discounted however for two reasons:

- Cooling the boards was initially conceived to use assisted convection – fans blowing into the bottom and another set exhausting from the top. The physical size of the circuit boards, however, when compared to the robot meant that there was no space for fans and thus cooling the 'blades' would be a major issue;
- All the boards were designed to be mounted directly onto surfaces and did not lend themselves to being mounted on runners; predominantly since the connections to and from the board often were made at two ends of the board.

3.3.1.1.2. Stack mounting concept

To allow ease of access a single modular electronics stack design was conceived. This concept allowed all the circuit boards and other control electronics to be housed entirely in one place; beneficial for ease of replacement as well as cooling. To ensure that the circuit boards didn't overheat, a 120mm fan attached to the front of the stack and two 80mm fans exhausted the warm air from the rear of the robot, shown in Figure 49.

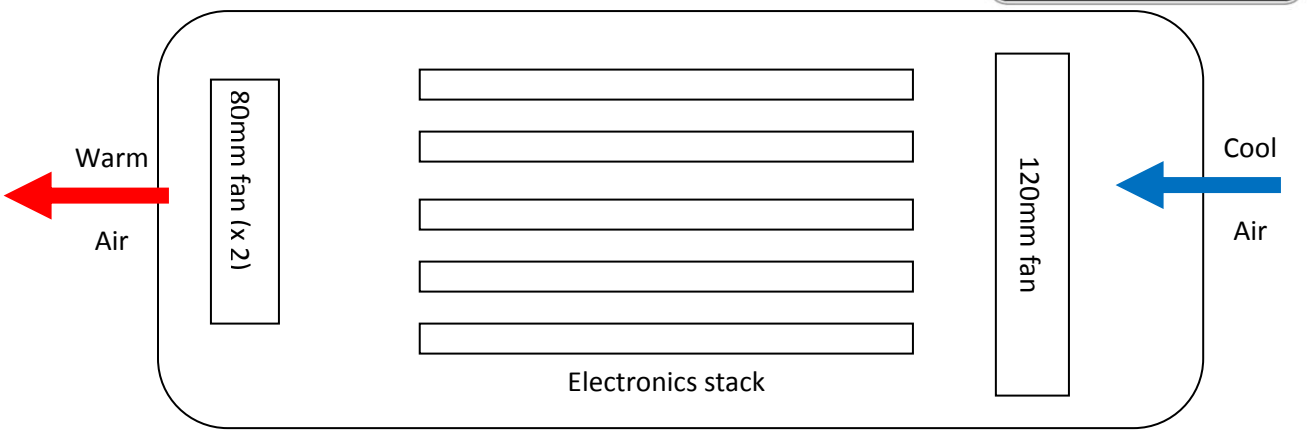

Figure 49 - Airflow representation through stack

Following the mechanical design, a width limitation was enforced to ensure that the stack would fit within the internal dimensions of the robot. One major problem with the design of the previous year was that it housed the motherboard in such an orientation that the USB and serial connections were put under significant strain when placed into the robot under the preceeding arrangment. The new design addressed this problem by rotating the motherboard through 90 degrees, thus totally removing this pressure. Figure 50 shows a SolidWorks drawing of the assembled stack.

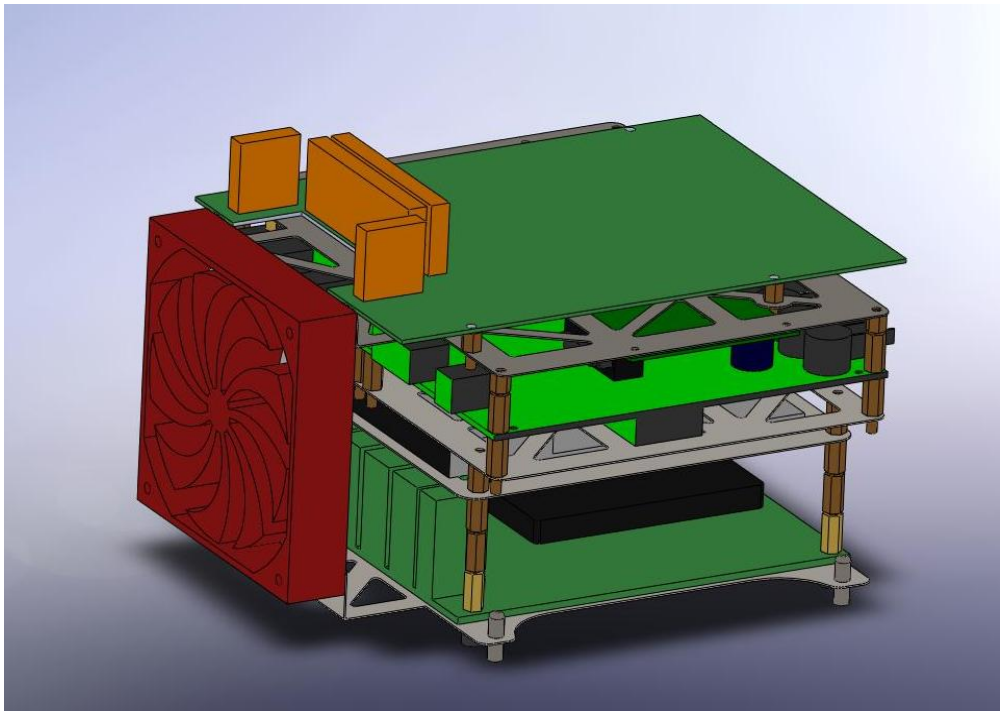

Figure 50 - The SolidWorks design of the electronics stack with 120mm fan (red)

The new stack design incorporated all electronic circuit boards, including the four motor control boards (two AX3500 – drive and flipper motor control and two AX500 – control of the four arm motors, two motors per board). From the top down, the following boards were included (Figure 51).

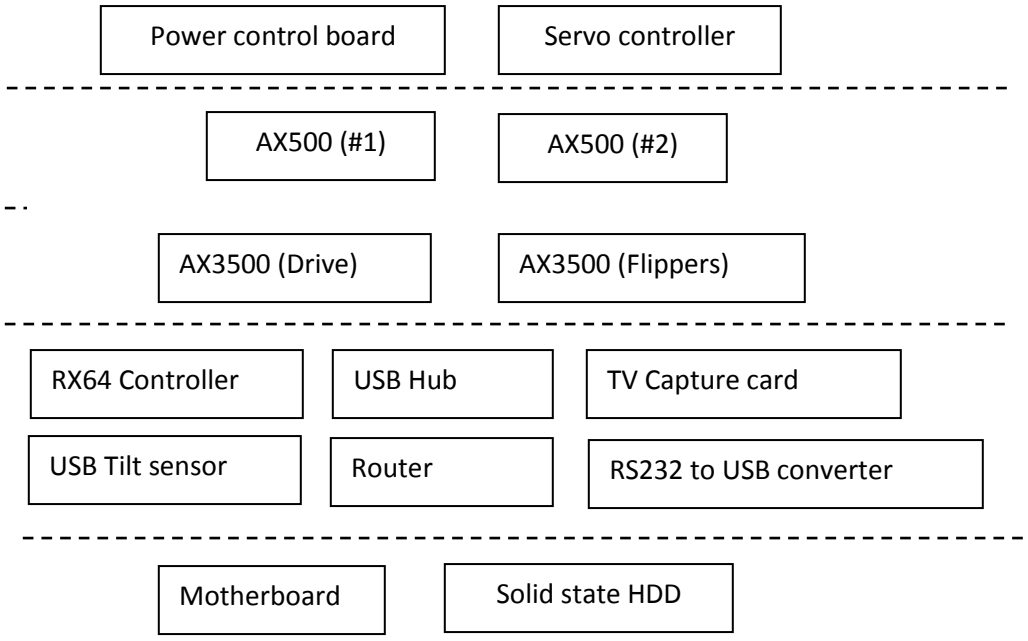

Figure 51 - Diagrammatic systems stack model by level

To ensure the most compact fit of all the boards the AX500s were mounted upside down and in a central position allowing the capacitors of both the AX500 and the AX3500 space in the stack. To further improve space saving the heat sinks on the AX500s were removed. This was deemed safe since the stall current drawn by the motors was only 3A and the AX500 are designed to cope with 15A per channel. Furthermore, they are designed to cope with two continuous 15A loads – the arm would not be used continuously.

For ease of construction and reduction of wiring complexity the stack was designed to keep the boards orientated in such a way that all power connections exited from the back of the stack and all data connections exited from the front of the stack (where the fan is located). This mainly applied to the motor control boards but care was taken to ensure the motherboard also adhered to this design rule also. Figure 52 shows all the connections made within the stack.

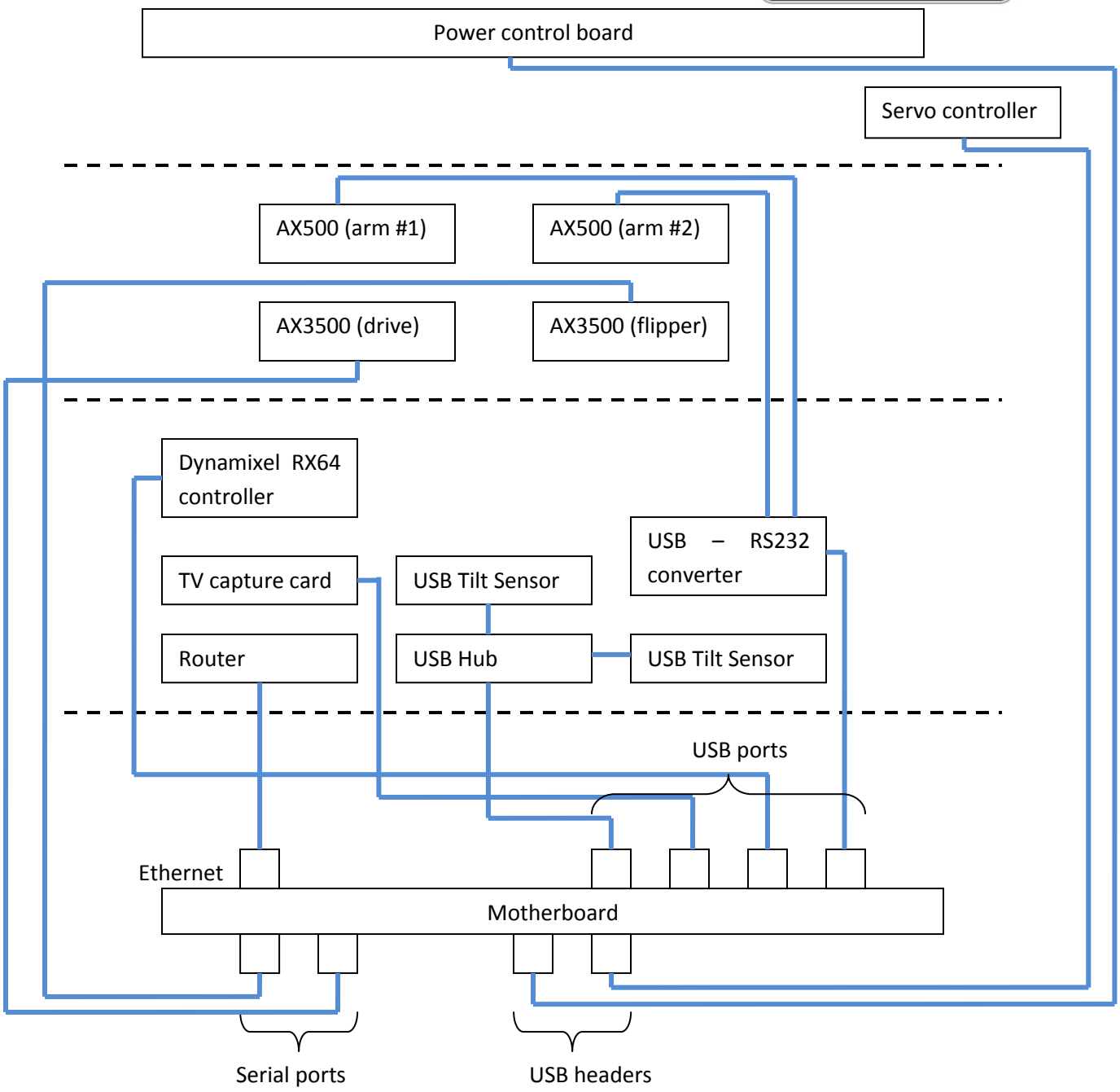

Figure 52 - Connections made within the stack

Figure 53 shows an exploded view of the stack displaying in more detail how the compact design worked. The router is show in the drawing but the other items that are stated above to share the same level are not shown. In addition, for the sake of simplicity, the stand-offs that provide the spacing in between the layers are removed.

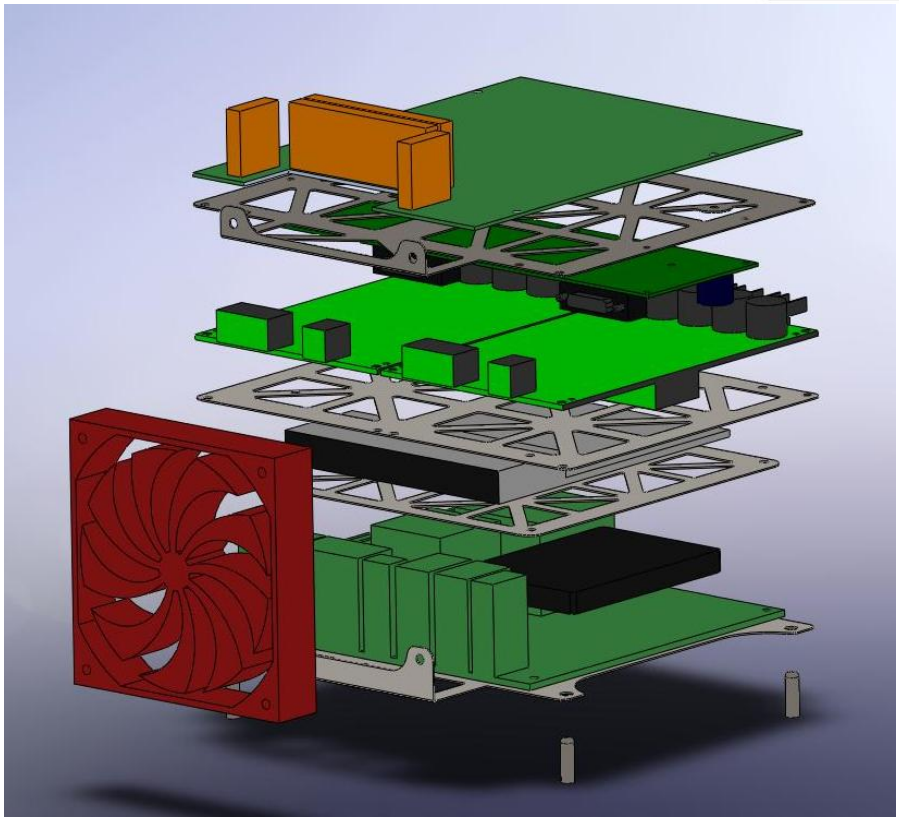

Figure 53 - Exploded view of the stack

Figure 53 shows the mounting stanchions that the stack located on. For ease of installation, the stack was designed with four 4mm holes in the base plate. These holes matched up with four M4 bolts bolted to the base of the robot, thereby locating the stack. Under the corners of the stack four foam pads were placed, providing impact and shock protection to the stack in much the same was that rubber engine mounts are used on a car. To secure the stack to the base of the robot four small catches were machined. These catches were bolted to the bottom of the robot and secured with nylock nuts, allowing the catches to be rotated using an allen key on the base of the robot and thus improving the ease of assembly and disassembly. An actual image of the stack can be seen in figure Figure 54.

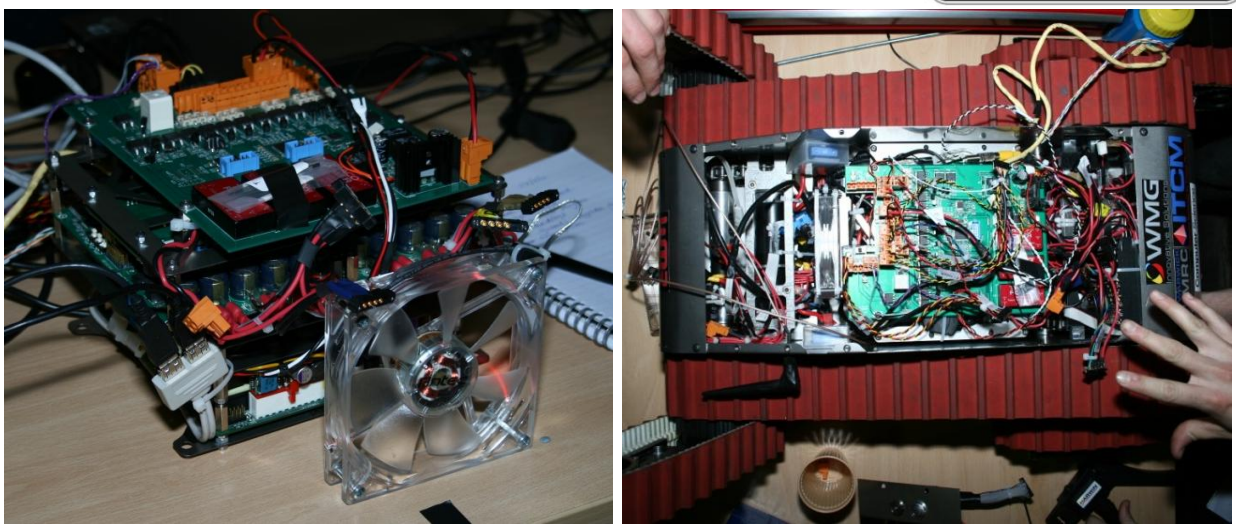

Figure 54 - Electronics stack (left: out of robot; right: in robot)

To ensure the ease of installation and removal of the stack, the wired connections to all the boards had to be as simple and easy to connect as the stack was to install. Various connectors were investigated, including one made by Harwin Interconnect. Following a discussion and meeting with representatives from Harwin it was decided that their connectors were ideally suited for use on our robot; especially since their connectors had been used in robotics applications before, including on some of NASA's robots.

3.3.1.2. Motor control boards

Disregarding servomotors, there are three different types of motors used on the robot; the drive motors (2 x RE50s), the flipper motors (2 x RE???) and the arm motors (3 x RE30s and 1 x A-max 30).

The largest of these are the two drive motors; controlling the left and the right tracks. As previously mentioned, these motors can draw over 9A when used continuously and can feasibly draw significantly more current when navigating some challenging terrain, such as steeply inclined slopes. To cope with these currents and the 24v supply used to drive the motors the Roboteq AX3500 60A dual channel motor control board was chosen. In previous years these boards had proven to be reliable and had performed well. The board also offers a wide range of user programmable settings to control every aspect of the motors performance. The board uses an RS232 interface for both re-programming the board and for sending and receiving commands.

To control the flipper motors similar requirements were needed. However, in addition to the specifications for the drive motors, the flipper motor control board needed to be able to read data from

the optical encoders on the motors. This was crucial to ensure the flippers could be driven to a desired angle. Again the AX3500 provided ample current capacity and, importantly, could also interface with the optical position encoders to allow the board to drive the motors in closed loop position mode. Table 3 shows the basic specifications of the AX3500 board.

Operating Voltage	12V to 40V DC
Number of Channels	2
Max Current per channel	-
30s	60A
1min	50A
3 min	40A
1h	40A

Table 3 - Basic AX3500 specification

The arm motors and their control are discussed in section 5.13.

3.3.1.3. Arm electronic design

To control the five degrees of freedom provided by the mechanical arm design an electronic system was required.

3.3.1.3.1. Servomotor circuit adaption

As a result of successful utilisation of Hitec HS422 servomotors in the self-stabilising gimbal, it was decided to further investigate the possibility of using a similar concept for arm control. Consequently, it was decided that the arm motors would be configured as servomotors; there are a number of advantages to this arrangement:

- Since servomotors use potentiometers as the position encoders, the position is absolute and not relative as it is with most optical encoders (as on the flipper and main track drive motors); therefore, a command for a motor to drive to an absolute position may be sent.

- Once a command is sent to the control circuitry the motor would be continuously driven until the potentiometer feeds back that the correct angle is achieved. This circumvents the problem of encoder

output division that would have to be used were the encoder attached to the motor shaft, since the gearbox on the front of the motor provides a large reduction ratio;

- The joint controlled by the servomotor setup could maintain the desired angle provided there was power to do so, meaning that, for example, if a weight was placed on the head of the arm causing it to sag, the potentiometers could detect this displacement and drive it back to its desired position;

- The internal circuitry of a servomotor may be commanded to drive a motor either in forwards or reverse direction, vitally allowing the arm joints to move in both directions.

Initial investigations were into the suitability of servo motor internal control circuitry to provide control systems. Servo motors consist of four main parts; the motor, a gearbox, a potentiometer and some simple control circuitry. The potentiometer and the control circuitry work together to provide a hardware-based PID loop. A standard analogue servo has three wires; Vcc, Gnd and Signal. The Vcc and Gnd provide power to the circuitry and also the motor. The signal wire provides the control signals from the servo control board to the internal servo circuitry. In order to command a servo to a particular angle a pulse of the corresponding width is sent. Figure 55[2] explains how the pulse widths relate to angles.

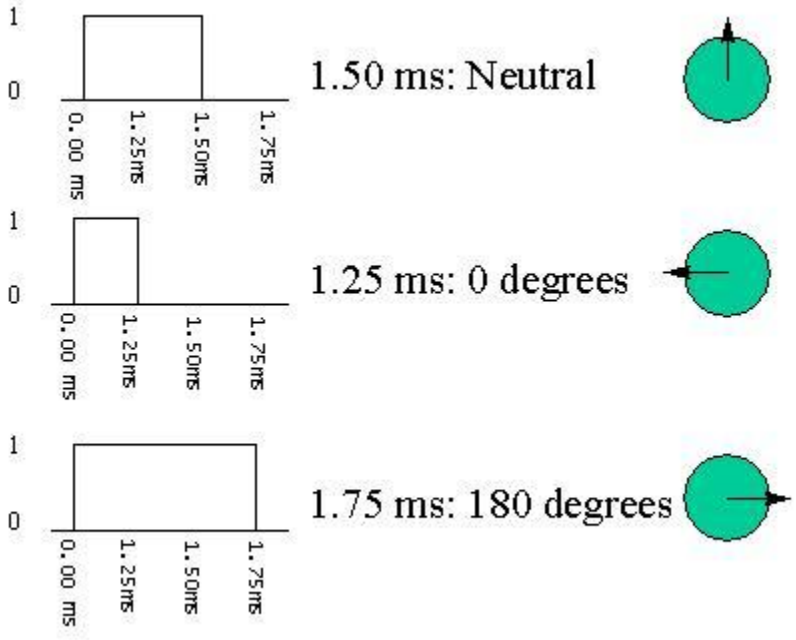

Figure 55 - How varying the pulse with width varies the angle

[2] http://www.seattlerobotics.org/guide/servos.html

Following investigations into the functionality of servomotors, it was realised that the internal servo electronics would have to be significantly adapted to cope with driving the proposed Maxon arm motors; a stall current of **3.35 amps** would have to be designed for. This is far in excess of the stall current of a standard servomotor from a Hitec HS422 servo. Power MOSFETS were proposed as a solution with a potential circuit redesign to cope with the additional current.

3.3.1.3.2. Roboteq AX500 motor control boards

At this point of the investigation however, simultaneous investigations into the previously used Roboteq AX500 motor control boards proved fruitful. Table 4 shows the basic specification of the board.

Operating Voltage	12V to 24V DC
Number of Channels	2
Max Current per channel	-
30s	15A
1min	10A
3 min	8A
1h	7.5A

Table 4 - Basic AX500 specification

It soon became clear that although a bespoke circuit based on the internal PID circuitry of a servomotor would be likely to work, Roboteq were experts in the field and could provide the team with a much more customisable solution. The communication protocol of RS232 was also of benefit since it could accept command line instructions should any of the board settings require to be changed remotely over an SSH connection. Comparing the arm motor specifications in 5.13.1 with the AX500 motor board specifications in Table 4 it is clear that the power requirements were well within the limitations of the board.

As mentioned earlier, a servomotor consists of four main components. The internal control circuitry was replaced by the AX500 and the Maxon motor and attached gearbox provided the motive power. The one remaining component was the position sensor. Due to the limited size available for position sensing, a small form factor potentiometer was required.

3.3.1.4. Harwin connectors

One of the biggest advantages of the Harwin connectors was the totally flexible configuration they offered. Their Mix-Tek range of connectors allows a designer to specify a mix of data connections, power connections and coaxial connections; ideal for developing bespoke connectors for the circuit board connections. The connectors also offer a variety of jackscrews to stop the connectors coming apart due, for example, to vibration. Harwin publish recommend maximum currents for data and power contacts (Table 5)[3].

Contact Type	Current Rating
Power	20 A
Data	3 A

Table 5 - Harwin connector ratings

Special consideration was paid to potential current loading through the connectors to ensure that none of the contacts was overloaded. The main drive motors for example are rated at 9.04A (max continuous current) so using the data connections to power them would have been dangerous. Their rating however is well within the limits of the power contacts. For this reason power contacts were used for the drive motors, flipper motors and also for the arm motors. In the case of the arm motors, they are rated at 3.44A (max continuous current) so could probably be run using data contacts since it was deemed unlikely that they would be running anywhere near their maximum current, however it was decided safer to use the power contacts than risk overloading them.

The following diagram shows how Harwin connectors were used to connect the AX3500 to the power supply and to the drive motors, Figure 56.

[3] Harwin product catalogue 10/11, p61

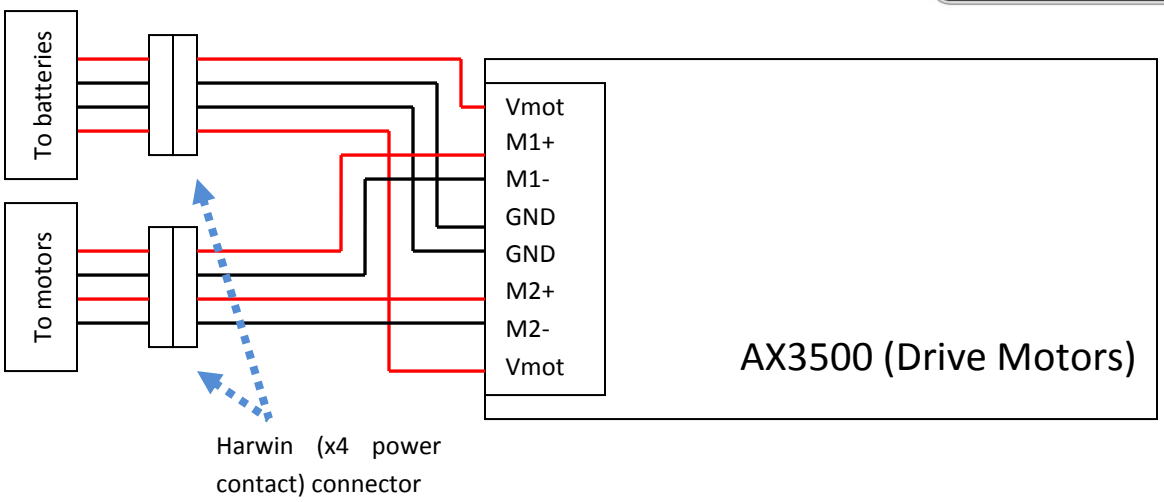

Figure 56 - Showing the location on the Harwin connectors at the rear of the AX3500

This configuration provided the motor control board with two separate 24v supplies and two ground supplies. This was done to ensure that the recommended current limit of the power contacts in the Harwin connector was not overloaded. In this case the AX3500 provides the power to two RE50 Maxon motors, each drawing 9.04A (max continuous current). This means that the potential current drawn by the AX3500 could be 18.08A, very close to the power contact current limit of 20A. Since the motors were going to be put under large loads on occasion, the potential for them to draw more than 9.04A amps each was very real and it was therefore decided that two power contacts would be used to provide power to the AX3500, as Figure 56 shows. This configuration proved very useful when re-programming the AX3500 as they could be powered up without connecting the motors, thus allowing non-moving testing to take place.

The major selling point of the Harwin Mix-Tek connectors is the ability to mix data and power contacts in the same connector. As previously discussed, the arm joints used potentiometers as position encoders. Each potentiometer has three connections; V_{batt}, Gnd and the output from the wiper. This means that each joint requires the following number of contacts, as shown in Table 6.

Device	Power contact	Data contact
Motor	2	
Potentiometer		3

Table 6 - Number of contacts

Since each AX500 can control two arm motors the number of required connections are illustrated in Table 7.

Device	Power contact	Data contact
Motor 1	2	
Potentiometer 1		3
Motor 2	2	
Potentiometer 2		1
TOTAL	***4***	***4***

Table 7 - Number of required connections

The two potentiometers share a common ground and V_{batt} meaning that the second potentiometer only needs one new connection and uses the same ground and V_{batt} as the other potentiometer.

The Harwin connectors also have an option that utilises special jackscrews that make the connectors panel mountable. The initial concept of using panel-mounting connectors was that the arm could be disconnected from the top panel without having to open up the robot. The final design of the arm meant that the arm was easiest to remove with the top panel connected. This didn't render the panel mounting connectors entirely useless however, as it enabled individual joints to be powered up using a power supply allowing the arm to be positioned without having to power up the entire robot.

The top panel mounted connectors consisted of three connectors, two for connecting the arm motors and their attached potentiometers, and one connector for connecting all the devices in the head. The large panel mounted data connector connects the following devices (Table 8).

Device	Data contact
IR cam	4
IP cam 1	2
IP cam 2	1
2 x 12v 40mm fans	2
Microphone	2
CO_2 sensor	3
LEDs	2
RX64 servo	4
TOTAL	***20***

Table 8 - Number of contacts for device

The front **basket** is also connected using a Harwin connector, connecting the following devices (Table 9).

Device	Data contact
Servo 1	3
Servo 2	3
Speaker	2
LiDAR Power	2
PC On Swtich	4
E-Stop	2
E-Stop Reset	2
TOTAL	***18***

Table 9 - Device connections

Where connections to and from the stack were required, if possible, Harwin connectors were used as a simple way of connecting multiple devices in one go. Figure 57 shows in a diagrammatic representation where the Harwin connectors were used.

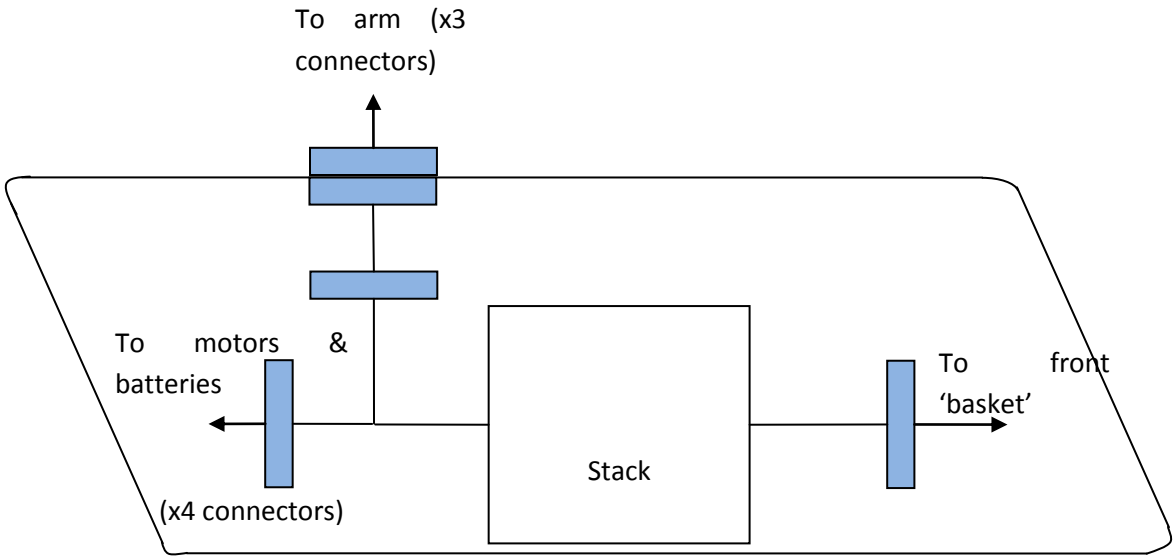

Figure 57 - Diagram of locations of Harwin connectors (blue)

3.3.1.5. Emergency stop (E-stop)

A necessary safety precaution, protecting both the robot and humans, is a method of locally stopping the robot, for example to stop an out of control robot or to avoid injury should a person find themselves in danger. The emergency stop circuit is unchanged from the previous years design and used a latched

relay to provide power to the motor control boards until the e-stop button is depressed and the circuit is broken thereby unlatching the relay and returning the robot to a 'safe' state.

The addition of an arm control using AX500 motor control boards allowed those too to be included in the e-stop circuit. Hitting the e-stop button not only immobilises the robot tracks, the flippers and arm motors are also stopped. The only joint that remains un-stopped is the pan of the head which is driven using an RX64 servomotor and is therefore on a different circuit. This was not a problem considering the limited torque the servomotor can provide. Additionally, the RX64 was set to provide only a minimal resistance torque to avoid damage should the arm or hear movement become impeded.

When the robot is first powered up by attaching a battery, the initial state of the e-stop circuit is 'safe' thus avoiding any possible mistakes of leaving the robot in a live state at the point of turning it off.

3.3.2. Autonomous robot

3.3.2.1. Higher specification computer to run the autonomous control software

Since the autonomous robot would be running the existing robot server, as well as all the software required to perform SLAM, a significantly more powerful on-board computer was chosen. Additionally, the computer was chosen to be as compatible as possible with the existing teleoperated computer. Some of the main design choices were:

- Small and lightweight.
- Combination of powerful processor and sufficient RAM to handle several running threads.
- Enough USB ports to connect all peripherals.
- No need for dedicated graphics card.
- Hard drive capacity not critical – enough space to run an operating system, and store the server code.
- Ideally, the hard drive should be solid-state, as the robot would likely suffer significant vibration during run, and may damage traditional drives.

The cost of the computer was not a prohibitive factor; it was decided that getting a powerful computer for a high price would justify itself by running the software well, and remaining useful in years to come.

3.3.2.2. Servo dropout issues

During testing of the autonomous robot, a persistent problem was noticed in that occasionally the HS422 gimbal servos would drop out unexpectedly, causing the LiDAR to fall. Looking at the datasheet for the servocontroller, a possible cause was identified. In the initial setup described above, the servos were powered off the 5V DC/DC converter. This was based on the allowable range for the servocontroller supply voltage, 4.8 – 7.2V. However, the datasheet also recommended that the value should be as high as possible to handle significant loads. Thus, a simple 6V converter was used solely to power the servos. This worked as expected, and the problem was eliminated in all future testing.

3.3.2.3. Increased space for maintenance and cooling

Last year's design of the electronics stack within the teleoperated platform caused some problems with cooling, which may have led to problems such as the weak wireless connection. Continuing with the simplistic design principle, the chassis was split up into 2 sections: the rear section containing the motor and power connections, and the front containing the PC and the peripheral components. Every effort was made to ensure that air could flow easily from the front to the back and out. Rather than create a stack of electronics, the PC was seated on the bottom of the chassis, and then the remainder of the components were bolted to the side or the lid. In this way, all the components were easily accessible during maintenance.

3.3.2.4. Final Layout

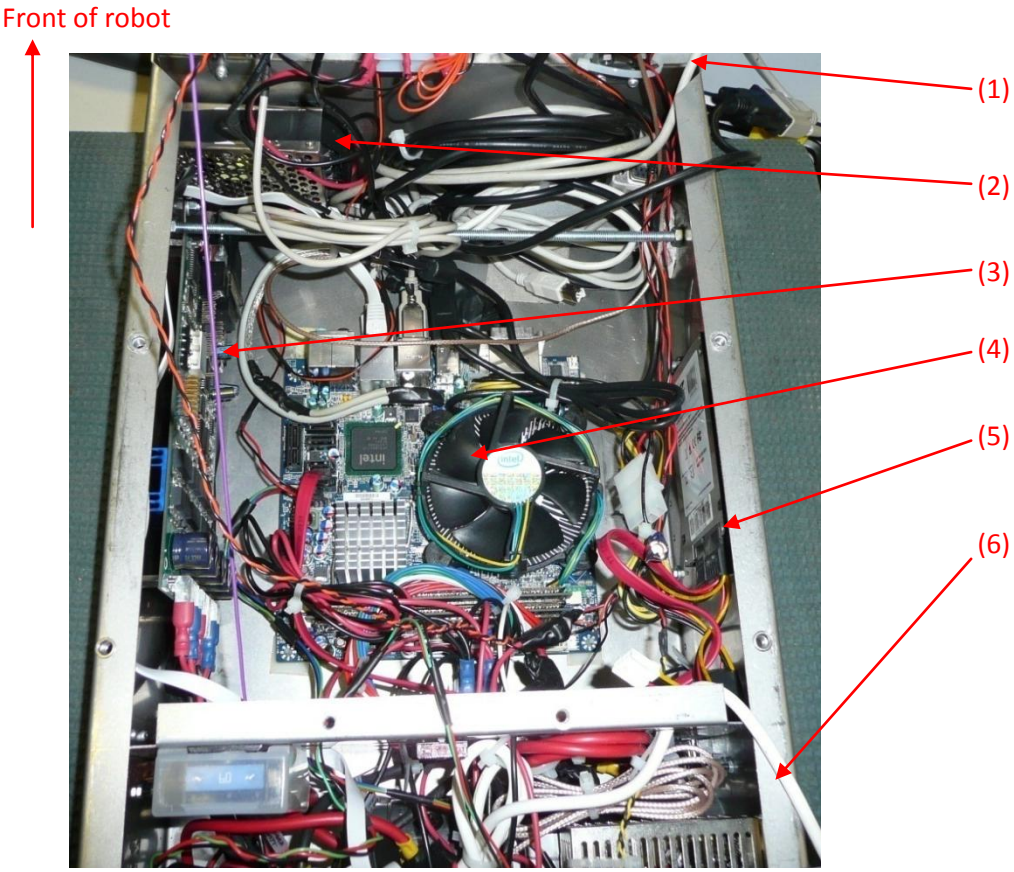

Figure 58 – Autonomous Front Interior

- Attached lid, with remainder of electronic components
- 5V DC-DC Converter, powering router, LiDAR, Phidgets Board
- Motor Control Board
- PC
- SSD Hard Drive
- Motor section, with relay system and 12V DC-DC Converter

As can be seen, all the components are arranged in the chassis such that each is accessible for modification or maintenance. Effort was made to ensure that components which connected to one another were placed in close proximity, to avoid clutter.

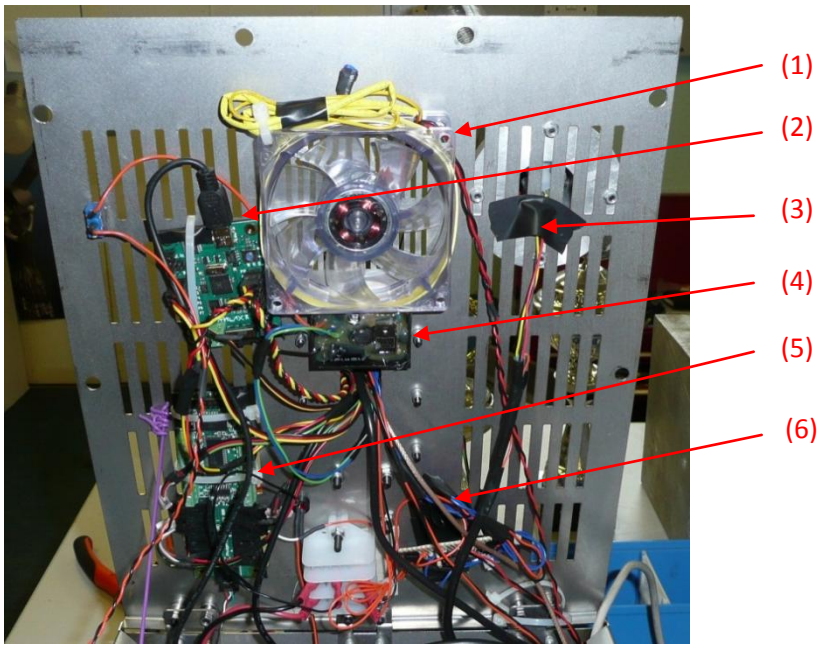

Figure 59 – Autonomous Lid-Mounted Components

- 80mm fan to create airflow from back to front.
- Parallax PropellorServoController – controls LiDAR gimbal and camera pan/tilt servos.
- Wires for compass/tilt sensor, which travel up carbon fibre tube.
- Power LED Driver.
- Phidgets Interface Kit.
- Insulated CO2 Sensor Amplifier

Figure 60 – Autonomous Electronics Diagram

3.3.3. Wireless Communication

One critical problem carried over from last year was the wireless connection between operator and robot. Although the exact cause was not known, some possible factors were identified and are discussed below along with their attempted solutions.

3.3.3.1. Routers

The existing routers were old and had been removed from their protective casing to save space and taped up with insulation tape, possibly causing overheating.

Figure 61 – Old Router

Several performance tests were done on the routers, both insulated and uninsulated, using the NetStumbler wireless network detection software. From the graph in Figure 63, it is clear that the wireless signal is quite unreliable, with many small lapses, and two large drop-outs. If connected to the robot, these outages would be enough to fully cut the connection between client and server.

The cause of this poor performance was undetermined due to further difficulties in testing (such as overheating). To eliminate the weak router performance, a new and more powerful router was purchased – the Buffalo Wireless-N Nfiniti Gigabit Router.

Figure 62 – New Router[4]

This initially was mounted on the autonomous robot to ensure no connection loss. The old router kept in the teleoperated stack was stripped of its tape, and had an external heat sink glued onto the metal plates to maximise heat dissipation. Simple testing showed a significant improvement in wireless performance.

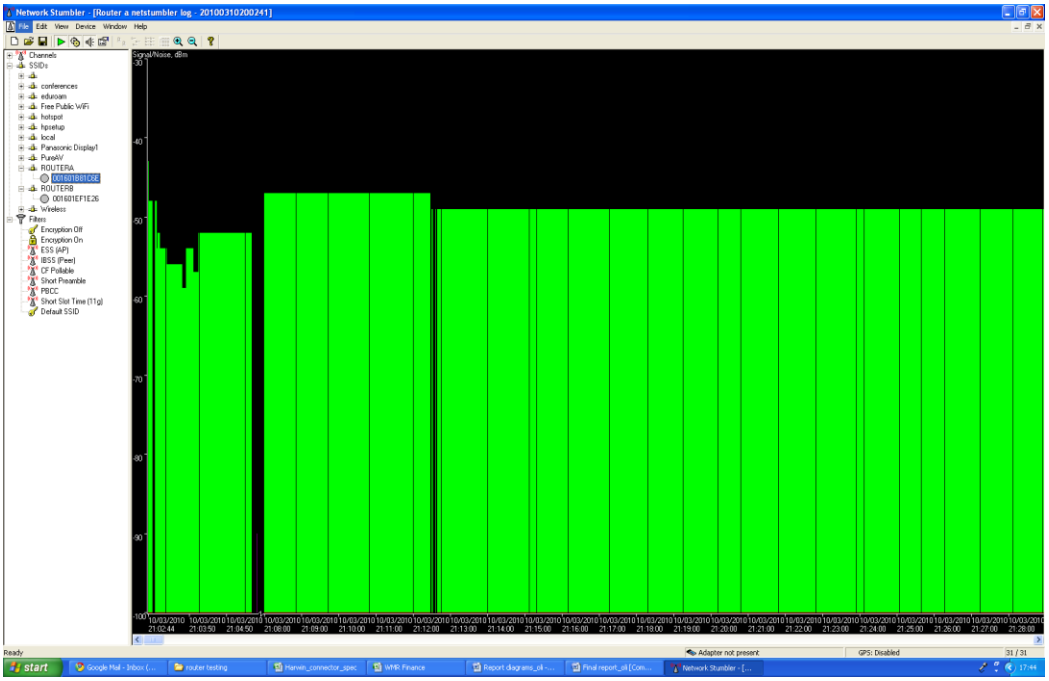

Figure 63 – NetStumbler Router Performance Graph

[4] http://www.product-reviews.net/wp-content/userimages/2008/01/buffalo-wzr2-g300n-nfiniti-router.jpg

3.3.3.2. Antennae

During the competition last year the wireless antenna was damaged and its reliability was unknown. Rather than attempt to fix it several new antennae of various sizes were purchased, as shown in Figure 64.

Figure 64 - Antennas

The connectors were Reverse SMA type, which meant they could be interchanged based on requirement. Initially it was planned to use the largest antenna mounted on the autonomous chassis. The teleoperated chassis would be equipped with the smallest antenna on the side to avoid collision with the arm.

3.3.3.3. Power

The 5V supply from the power board in the teleoperated robot was identified as problematic, possibly causing the router to drop out. Using a dedicated 5V DC-DC converter (the same Sunpower model as used in the autonomous) eliminated this problem.

3.3.3.4. Wireless Interference

A significant limitation of the wireless tests performed before the competition was that they did not accurately simulate the competition conditions, namely in terms of the wireless interference from other

traffic during competition runs. The competition rules specified that all competitors must use the 802.11a WiFi protocol, which meant that if several teams had their wireless networks running during a run, the signal could suffer drastically from interference.

This problem was difficult to solve definitively due to a lack of viable options. After some research, the most effective method of attacking this problem was to use more sophisticated channel sniffing software (such as NetStumbler, which was used previously) and focus more on choosing an empty channel, even during a run, if the signal were to suffer. It was also hoped that even if wireless interference were to occur the previous measures taken would help to limit its effects.

3.4. Tele-operation

3.4.1. New control system for ease of operation

3.4.1.1. Design for speed and manoeuvrability

It was pointed out from last year's efforts that a key aspect to focus on when modifying the control system was maximising the speed of movement and the ability to manoeuvre around obstacles. This would become more complex with the addition of a 5 DOF arm.

In the existing configuration, each track was controlled by one joystick for differential motion, and the D-pad and numbered buttons were used to control the arm joints (allowing for pan and tilt of the head). Even without testing, it was clear that although this would allow full manoeuvrability, the movement would be slow. An alternative control configuration was developed. When in this mode of control:

- The arm would be in a driving position.
- The right joystick would control both tracks.
- The D-pad would control the top two arm joints, effectively allowing the operator to look around while moving, with the D-pad.

Figure 65 – New Controller Layout

3.4.2. Modifications to GUI

3.4.2.1. CO2 Gauge

The hardware specifics of the carbon dioxide sensor are discussed further in **Error! Reference source ot found.**. The software was designed to handle the raw sensor input. The following assumptions were made:

- In ambient conditions, the sensor value would remain stable at some value between 0 and 999.
- During a run, when in the presence of an increase in ambient CO_2 the value would slowly drop.

To maximise the variation in the GUI value, the software was written as follows:

- To begin with, take 1000 values and average them, to obtain the sensor's base value (this can be recalibrated later).
- In a loop, at specified intervals (perhaps 1 or 2 seconds), take a new value, and subtract it from the base value.

In this way, even a very small change would appear clearly. For example, a change of 20 millivolts would result in the gauge increasing from 0 to 20. The nature of the sensor requirement was that it needed to detect the presence of CO_2 levels above atmospheric, with no thought to absolute values of CO_2

concentration. This simple setup in the GUI was deemed sufficient in the competition to score points for CO_2 identification.

Figure 66 – CO2 GUI

3.5. Autonomous control and Mapping

3.5.1. Objectives

The following objectives are proposed:

- Produce full SLAM; that is,create a real-time map of the robot's surroundings, with an accurate knowledge of the robot's position within the map. Further, this map should be easily accessible by the current operator via a simple interface. Finally, to meet the requirements of the RoboRescue rules, the final map should be automatically saved in the GeoTIFF format.
- Produce software capable of controlling the robot to autonomously explore and map the yellow area of a RoboCup Rescue arena. This software should, again, be easily accessible to any operator with a graphical or command-line interface.
- In the event that a choice is presented between partial achievement of both objectives 1 and 2; and complete achievement of objective 1 only; the latter would be preferred.
- The software should be both portable and scalable, i.e. it should be easy for future teams to add new hardware interfaces to it, and port the code to the teleoperated robot for mapping.
- If given time, the LiDAR data should be combined with data from front-facing sonar sensors, to increase accuracy at short distances.

3.5.2. Milestones

The following milestones are proposed:

- Investigate simultaneous localisation and mapping, particularly on RoboCup Rescue robots and using LiDAR/sonar.
- Working with the WMR team, determine the suitability of current sensors and their implementation on the robot.Create software plan to work best with existing hardware.
- Working concurrently with WMR's progress on the autonomous robot, produce the code required to perform SLAM, testable on simulated data.
- Implement software on the robot, interface with the required sensors and the motor controller. Preliminary testing of SLAM code.
- Interface the mapping software with the current operator control software, such that the operator control software may access the most recent map; or design a sensible interface from which the operator could access the information.
- Final testing of software on robot, using practice yellow arena.

3.5.3. Deliverable

The computer science team will be expected to deliver software to achieve the objectives laid out above. The robot should be able to perform SLAM without human intervention, and be able to navigate autonomously within the yellow arena. From the point of view of WMR, there will be hardware requirements and milestones to be met so that the computer science team can meet their objectives.

3.5.3.1. Hardware Specification

The current hardware may be changed if required later; the setup agreed with the members of the computer science team is:

Component	Detailed Description
Computer	Intel Core 2 Duo Mobile T5600 (1.8GHz) 2 GB of RAM 16GB Solid State hard drive
Operating System	Ubuntu v9.10
LiDAR	Hokuyo URG-04LX
Sonar	MaxSonar EZ3
Tilt Sensor	OceanServer OS5000 Digital Compass
Compass	Same as above
Router	Buffalo Wireless Nfiniti Dual-Band

Table 10 – Autonomous Hardware Specification

The robot itself will be designed as much as possible to meet the requirements of the computer science team. Some general goals, which have been discussed above, are:

- Solid design, which can easily accommodate all the hardware, in whatever configuration is deemed most suitable for SLAM.
- Differential drive system, with speed control and position control available for the tracks.
- Enough battery life to allow a full run (at least 20 minutes).

3.5.4. SLAM mapping using LiDAR

The SLAM algorithm combines the processes of creating a map of an unknown environment and localising the entity within it. The SLAM algorithm combines these two processes in an iterative loop.

Initially, the robot is supplied with an image of the environment from the LiDAR data. This is then used as an estimate of the environment. It then extracts the features such as walls and obstacles and uses them to determine its position in the environment.

The end result is a generated hypothesis which outlines which features it has seen before and which ones are new. Walls that have been seen before have estimates of where they were thought to have been. Using the fact that they have just been seen again, the estimate of their position can then be improved upon. This process goes through an Extended Kalman Filter (EKF) which minimizes the errors from all the sensor data consisting of the motors, compass, LiDAR and sonar data. The EKF converges the mean errors in the state estimation creating a new estimate of the positional data.

The improved accuracy data from the LiDAR data of the walls is then added to the occupancy map which is a representation of the local environment. Using this map and the position of the robot, the software then searches for possible paths which are on the threshold of the newly seen walls and the already seen features in order to verify the new positional data. When these points are determined the software then implements a route planning algorithm which navigates the robot to one of these locations where it will then repeat the process in order to scan new areas.

3.5.5. Gimbal and tilt sensor array for smooth LiDAR/Camera data

A major problem with the LiDAR scanning and mapping is that it presumes the LiDAR is horizontal. This is clearly not the case in real-world scenarios, nor in the arena where there are slopes placed throughout. If the robot was on a slope, the LiDAR would be either pointing at the ground or over the walls of the arena. In either case this would cause a problem and would likely disrupt the entire mapping process.

To counteract this the LiDAR was fitted onto a dual-servo gimbal. The pitch and roll of the gimbal was controlled by the OS5000 tilt sensor, effectively stabilising the LiDAR.

Figure 67 – LiDAR gimbal (Active robots)

The HS422 servos were controlled with a simple controller (Parallax USB Servo Controller) which provided more than enough connections. This was powered by USB, and required an additional 4.8-7.2V supply for the servomotors, which was taken from the SunPower 5V converter.

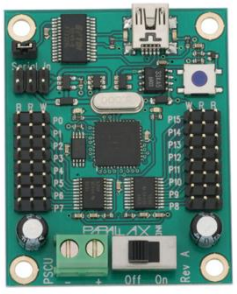

Figure 68 - Servocontroller

In the software, every reading from the tilt sensor was applied to the appropriate servo in a perpetual loop. Given the mechanical constraints of

the gimbal, the angle limits were set at -45° and +45°. The degree reading from the tilt sensor was converted in the code to correspond to the correct pulse-width-modulated signal to the servo controller.

Angle (°)	Pulse Width (µs)
-45	550
0	750
45	950

Table 11 - Gimbal Angle/PWM Conversion

$$1° = \frac{200}{45} = 4.44$$

Equation 1 – Gimbal Angle/PWM Conversion

This conversion factor was simple to implement and it was possible to adjust this value once testing had begun. For example, by using a moving average of the tilt data, the gimbal movement can be damped, if it is found that the LiDAR is suffering from vibration effects.

3.5.6. Autonomous victim identification

The autonomous victim identification software works on a voting system which is compiled of the various different sensors used by the robot. Each individual sensor runs a series of tests on a potential victim site and calculates the probability of it containing a victim by comparing it to an array of test images or by meeting some other coded parameter. All the individual systems then submit their value for the site and, if the total is above a certain threshold, the site is marked as a victim and a marker is placed on the map. The robot will then navigate away from this area in search of new victims.

3.5.6.1. Shape and edge detection

One of the main forms of victim identification is face and edge detection utilised on the visual spectrum web-camera. This software works by detecting sharp changes in the contrast of the image which might represent the edges of a shape. These edges are then compared with a library of test images which consist of various different orientations of recognised shapes. In the competition all the victims in the autonomous arena will be located inside boxes with circular viewing holes. It is very important therefore to have an array of ellipses in the database as the robot will most likely be viewing these circular holes

from an angle making them appear as ellipses. The software works in such a way that if the image edge features match any of the images in the database then the software will flag it as a recognised shape and take appropriate actions. In the case of a potential ellipse it compares the colours on the inside of the ellipse to those on the outside and if the inside is significantly darker i.e. a hole, then it votes that this could be the location of a victim and tells the robot to navigate towards it. Once at a certain distance from the hole, the robot will then perform face recognition using edge detection and compare this with test images from its database. The information on the victim card is easier to read as it takes the form of various different black symbols on a white background which have straight edges. These shapes are easily matched to a database of test images and are used alongside the face recognition software in the voting system for the victim identification process.

Figure 69 – Face and text recognition

The accuracy of this method depends largely on the size of the test database and becomes increasingly more diverse when more images are added. In this project thousands of test images for faces, ellipses, victim cards and warning signs are included in the database. Additional features of this software include a library of objects that are similar in shape to these objects. These test images are used as a way of discounting objects which may otherwise be mistaken for useful objects increasing the accuracy of the software.

3.5.6.2. Infra red blob detection

The infra-red blob detection software uses a scan line algorithm in conjunction with the Infra-red camera. The algorithm separates the image from the IR camera by placing a temperature threshold on

each pixel and displays 'hot' or 'cold' in either white or black respectively. For each frame the algorithm goes through each pixel and assigns it black or white, transforming the picture into a binary image. The software then scans through this binary image and discounts all the black pixels. When it comes across a white pixel it stops and searches the surrounding pixels to find new white ones. As new white pixels are found their surrounding pixels are then searched, eventually propagating into a blob. Once no new white pixels are discovered, the program then continues its search for new white pixels from where it last stopped ignoring the pixels which it has already found. When it then encounters the next new white pixel it repeats creating new blobs. Each blob is classified as a collection of white pixels with size and position data. If any blobs fall into a certain parameter then they are targeted to be potential victims and their positional data is relayed to the navigation system as an angle relative to the current bearing. The robot then uses a path planning algorithm to plot a path to this location.

3.5.6.3. CO2 intensity test

The CO2 sensor will operate differently than some of the other sensors. The nature of the reaction that takes place is very slow. Preliminary testing of the sensor (by breathing on it, for example) showed a sharp increase in the output voltage, and then a very gradual drop back to its base value. Thus, it will not be possible to take a 'snapshot' reading of a victim, as with the cameras. Instead, the best way to operate it would be to leave it running throughout the run, and take its value when the robot is attempting to identify a victim.

3.6. Sensors

3.6.1. Web cameras

Both robots use visual spectrum web cameras as a primary means of victim identification and in the case of the tele-operated robot navigation. The autonomous robot uses a *Logitech Quickcam 5000* web camera for its victim identification as this type has the required resolution and is compatible with the vision software. The tele-operated robot uses 2 web-cameras for navigation and victim identification. An Axis 207 web- camera is located in the front of the head in an optimal driving position and another Axis 206 is tilted downwards on the back of the head for backwards navigation and a good view of the robot body in tight spots.

Product Selection Guide						
Model	Connection			Max resolution	Max frame rate	Light sensitivity range
AXIS 206	Network 10/100	Camera	Ethernet	640x480 pixels	30 fps	4-10 000 lux
AXIS 207	Network 10/100	Camera	Ethernet	640x480 pixels	30 fps	1-10 000 lux

Table 12 - Camera Specification

As can be seen from Table 12 the two cameras are nearly identical. The only advantage of the AXIS 207 is that it can be set to a range of different resolutions which is preferable for data compression. This is a very important factor as the data compression vastly affects the amount of data being transmitted back to the client and therefore the lag in the camera feedback.

Resolution	JPEG compression level			
	Low	Medium	High	Very high
1280x1024	130	66	44	34
1280x960	117	60	36	30
1280x720	93	47	28	24
640x480	55	35	20	16
320x240	18	12	8	5

Table 13 - Camera Compression Rates

From Table 13 it can clearly be seen that a higher compression level results in a significantly smaller package sent back to the client.

Two visible spectrum cameras were used on the robot, one forward facing and the other facing the rear. These were designed to be the main driving aids and were fitted with wide angle lenses to further improve the vision whilst driving. The improvement in field of view (FOV) was drastic and can be seen at Figure 70.

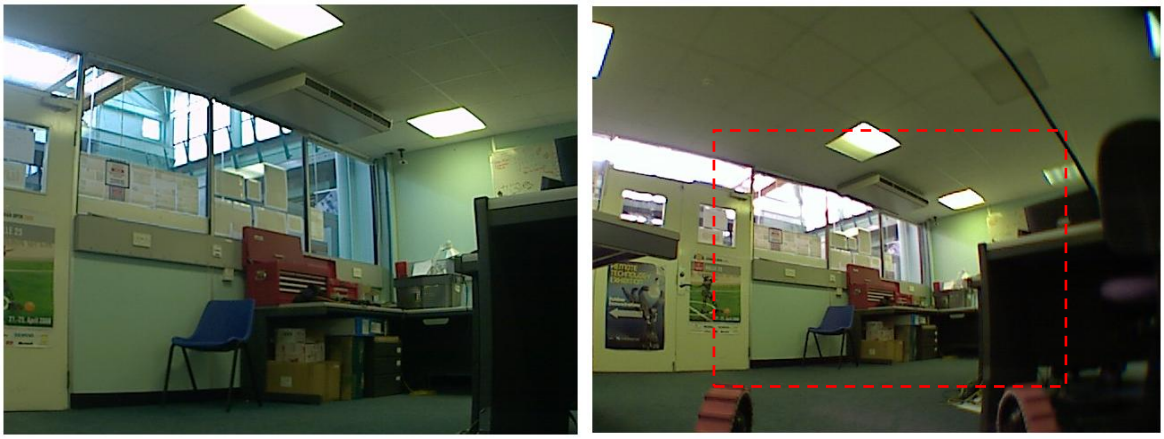

Figure 70 - Views from the IP cameras before the wide angle lenses (left) and after (right). The annotation shows the original FOV.

Both cameras are IP based network cameras that connect directly to the router using Ethernet patch cables and took their power from the power board. One the top panel at the base of the arm two panel mounted couplers transferred the signals from the patch cable connected to the camera to another plugged directly into the router.

Since the IP cameras act as a server and are assigned their own IP addresses by the router, accessing the images broadcast by them is easy and simply a case of typing the relevant IP address into a web browser and the moving image is then served to the client. Figure 71 shows a picture of an Axis 207 IP camera in its complete state. For use on the robot the two cameras (one axis 207 and one axis 206) were stripped down to reduce weight and save space.

Figure 71 - An axis 207 IP camera in its pre-stripped state[5]

3.6.2. Infra-red camera

Infra-red cameras detect areas of heat and display them in the visible spectrum using representative colours for the thermal range. They can also be used to create a binary image using a threshold heat value which translates it into black and white for blob detection.

The IR cameras used in both the tele-operated and autonomous robots are from the same manufacturer, with two different versions: a FLIR Photon 80 and 160, the only difference being their resolutions.

Model	Resolution	Spectral range	Thermal sensitivity
Photon 80	80x60	7.5 - 13.5 µm	<85mK
Photon 160	160x120	7.5 - 13.5 µm	<85mK

Table 14 - IR Camera Specification

The FLIR Photon 80 core was once again chosen as a highly capable thermal imaging unit. The camera has a RS232 interface to allow on board settings such as hue, rotation, colour output to be adjusted but uses a standard composite output for video. The composite output from the IR camera was fed into a USB TV capture card with a composite input. Individual frames from the camera could then be captured as required. Figure 72 shows an example of an image captured using the IR camera.

[5] http://www.net-shop.co.uk/CategoryImages\AXIS207l.jpg

Figure 72 - An image captured using the on-board IR camera

3.6.2.1. TV Capture Card

Last year's team used a Hauppauge USB-Live 2 Capture Card to transfer the analogue video from the IR camera to the PC. A small server was written in C to run in the background and grab frames from the capture card. The Java robot software would connect as a client to the capture program to load IR frames into the GUI for blob detection.

Due to hardware constraints this year, a different approach was taken. The capture software would only work with an identical capture card, which was no longer being manufactured. The only capture card found that was compatible with Ubuntu (a Linux based OS) and had the required interface with the IR camera was an EasyCap DC60 card. After attempting various configurations and techniques for grabbing data, the one settled on proceeded as follows:

- Using the MPlayer application for Ubuntu, a command-line script was written to grab several frames from the camera.
- The images were saved onto the computer in a known folder.

- During a competition run, the operator would have command-line control of the robot's computer via Putty and WinSCP.
- When a victim was visually identified an IR capture was performed by running the MPlayer script.
- The saved frames could then be opened remotely using WinSCP which would show an IR image of where the camera was pointing.

An unintended benefit of this method is that the required network bandwidth would be reduced since streaming IR feed would be unnecessary.

3.6.3. Phidgets Interface Kit

The Phidgets board was used to interface with a range of sensors. Not only could it connect proprietary Phidgets sensors (such as the sonar), but any sensor with an analogue output between 0 and 5 volts. The board chosen had 8 analogue inputs, which was deemed more than enough to satisfy the sensor requirements for each robot.

An additional benefit was that the kit was setup to be easily programmed in a range of languages (including Java) using a free set of libraries. With this, the software interface to the sensors was easy.

3.6.4. CO2 sensors

CO_2 sensors are used to measure the CO_2 concentration in the air. As the concentration rises the output voltage changes in proportion with the rise, producing varying voltage levels for different concentrations and thus a measurement of the ambient concentration.

When the sensor is exposed to CO2 an electrode reaction occurs：

Cathodic reaction：

$$2\mathrm{Li}^{+} + \mathrm{CO2} + \frac{1}{2}\mathrm{O}_2 + 2\mathrm{e}^{-} = \mathrm{Li}_2\mathrm{CO}_3$$

Anodic reaction：

$$2\mathrm{Na} + + \frac{1}{2}\mathrm{O}_2 + 2\mathrm{e}^{-} = \mathrm{Na2O}$$

Overall chemical reaction :

$$Li_2CO_3 + 2Na + = Na_2O + 2Li^+ + CO_2$$

This reaction produces an electromotive force (EMF) from the electrodes which is in compliance with the Nernst's equation:

$$EMF = Ec - (R \times T) / (2F) \ln (P(CO_2))$$

Where: $P(CO_2)$ $=CO_2$ partial Pressure, E_c = Constant Volume, R = Gas Constant volume, T^- = Absolute Temperature (K) and F = Faraday constant.

Below is a circuit diagram of the CO_2 sensor:

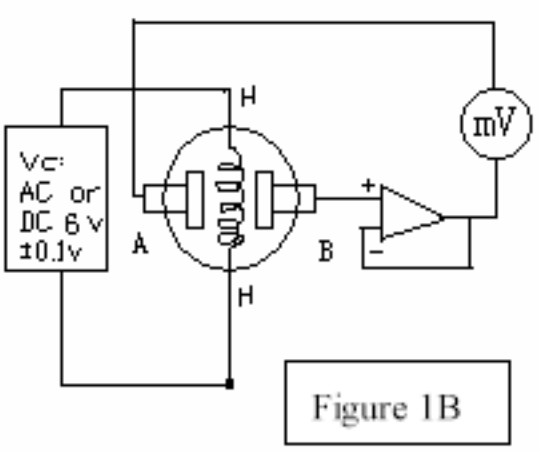

Figure 73 – CO_2 sensor circuitry

The variation in the CO_2 sensor with concentration changes (e.g. breathing on the sensor) was observed to be in the millivolt range, unsuitable for integration with the ADC kit (the Phidgets interface kit). Thus, the sensor output was amplied using a simple amplifier circuit. An LM324 was selected since it can operate on a single rail supply and the gain resistors were placed in a simple non-inverting circuit. The circuit shown in **Error! Reference source not found.** was taken from another project, which used the ame sensor. The circuit was modified slightly, then laid out on a PCB using the Altium DXP layout software.

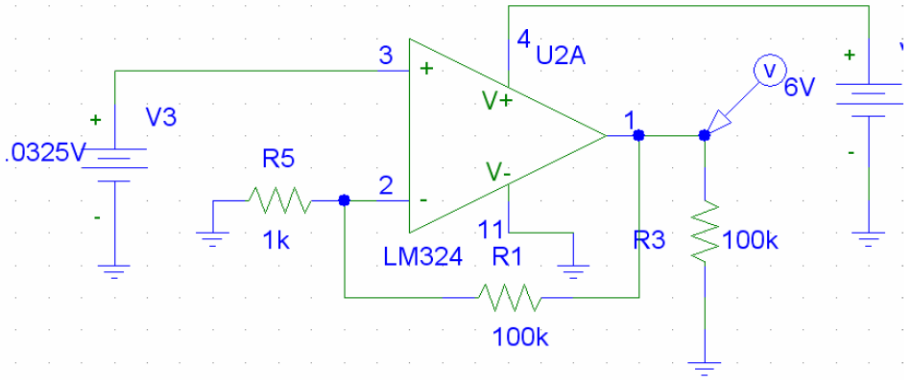

Figure 74 – CO_2 sensor amplifier

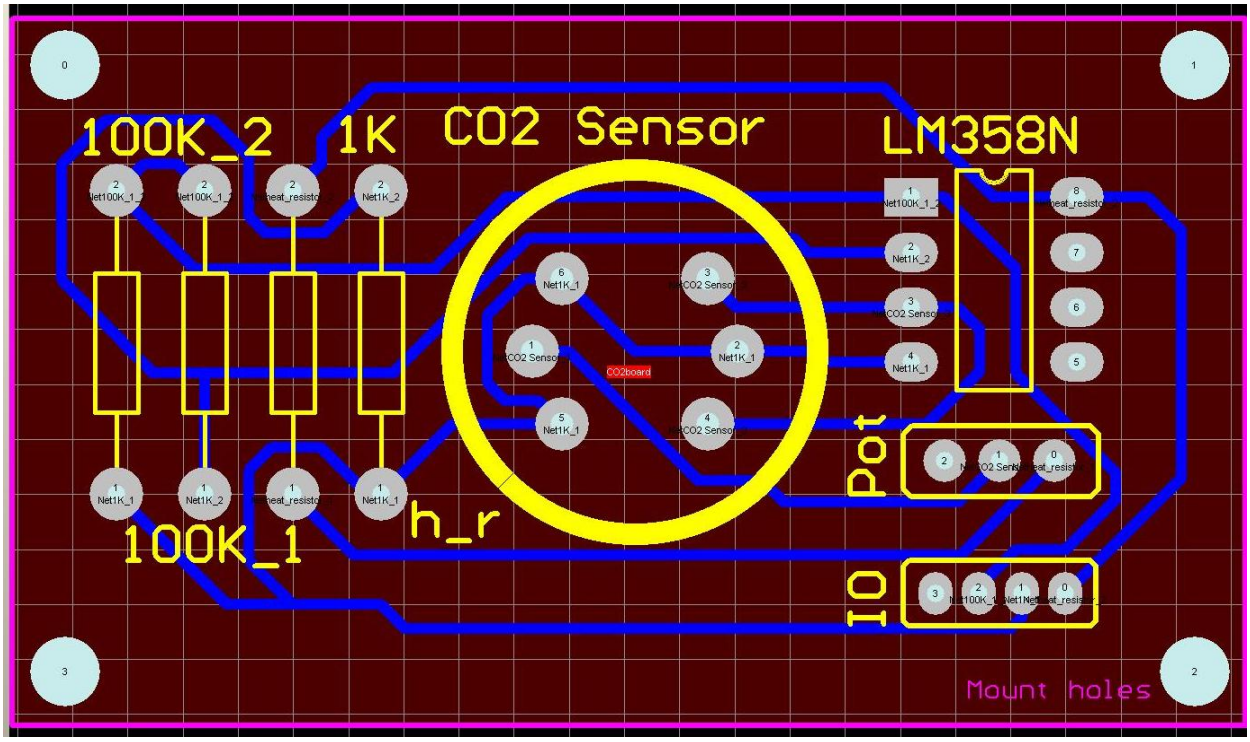

Figure 75 – CO_2 sensor amplifier PCB

It was decided to power the LM358 op-amp using a 12V supply. Since the CO_2 heater required 6V, a potentiometer and a heating resistor were placed in between the positive supply and the sensor. The resistance across the heater was measured at 30Ω, and, using the potential divider formula, a value for the potentiometer could be obtained:

$$V_{out} = \frac{R_2}{R_1 + R_2} V_{CC}$$

$$R_1 = 30\Omega$$

Equation 2

The potentiometer (Bourns 3296) had a maximum power rating of 0.5W. Assuming this was placed in the circuit:

$$I_{heat} = \frac{V}{R_{heat}} = \frac{12}{30} = 0.2A$$

Equation 3

$$Power\ dissipated\ by\ potentiometer\ P = I_{heat}^2 R = 1.2W$$

Equation 4

This was more than double the rated power dissipation – to fix this, the resistance was split between the potentiometer and a fixed 15Ω resistor (labelled h_r on the PCB diagram).

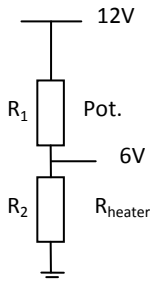

Figure 76 – Potential divider

3.6.5. Sonar

The Phidgets Sonar (Figure 77) Sensor was specified to detect objects in a range from 0 to 0.5m, with a 20mm resolution. This range actually exceeded that of the LiDAR, so it was thought that they would be useful to mount on the autonomous robot, and use both methods of ranging for higher accuracy and reliability.

Figure 77- Phidget sonar

To interface the sonar data with the PC, an analogue-to-digital converter was required. One of the reasons this particular sensor was purchased was the fact that it could be used with the Phidgets Interface Kit that was already working with the CO_2 sensor. The raw value read from the kit (an integer between 0 and 999, representing 0 and 5 volts), had to be converted to cm, using Equation 5.

$$Dicstance\ (cm) = SonarValue \times 1.29\mathbf{6}$$

Equation 5

In addition to providing ranging data for mapping, the sensor also was very useful for simple proximity detection in drop sensing. In this situation, a sensor would be mounted on the front of the robot pointing downwards. If the robot were to drive over a significant drop the sensor value would change instantly and the robot could be stopped to prevent fall damage.

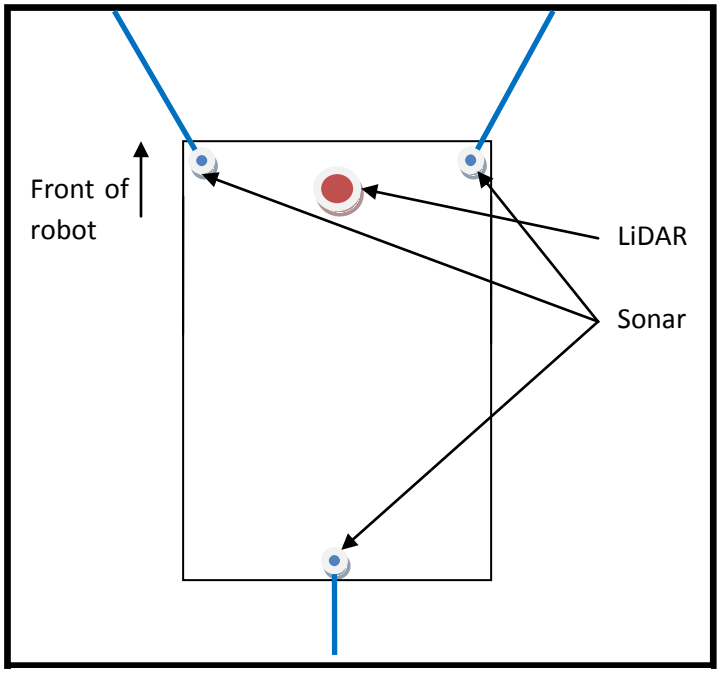

Figure 78 – Sonar and LiDAR configuration

3.6.6. Two way communication

Being able to verbally communicate with the victims provides more points in the competition for identifying their state. With the installation of a microphone and speaker onto the tele-operated robot the aim was run a two-way communications system across the network.

There are many commercially available pieces of software for two way communications over the internet (e.g. Skype). These however cannot be used in our situation as there is no internet connection available. The software must work over a Local Area Network (LAN) and also between the Linux operating system of the robot and the Windows operating system of the controller laptop. There must also be the ability to control the software on the robot computer using the command line.

There was not enough time before the competition to develop such a system. During the competition some trials were carried out to attempt to set-up two way communications but with limited success. Programmes such as Ekiga and Asterix showed some promise as possible solutions. It is recommended that further work be carried out next year to solve this problem.

3.6.7. LiDAR

To allow both the autonomous and the tele-operated platforms to map their environments a small Light Detection And Ranging (LiDAR) laser scanner was used. The concept of the LiDAR is relatively simple; a laser is fired out at a known angle and the time taken for it to return having reflected off an object is measured. Using simple speed, distance, time calculations the distance of the reflecting object from the LiDAR can be given. The process in then repeated through the entire 240° so that a 2D scan can be produced. Figure 79 shows an image of the Hokuyo URG-04LX that was used on both robots.

Figure 79- The laser scanner that was used on both the autnomous and tele-operated platforms

3.6.8. Head LEDs

To ensure that the robot's cameras could see under low or zero light conditions, illumination had to be provided. A simple yet highly effective solution was found in a pair of ultra bright LEDs; Luxeon 1W Star. These ultra bright LEDs have a small aluminium heat sink attached to them to avoid overheating. In order that these LEDs could be driven correctly a power LED driver circuit was used. The input to the driver circuit was connected to a socket on the power board that could be remotely cycled, thus allowing the LEDs to be turned on and off remotely.

3.6.9. Microphone

A very simple Electret microphone was placed in the head to allow noises and sounds emitted by the victim to be detected. Experiments proved that the microphone could simply be wired into the auxiliary input to the motherboard and in such a configuration would provide adequate sound quality to be able to recognise voices and distinguish between sounds.

4. Robot Head

As part of the aims and objectives for the 2009/10 tele-operated robot it was decided that the robot head would undergo major modifications for improved sensory feedback. As in previous years a network axis and infrared (IR) camera would be used for navigation and identifying heat sources, respectively. This academic year, the addition of a rear-facing network axis camera, microphone, CO2 sensor, servomotor for pan and LED's required a complete re-design of the head. As with many designs of the 2009/10 tele-operated robot, the ease of manufacture with laser cutting sheet steel would be taken advantage of for the head design. The biggest challenge was to position all the components in such a way that no sensors would protrude below the base of the servo motor and the design was as compact as possible. An image of the final head design is shown in Figure 80.

Figure 80 - Final head design

The proposed design was aimed at solving some of the major problems faced with last year's head design and was mainly to do with accessibility. Considering each sensory component has multiple wires going to it, it is important to include enough room for these. Modifications to Ethernet cables and connectors for downsizing often make these unreliable. We also wanted a modular design which was visually appealing and made access to components easy. This was achieved by attaching all the sensory components to the servomotor, which was then attached to the robot arm and front plate. This meant the head cover could be detached from the front plate independently, resulting in open access to all components, as shown in Figure 81.

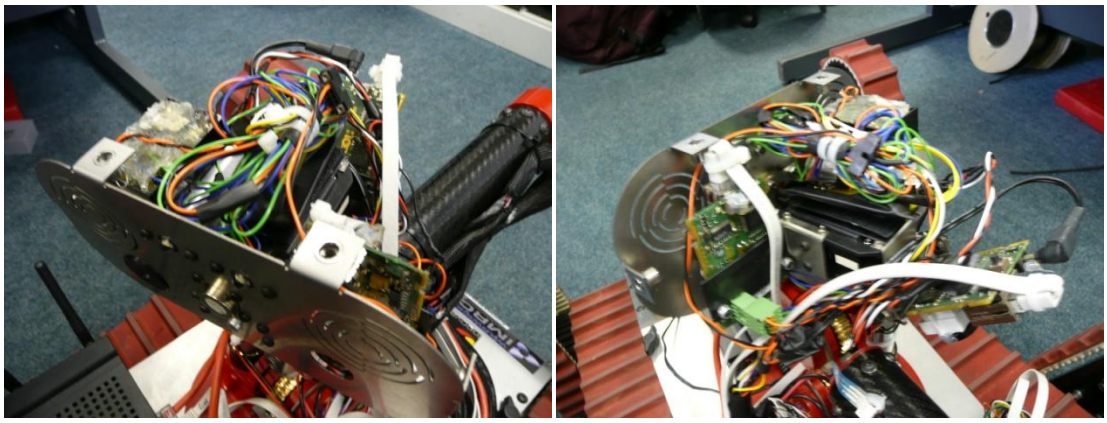

Figure 81 - Head without cover

The head was entirely designed in SolidWorks including all modeled components for ensuring correct geometries, as shown in Figure 82.

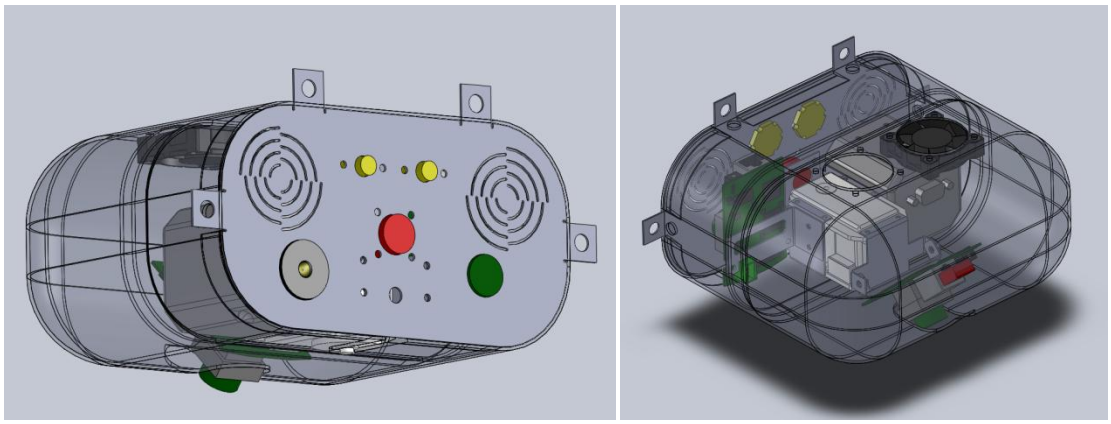

Figure 82 - CAD model of head design

The front head plate and sensory component attachments were manufactured using laser cutting of 0.9mm thick sheet steel and manually bent. This had the advantage of being able to detach components

separately if needed. The inclusion of a rear camera meant a swivel mechanism would have to be designed to allow the viewing angle to be changed. This is because the entire head is tilted forwards by an angle of approximately 30 degrees in the driving position, meaning the rear camera would be looking upwards if it was mounted vertically. This simple mechanical swivel mechanism is shown in Figure 83 and is easily adjustable by two screws on either side.

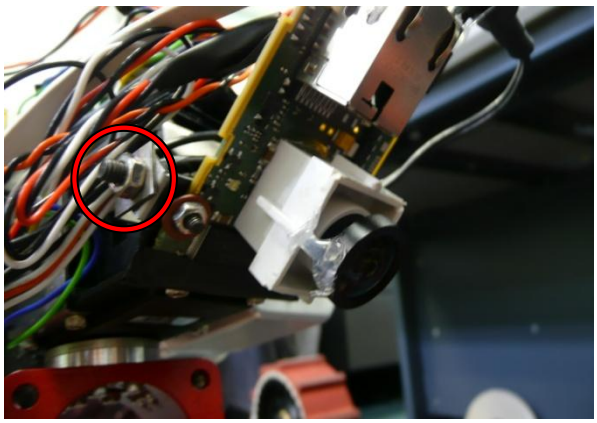

Figure 83 - Rear camera swivel mechanism (circled)

A cut-out has been designed into the head cover to allow for the rear camera tilting motion, as shown in Figure 84.

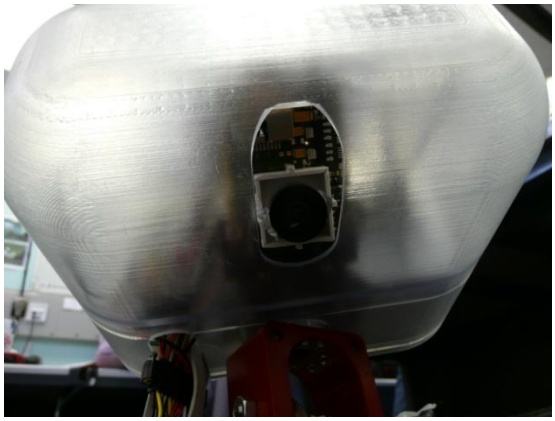

Figure 84 - Rear camera head cover cut-out

Two more cut outs have been included in the head cover to allow it to be detached from the arm. One cut-out is for the servomotor to arm connection and the other is for the electronic connections, as shown in Figure 85.

Figure 85 - Servo motor and electronic wires head cover cut-outs

The use of Harwin connectors for all components in the head meant these could be detached from the arm in an instant, as shown in Figure 86. Making all the Harwin connectors for these was initially time consuming however saved a lot of time and effort when connecting and disconnecting components at the competition. It is important to ensure all exposed circuit boards and metal parts are well insulated to avoid shorting out of components. This was done using insulating tape.

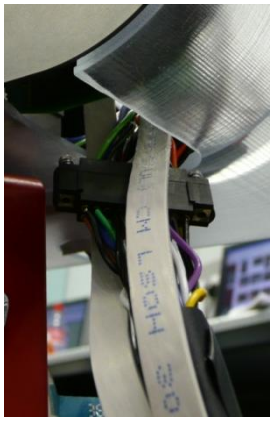

Figure 86 - Main head Harwin connector

A separate connector was made for the fans in the head cover, considering the head cover would be frequently removed and was independent to all other components. The fans in the head were necessary to provide sufficient cooling and were sucking air into the head to create positive pressure and keep out any dust. The fan connector and fans are shown in Figure 87.

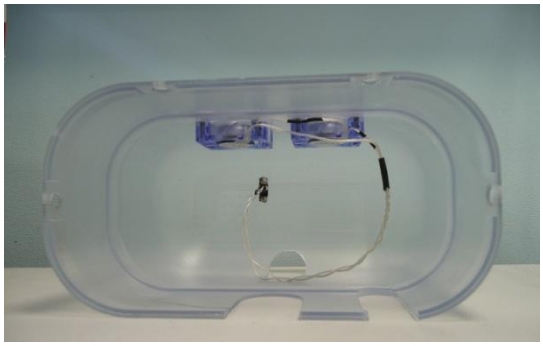

Figure 87 - Fan connector and fans

The head cover itself was designed in CAD and manufactured using the stereolithography rapid prototyping method. The CAD drawing and actual head cover are shown in Figure 88 for comparison. The final head cover design had to be slightly modified using a *Dremel* hand drill to create a new notch for the cables, as seen in Figure 88. It was previously anticipated that the cables could fit in the servomotor notch, however when tested these often hindered the head's tilt motion.

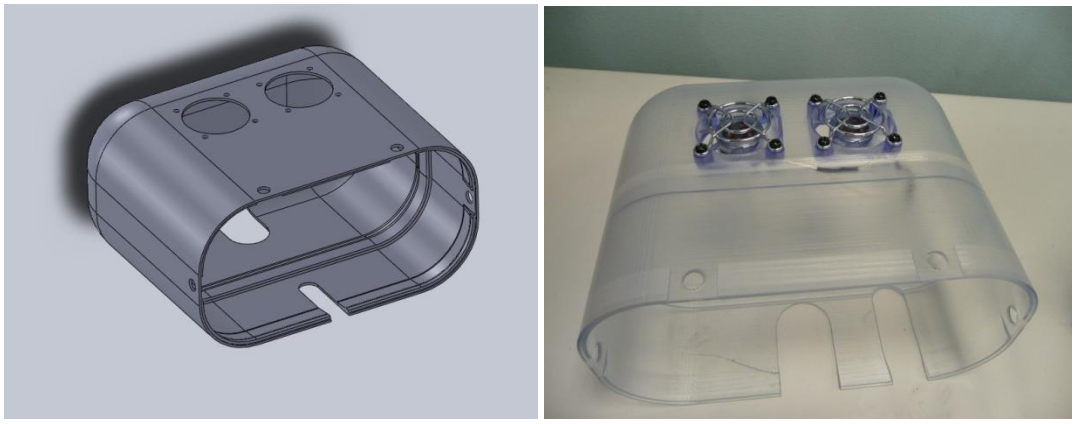

Figure 88 - CAD model and actual image of head cover with fans and finger guards

This method of manufacture, also known as *3D printing*, is ideal for such complex geometries. There is no material wastage in the manufacturing process, the finished product is lightweight, serves its purpose of protecting the sensory components and is visually appealing. The high precision laser used in the process has a resolution of 0.1mm and components such as the head cover can be produced within 12 hours, including curing time in the oven.

Stereolithography is an additive manufacturing technology and is based on the principle of curing a liquid photopolymer into a specific shape (Kalpakjian & Schmid 2006). A platform which can be lowered

and raised is contained within a vat which is filled with a photocurable liquid-acrylate polymer, as illustrated in Figure 89. As described by Kalpakjian & Schmid (2006), at its highest position (depth *a* in Figure 89), a shallow layer of liquid exists above the platform. A laser generating an ultraviolet (UV) beam is focused on a specific surface area of the photopolymer and moved in the *x-y* plane. The beam cures the portion of the photopolymer making it a solid body. The platform is then lowered sufficiently to allow the cured portion of the polymer to be covered with another layer of liquid polymer, and the sequence is repeated. After the build stage is complete parts are immersed in a chemical bath to remove any excess resin and cured in a UV-oven. The part has been set up in the stereolithography machine so there is no need for support structures.

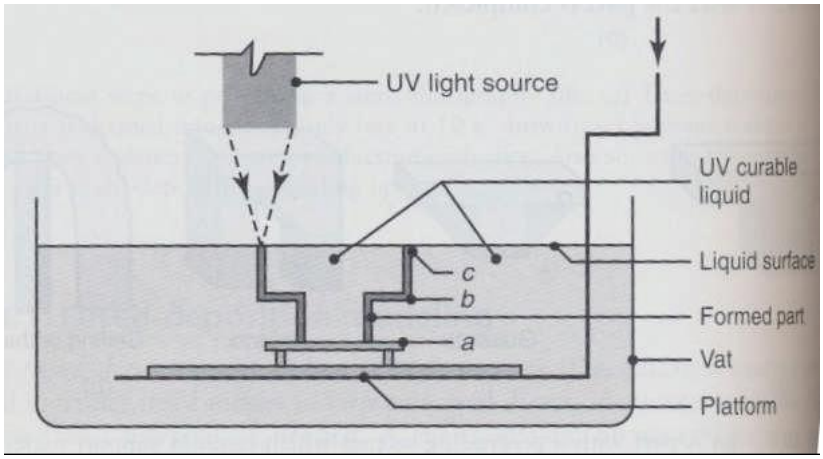

Figure 89 - Illustration of the stereolithography process (Kalpakjian & Schmid 2006)

A low shutter speed image of the laser curing the photopolymer is shown in Figure 90. The facility for stereolithography is readily available at the *Rapid Prototyping and Tooling* centre of the WMG.

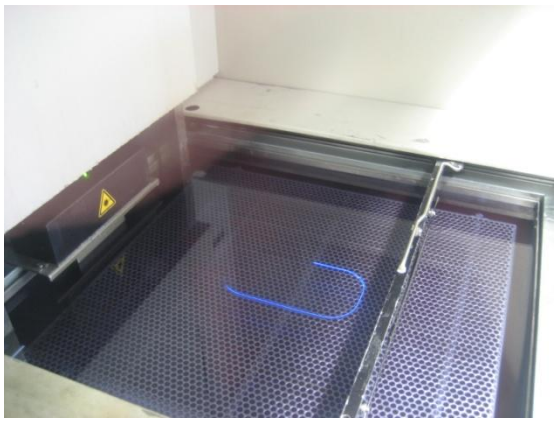

Figure 90 - UV laser curing photopolymer

A chamfer has been included in the head cover design for structural rigidity and is shown in Figure 91. Notches for the head cover to face plate connection and a lip for the front plate to sit in have also been included in the head cover design for easier alignment. This is shown in Figure 91.

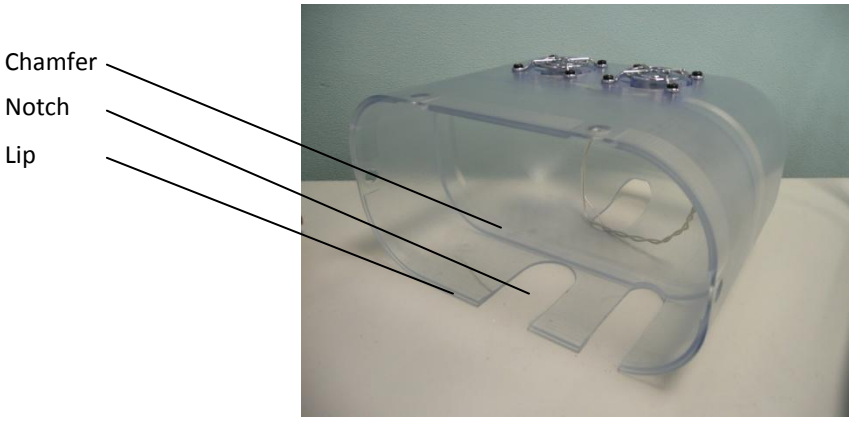

Figure 91 - Chamfer and notches in head cover design

The servomotor (RX-64 Dynamixel) can be detached from the robot arm, hence detaching the entire head. This is achievable using one screw and makes removing the head from the robot arm easy. This is useful when testing and transporting the arm.

As already mentioned it was important to ensure all components were positioned so that none would protrude below the base of the servomotor. This is so when the head is tilted by the robot arm third joint, any collisions between the head and arm are avoided. Limits have been set on the third joint and servomotor to ensure there is enough slack in the wire connections. The head design proved its functionality and modularity at the competition where access to components was quick, the entire head could be detached within seconds and components were protected during collisions.

5. Robot Arm

5.1. Tele-operated Arm

A highly dexterous arm is an essential component for a successful teleoperated rescue robot. The arm controls the position and orientation of the head and the manipulator. The robot head and the simple manipulator can be seen in Figure 92. The head encases the cameras and sensors for the robot. These are used for driving the robot remotely and for identifying victims.

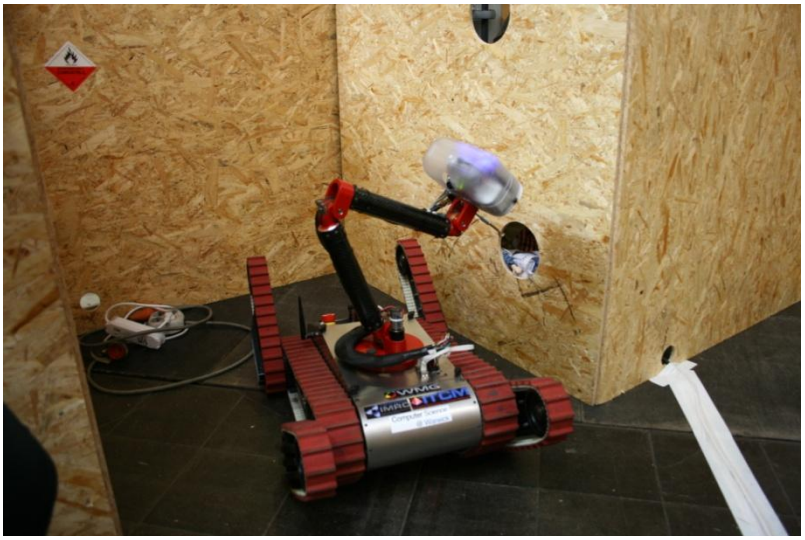

Figure 92 - Arm supporting the head and manipulator, picture taken at the Robocup European Open 2010

It is essential that the cameras have good visibility, allowing the operator to manoeuvre the robot safely around the arena or disaster zone. The front and rear web cameras must show as much of the environment as possible. It is also important that they have a clear view of the robot, to help the operator avoid collisions between the robot and its environment. A wide angle lens is used to improve the field of view of the web cameras.

A fixed web camera would provide sufficient visibility for a robot which was only required to navigate a simple environment (such as the yellow section of the Robocup arena). In this case, the camera position and orientation would be optimised for driving forwards. However, the tele-operated robot must be capable of navigating complex environments (recreated by the orange and red sections of the arena), as well as locating victims in restricted-access areas. In order to be successful in these sections of the

arena, it is essential to have greater control over the position and orientation of the head. This gives rise to the requirement for a highly dextrous arm to support the head.

5.2. Previous Design (08-09)

Last year's team designed a four degrees of freedom arm, which is shown in Figure 93. This arm was constructed using Dynamixel servos and laser cut stainless steel panels. The arm proved very useful in the 2008-2009 Robocup competition.

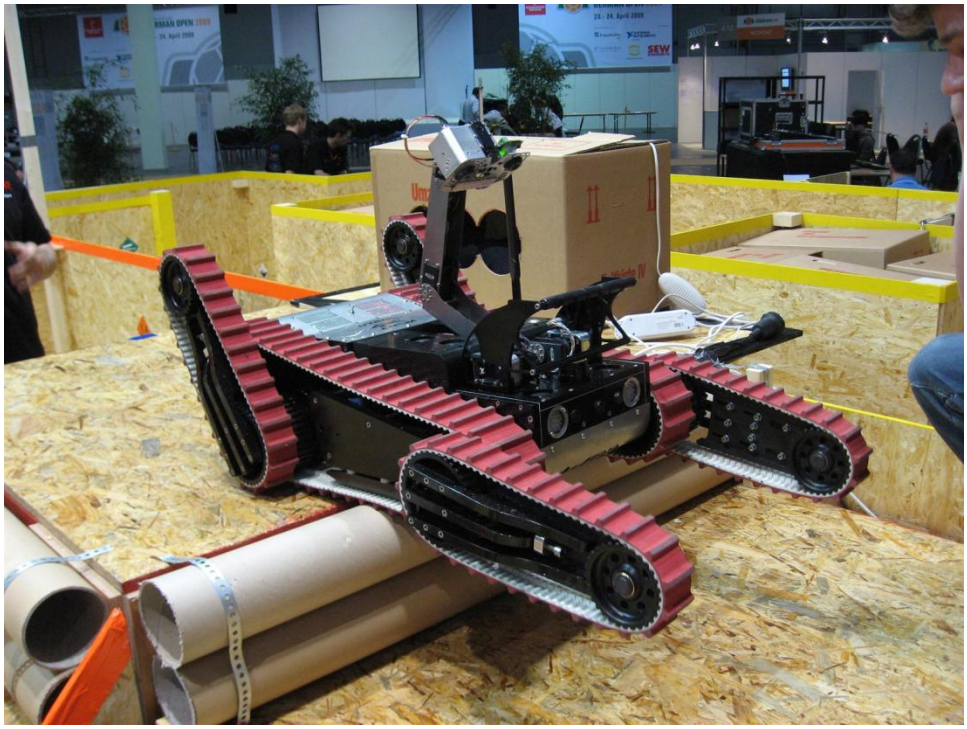

Figure 93 - Arm design from previous year

The first arm joint consisted of two Dynamixel RX-64 servos. The second joint used one RX-64, and the third and fourth joints used RX-28 servos. The servos were doubled up on the first joint to provide the large torque required to hold the arm. The last two joints used smaller RX-28 servos, as they required much less torque. This also reduced the size and weight of the arm. The servos were mechanically connected using laser cut stainless steel sections. These had a C-shape cross-section to provide some rigidity to the arm.

This design had several limitations; one contributing factor were the servos, typically used in light weight, low torque applications (such as model aircrafts). The Dynamixel servos, despite being high specification, were only just capable of supporting the head (approximately 1 kg). This limitation meant that the weight of the head had to be kept to a minimum and that the arm could not support a manipulator.

The second problem was the lack of rigidity. A rigid arm is required to hold the cameras and sensors steady whilst navigating rough terrain. If the web cameras are not stable, they will produce very poor quality images. This is magnified by the lag, low resolution and high compression of the web cameras.

The third problem was the lack of strength. The stainless steel construction was damaged in an incident where the robot tipped over in the step field section of the arena. This bent the stainless steel sections and fused the servos. The requirement for rebuilding the arm raised the questions of a redesign encompassing several improvements.

5.3. Requirements

Table 15 gives a list of requirements for the new teleoperated robot arm. Quantification has been given where possible.

Requirement	Quantification
Rigid	The arm must provide a rigid platform for the head and the manipulator. The last joint must not exceed an accumulative play of 10 mm (position) or ± 5° (orientation).
Strong	The arm must be capable of supporting its own weight, a 2 kg head and a 1 kg payload attached to the manipulator.
Speed	The arm must be capable of achieving any position and orientation within 5 seconds. The motor control would ideally use acceleration/deceleration curves to avoid shock to the head.
Reach	The arm should be capable of raising the height of the head to 1 m above the ground to enable victim identification. It must be able to reach to the front and back of the robot for pick and place operations with the manipulator.
Control	The arm should be easy to control with one operator from the standard GUI. Options for inverse kinematics or individual joint control should be provided. Presets would speed up common positions and orientations.
Weight	One of the main objectives of this year is to reduce the overall weight of the robot. This can only be achieved by minimising the weight of the arm (maximum 5 kg).
Power	The arm must be powered using either 12 or 24 volts (as determined by the motor control boards). Ideally it will draw little to no current whilst stationary to conserve battery life.
Cost	Approximately £3000 has been allocated from the project budget for the development of the arm.

Table 15 - Arm requirements

5.4. Arm Nomenclature

The following nomenclature has been developed for clarity and speed when referencing the arm. The joints are labelled Joint A, B, C, D and E, starting at the base. The joint angles are labelled θ1, θ2, θ3, θ4 and θ5, starting at the base. Joint A is typically referred to as the Arm Base. Working up from the Arm Base, there is the Lower Arm, the Upper Arm and the Head. Figure 94 shows a simplified schematic of the arm.

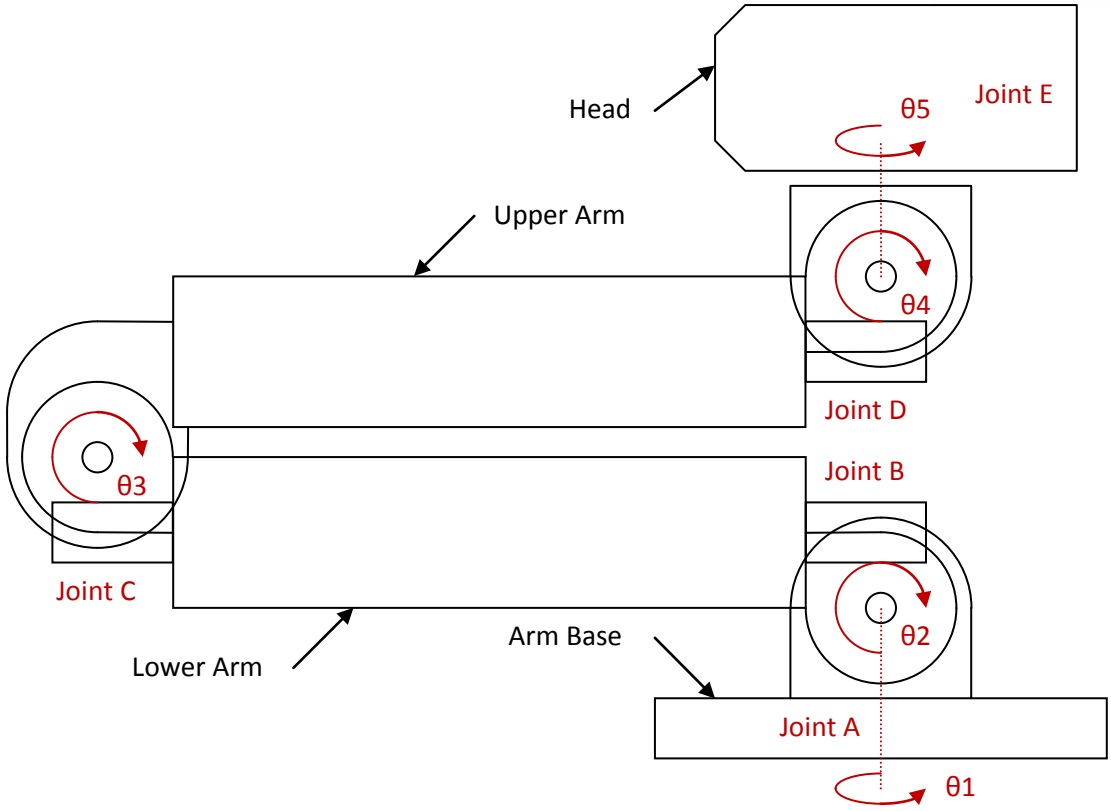

Figure 94 - Arm nomenclature

5.5. Mobility

Degrees of Freedom (DOF) is defined as the number of independent movements (displacement and rotation) of a rigid body. An unrestrained rigid body in 3D space has six degrees of freedom: three translational (XYZ) and three rotational. Two or more rigid bodies in space are collectively called a rigid body system. Joints connect the rigid bodies and provide the required kinematic constraints. There are different types of joints including revolute, prismatic, spherical, cylindrical and screw. The arm is a rigid body system, which uses revolute (R) joints. A revolute joint provides five constraints (three translational and 2 rotational). This leaves one rotational motion (and thus one DOF). Rigid bodies and kinematic constraints are the basic components of mechanisms. The motion of constrained rigid bodies can be analysed from their geometrical relationships or by using Newton's Second Law. The DOF of a mechanism can be calculated by using the Gruebler-Kutzbach equation.

5.5.1. Gruebler-Kutzbach Equation

$$F = 3 (N - 1) - 2 L$$

Where:

F is the total Degrees of Freedom in the mechanism
N is the number of links (including the frame)
L is the number of joints (one Degree of Freedom)

For the robot arm:

$$F = 3 (6 – 1) – 2 x 5 = 5$$

The number of Degrees of Freedom of a mechanism is also known as the mobility. The mobility is the number of input parameters that must be independently controlled to bring the mechanism into a particular position. This can be seen from the joint control option in the arm Graphical User Interface (GUI). There are five joints which can be independently controlled from the GUI. Alternatively, the inverse kinematics option can be used to control all five joints from world space coordinates.

5.6. In Practice

Five degrees of freedom provides excellent control over the position and orientation of the head. Figure 95 shows the head in a configuration where it can see the entire robot chassis and tracks in the field of view. This is especially useful for determining which part of the robot has become caught on the arena. Figure 96 shows the arm in its full forward position, this demonstrates the maximum reach of the arm.

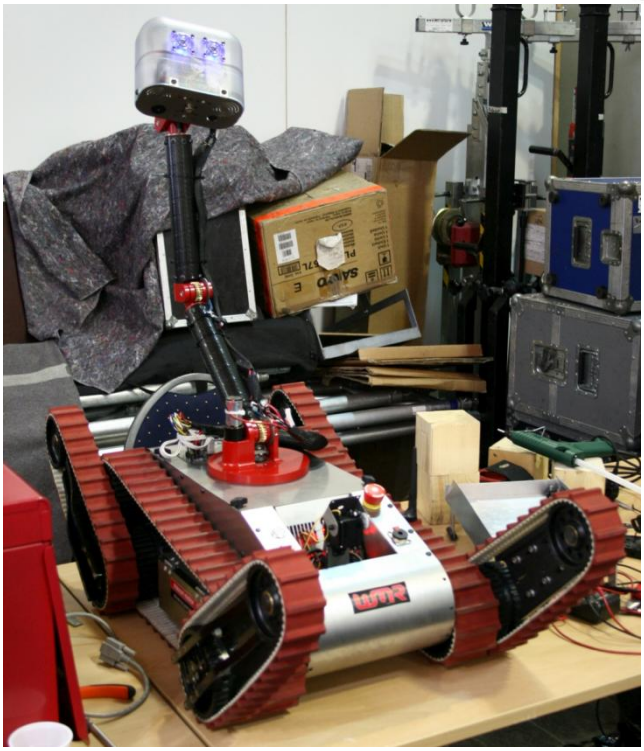

Figure 95 - View of the entire robot from the web cameras

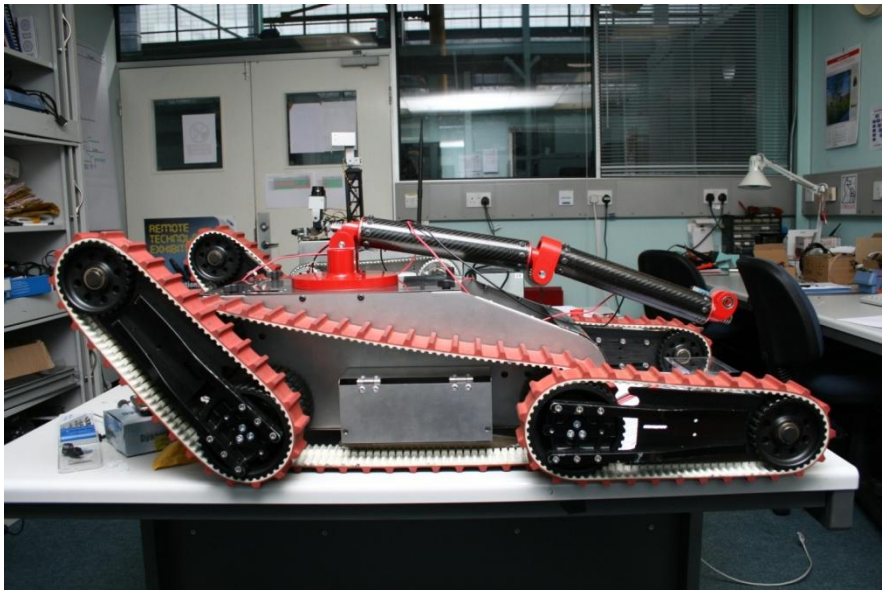

Figure 96 - Arm in forward orientation

5.7. Materials

One of the main objectives of this year was to reduce the overall weight of the robot. Thus, it was essential that the weight of the arm was kept to a minimum. Other important considerations when choosing materials for the arm included strength, rigidity, machinability, availability and cost. Table 16 gives the main components of the arm, the corresponding material and the justification for choosing this material.

Component	Material	Justification
Tubes	Carbon fibre	**Carbon fibre tubes are strong, rigid and light weight.**
Joints	Power coated aluminium	**Aluminium is easily machined on the five axis CNC (Computer Numerically Controlled) and is light weight.**
Worm	Surface hardened steel	**Steel is strong enough to prevent shearing of the worm teeth and is surface hardened to reduce frictional wear.**
Wheel	**Brass**	**Brass has a low coefficient of friction and reduces the wear to the worm.**

Table 16 - Justification of material choice

5.8. Costing

Table 17 gives a simplified costing of the arm. This sums to £1780. The true cost of arm, including machining, was significantly higher.

Component	Description	Supplier	Quantity	Cost	Total
Tubes	0.5 m carbon fibre 45.2 mm OD	Carbonology	2	£35	**£70**
Motors	A-max 26 + GP32C 246/1	Maxon Motors	1	£300	**£300**
Motors	RE30 + GP32C 23/1	Maxon Motors	3	£300	**£900**
Motors	RX-64	Dynamixel	1	£250	**£250**
Worm	WH1.25-1	HPC Gears	3	£15	**£45**
Wheel	PM1.25-24-1	HPC Gears	3	£30	**£90**
Potentiometers	ThinPot	SpectraSymbol	3	£15	**£45**
Potentiometers	SoftPot	SpectraSymbol	1	£15	**£15**
Potentiometers	1–3 N wiper	SpectraSymbol	3	£5	**£15**
Raw materials	**Aluminium**	**Stores**	**10 kg**	**£5/kg**	**£50**

Table 17 - Costing of arm

5.9. Membrane Potentiometers

The arm uses rotary membrane potentiometers to measure the absolute angle of each joint. An example of a stripped down joint, exposing the membrane potentiometer, is shown in Figure 97. All of the membrane potentiometers used on the arm are produced by SpectraSymbol. Joint A uses a SoftPot potentiometer. Joints B, C and D use ThinPot potentiometers. Joint E uses a servo, which has a built in potentiometer.

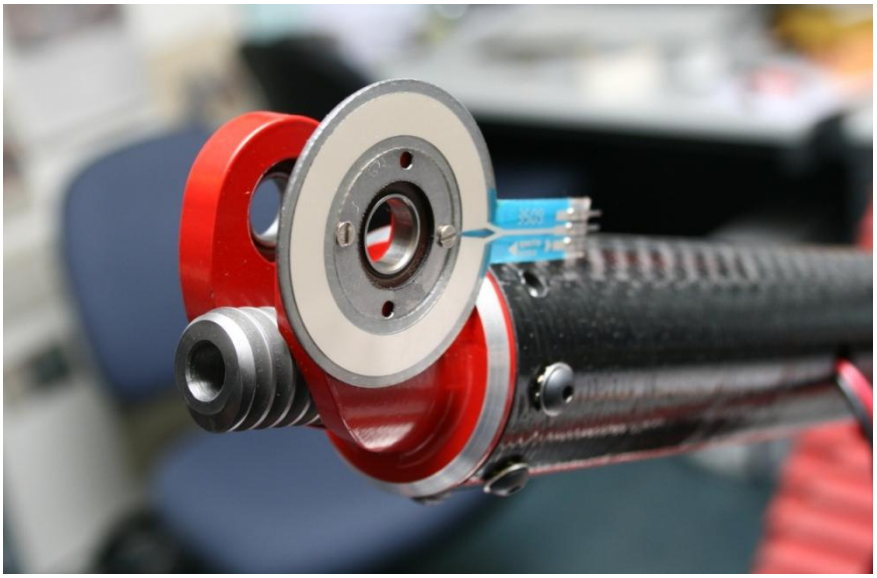

Figure 97 - Membrane potentiometer

5.9.1. How It Works

The membrane potentiometer is a resistive element which consists of a conductive resistor, a sealed encasement and a simple wiper assembly. The wiper is a non-conductive mechanism that depresses the top circuit actuating the potentiometer. The top and bottom circuits are separated by 0.15 mm of spacer adhesive build-up. Contact between the circuit occurs by pressure (typically 0.7 - 1.8 N) from the wiper on the top circuit. Both SoftPot and ThinPot potentiometers use a three wire system with two resistive output channels and an electrical collector channel. Figure 98 shows the construction of the membrane potentiometer. Figure 99 shows the electrical circuit and connection.

Figure 98 - Membrane potentiometer

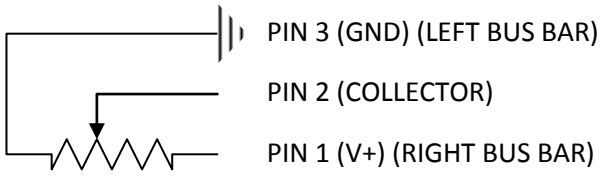

Figure 99 - Electrical circuit

5.9.2. Specification

The specification of the potentiometers is given in Table 18. ThinPot and SoftPot potentiometers are identical, except for their diameters. ThinPot potentiometers have an ID (inside diameter) of 15.4 mm and an OD (outside diameter) of 35.4 mm, while SoftPot potentiometers have an ID of 45.4 mm and an OD of 25.4 mm. A schematic of a SoftPot potentiometer is given in Figure 100 and Figure 101.

Property	Units	Specification
Life Cycle		> 1 million
Actuation Force	N	0.9 to 2.2 at -40°C 0.9 to 2.2 at -25°C 0.7 to 1.8 at +23°C 0.7 to 1.8 at +50°C
Operating Temperature	°C	-40 to +50
Humidity		No affect at 95% RH, 4hrs, 50°C
IP Rating of Active Area		IP64 (Dust Proof, Splash Proof)
Resistance	Ohms	10k

Resistance Tolerance	%	±20
Linearity	%	±3 to ±5
Repeatability		No hysteresis
Power Rating	W	1 W maximum at 25°C 0.5 W recommended
Resolution		Analogue output theoretically infinite
Dielectric Value		No affect at 500VAC for 1 minute
Backing		3M Pressure Sensitive Adhesive (PSA)
Connector		Crimpflex Short Male Pins (MP)

Table 18 - Potentiometer specification

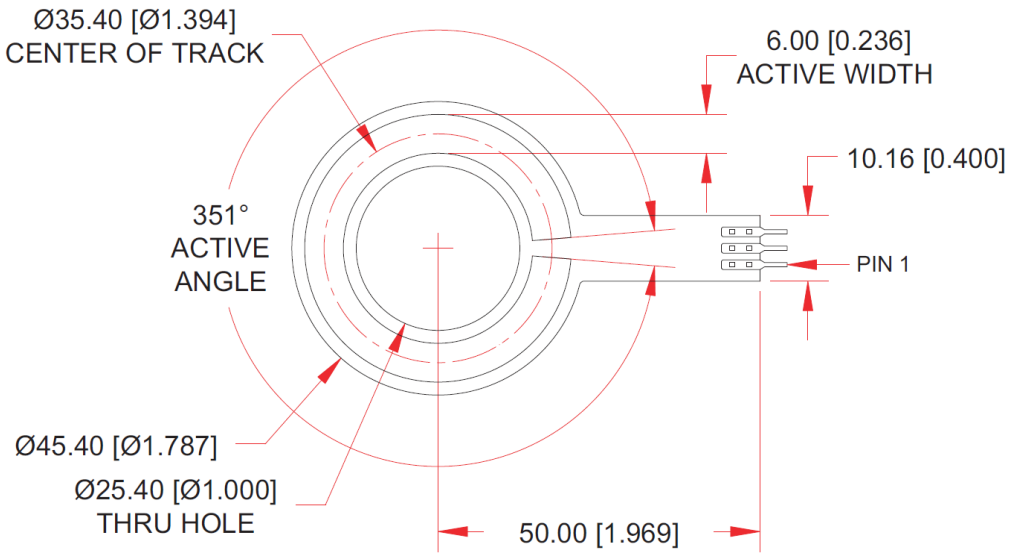

Figure 100 - Schematic of ThinPot

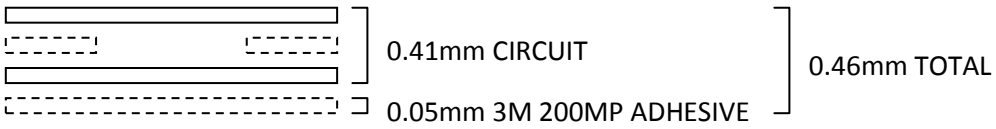

Figure 101 - Material cross-section

5.9.3. Justification for Choice of Potentiometers

There are two companies which produce membrane potentiometers. Both companies were approached.

Company	Products
SpectraSymbol	SoftPot, HotPot, ThinPot
Hoffmann + Krippner	Sensofoil

Table 19 - Membrane potentiometer companies

Both companies make custom membrane potentiometers and have a very limited range of standard membrane potentiometers. These standard potentiometers are meant as a demonstrator for their technology. For this reason, we were originally interested in making our own custom membrane potentiometers. Unfortunately the lead time for custom potentiometers proved too long and the custom tooling too expensive, thus we settled for a standard potentiometer. SpectraSymbol ThinPot and SoftPot were selected based on their small outside diameter.

5.10. Joint Angle Limits

Each of the arm joints has a lower and upper angle limit. If the limit is exceeded the arm may collide with itself or the potentiometer may exceed its operating range depending on the joint. If the operating range of the potentiometer is exceeded, the motor control board will try to drive the arm joint around to zero. Both of these cases will result in permanent damage to the arm and arm motors. For this reason, the joint angles are enforced through the software. It was thought that electromechanical limits would be a good idea. However, these proved too difficult to implement. Table 20 shows the angle limits for each of the arm joints.

Joint	Joint Angle	Lower Limit (degrees)	Upper Limit (degrees)
A	θ1	0	350
B	θ2	0	180
C	θ3	0	180
D	θ4	0	180
E	θ5	0	350

Table 20 - Joint angle limits

All of the membrane potentiometers have a range 351 degrees. The range between the joint angle limits, for each joint, is less than the range of the potentiometers. The potentiometers are positioned so that joint range lies in the middle of the potentiometer range. This gives the greatest area for error.

5.11. Torque Calculations

Simple torque calculations were done to determine the best motor, planetary gearbox and worm/wheel combination. The greatest torque experienced by the joints occurs when the arm is in its fully outstretched position. This is shown in Figure 102. To quantify the torque at Joint B, the weight of the arm is divided into the head and three motors.

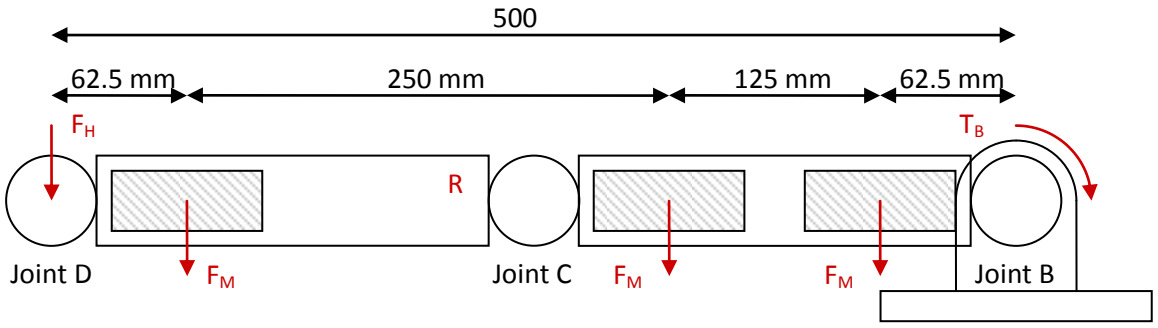

Figure 102 - Calculation of torques

$$T_B = (F_H \times 0.5\ m) + (F_M \times 0.4375\ m) + (F_M \times 0.1875\ m) + (F_M \times 0.0625\ m)$$

Where:

$$F_H = 2\ kg \times 9.8\ m/s^2 = 19.6\ N$$

$$F_M = 0.4\ kg \times 9.8\ m/s^2 = 3.92\ N$$

$$T_B = (19.6\ N \times 0.5\ m) + (3.92\ N \times 0.4375\ m) + (3.92\ N \times 0.1875\ m) + (3.92\ N \times 0.0625\ m) = 12.5\ Nm$$

This means that the output torque of the worm/wheel must be at least 12.5 Nm to support the arm in its outstretched position. The following motor, planetary gearbox and worm/wheel combination was selected through an iterative process. The calculations for the final selection are shown below.

The Maxon RE-30 has a nominal torque (maximum continuous torque) of 0.085 Nm. The Maxon GP32C was selected with a reduction ratio of 23:1, while the worm and wheel provide a reduction ratio of 24:1. Thus the total reduction is 552:1.

$$T_T = 0.085\ Nm \times 552 = 47\ Nm$$

If we assume that the worm and wheel is 30% efficient, the effective torque is:

$$T_E = 47\ Nm \times 0.3 = 14\ Nm$$

This is slightly greater than the required torque of 12.5 Nm. For simplicity, the same configuration is used for Joint B, Joint C and Joint D.

5.12. Speed Calculations

The Maxon RE-30 has a nominal speed of 8050 rpm. Through a 552:1 reduction, the output speed of the worm/wheel is 14.6 rpm. Thus it would take just over four seconds to complete one revolution.

Similarly with Joint A, the Maxon A-max has a nominal speed of 8820 rpm. Through a 1640:1 reduction ratio (246:1 provided by the GP32C gearbox and 80:12 provided by the internal gear), the output speed of Joint A is 5.4 rpm. Thus it would take just over eleven seconds to complete one revolution.

5.13. Motors & Gearing

Maxon Motors were selected to provide all of the motors for the arm based on their reputation and competitive cost after negotiating a 35% discount. In Figure 103, the carbon fibre tubes have been removed to show the location of the motors.

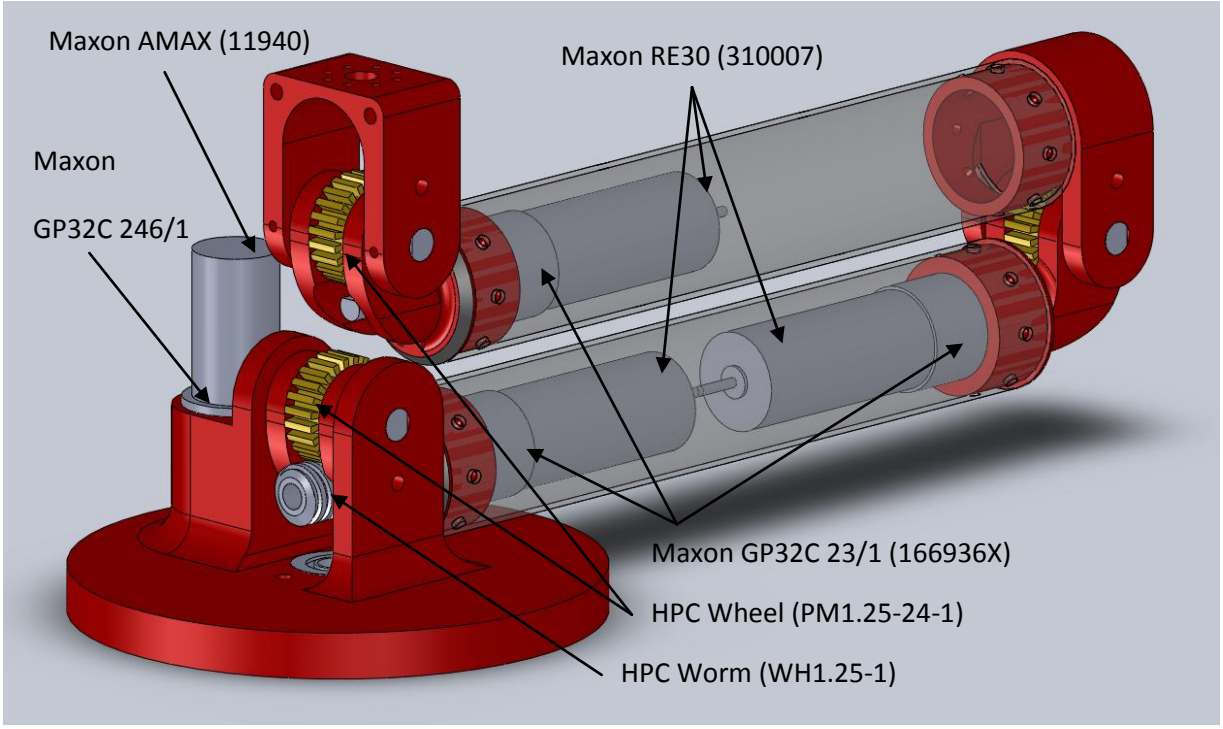

Figure 103 - Motors and gearboxes

Table 21 shows the motors and gearboxes for each of the joints. The Maxon GP32C 23/1 were ordered with custom made shafts. These were 8 mm OD as opposed to 6 mm and 30 mm long as opposed to 12 mm. This modification was made to fit the worm gear from HPC Gears.

Joint	Motor	Reference Code	Gearbox	Reference Code
A	Maxon A-max 26	110940	Maxon GP32C 246/1	166949
B	Maxon RE30	310007	Maxon GP32C 23/1	166936X
C	Maxon RE30	310007	Maxon GP32C 23/1	166936X
D	Maxon RE30	310007	Maxon GP32C 23/1	166936X
E	Dynamixel Servo RX	RX-64		

Table 21 - Motors and gearboxes

5.13.1. Maxon RE30 & A-max 26 Specification

Property	Units	RE30 310007	A-max 26 110940
Nominal voltage	V	24.0	24.0
No load speed	rpm	8810	8820
No load current	mA	164	31.7
Nominal speed	rpm	8050	6730
Nominal torque (max. continuous torque)	mNm	85.0	17.2
Nominal current (max. continuous current)	A	3.44	0.704
Stall torque	mNm	1020	77.6
Starting current	A	39.3	3.04
Max. efficiency	%	87	79
Terminal resistance	Ohms	0.611	7.90
Terminal inductance	mH	0.119	0.770
Torque constant	mNm/A	25.9	25.5
Speed constant	rpm/V	369	374
Speed/torque gradient	Rpm/mNm	8.69	116
Mechanical time constant	ms	3.03	15.7
Rotor inertia	gcm2	33.3	13.0
Thermal resistance housing-ambient	K/W	6.0	13.2
Thermal resistance winding-housing	K/W	1.7	3.2
Thermal time constant winding	s	16.2	12.4
Thermal time constant motor	s	714	772
Ambient temperature	°C	-30 to 100	-30 to 85
Max. permissible winding temperature	°C	125	125
Max. permissible speed	rpm	12000	10400
Axial play	mm	0.05-0.15	0.1-0.2
Radial play	mm	0.025	0.025
Max. axial load (dynamic)	N	5.6	5
Max. force for press fits (static)	N	110N	75

Max. radial loading, 5mm from flange	N	28	20.5
Number of pole pairs		1	1
Number of commutator segments		13	13
Weight of motor	g	238	117

Table 22 - Motor specification

5.13.2. Maxon GP32C Specification

Property	Units	GP32C 23/1 166936X	GP32C 246/1 166949
Planetary gear head		Straight teeth	Straight teeth
Output shaft		Stainless steel	Stainless steel
Shaft diameter	mm	8	8
Bearing at output		Ball bearing	Ball bearing
Max. radial play, 5mm from flange	mm	0.14	0.14
Max. axial play	mm	0.4	0.4
Max. radial load, 10mm from flange	N	140	140
Max. permissible axial load	N	120	120
Max. permissible force for press fits	N	120	120
Recommended input speed	rpm	<8000	<8000
Recommended temperature range	°C	-20 to 100	-20 to 100
Reduction		23:1	246:1
Reduction absolute		576/25	421824/1715
Max. motor shaft diameter	mm	4	4

Table 23 - Gearbox specification

5.14. Worm/Wheel Force Calculations

After the first construction of the arm, it was realised that the initial torque/force calculations were incorrect. The first calculations failed to take into account the lever action caused by the PCD (pitch circle diameter) of the worm and wheel. This is illustrated in Figure 104.

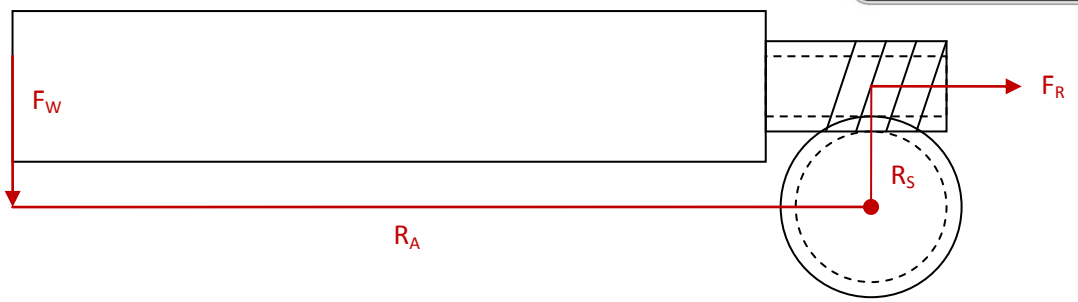

Figure 104 - Calculation of the force pulling the worm gear out

$$F_W \times R_A = F_R \times R_S$$

Where:

F_W is the force acting on the end of the arm

R_A is the length of the arm

R_S is the PCD of the worm gear + PCD of the wheel

F_R is the reaction force required to balance the arm

The worst case scenario occurs when the arm is fully outstretched, creating the largest torques and forces in the arm. In this situation the total length of the arm from Joint B to Joint D is 690 mm. The weight of the head is 0.8 kg. The weight of the lower and upper arms is 4 kg. The centre of gravity is strongly biased towards Joint B, as this section of the arm contains two motors rather than one. The distance between the worm gear and the wheel gear is 25 mm.

$R_A = 0.69$ m

$R_S = 0.025$ m

$F_W = (2 \text{ kg} \times 9.8 \text{ m/s}^2) + (4 \text{ kg} \times 9.8 \text{ m/s}^2) \times (2/3) = 45.7$ N

$F_R = F_W \times R_A / R_S = 45.7 \text{ N} \times 0.69 \text{ m} / 0.025 \text{ m} = 1261$ N

The maximum permissible axial load that can be supported (in both tension and compression) by the Maxon gearbox GP32C 23/1 is 120 N. Thus, with the proposed arm design, the arm loading would almost certainly damage the gearboxes. For this reason, the bottom two joints (Joint B and Joint C) were modified as they experienced the greatest forces. Figure 105 shows the modification to Joint B and Figure 106 shows the modification to Joint C.

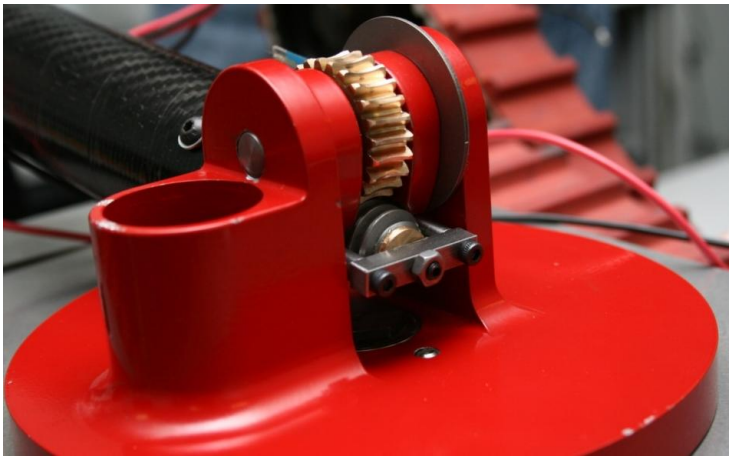

Figure 105 - Modification to Joint B

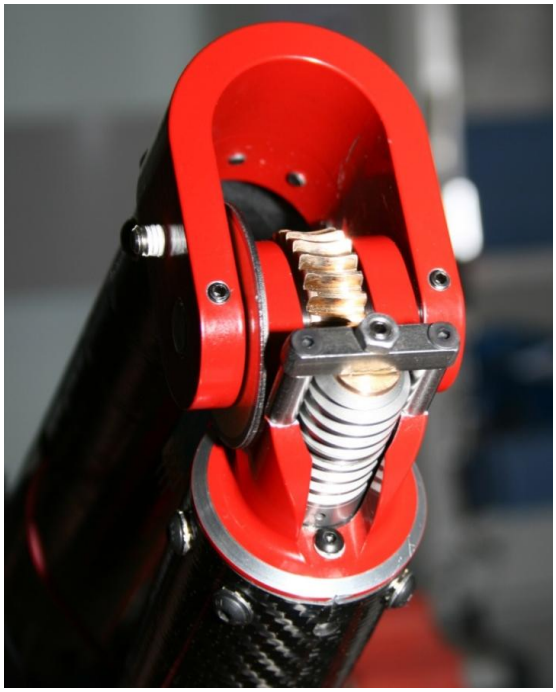

Figure 106 - Modification to Joint C

5.15. Arm Kinematics

Simple inverse kinematics is used to control the arm. The playstation controller is used to manoeuvre the arm in world space Cartesian coordinates. This position is then translated to joint angles. Figure 107 and Figure 108 explain the calculation of these angles.

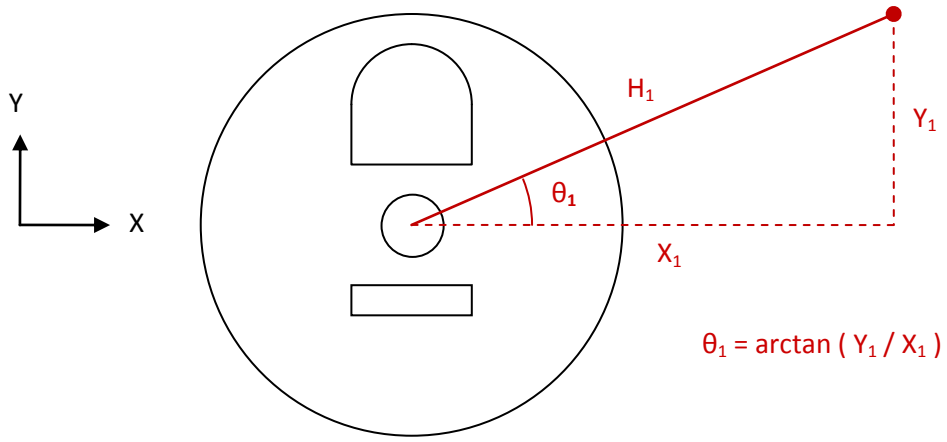

Figure 107 - Calculation of angle θ1 (Joint A)

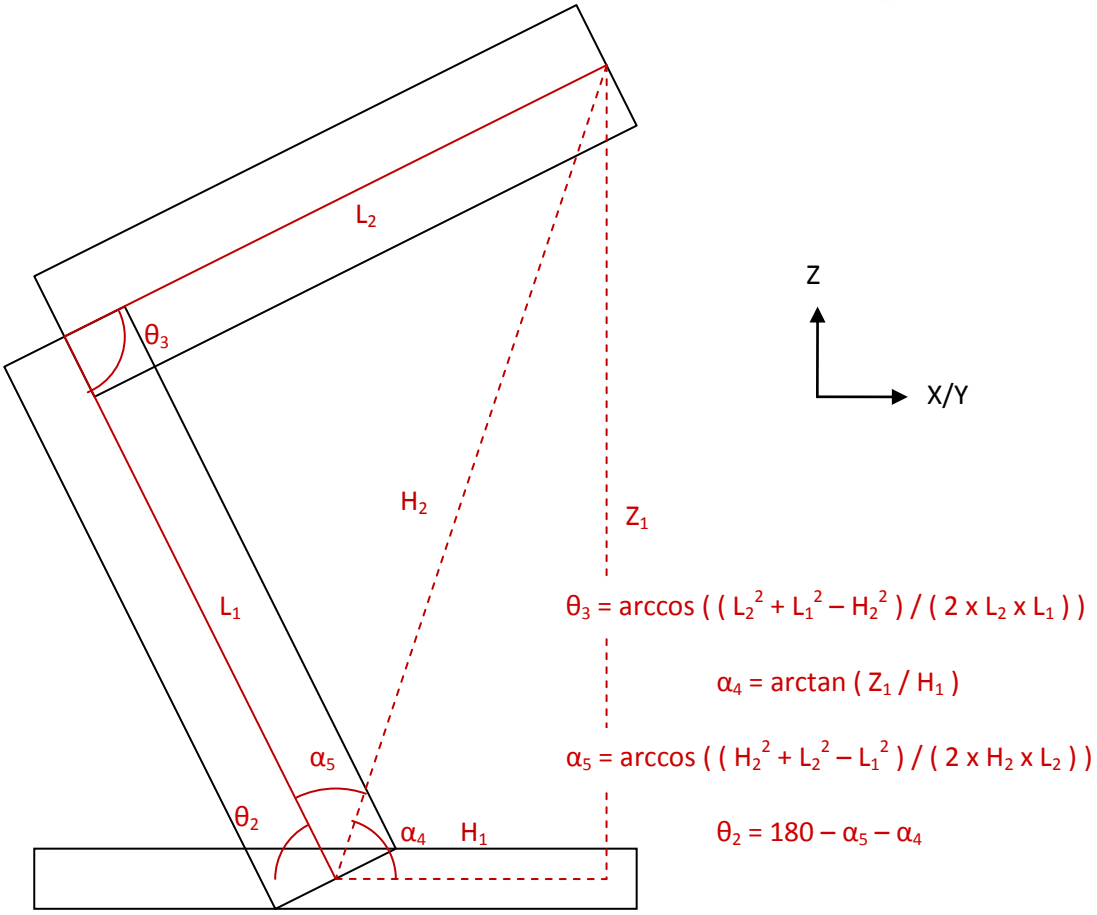

Figure 108 - Calculation of angles θ2 (Joint B) and θ3 (Joint C)

5.16. Construction

Development of the arm started on paper, but quickly moved to CAD (SolidWorks 2009). Several designs were developed before the final. The entire arm was modelled and assembled prior to manufacture. This ensured that mechanically it functioned correctly and that all the parts fitted perfectly. The CAD data was then used to machine the various components on the five axes CNC (Computer Numerically Controlled) machine. The following images show the design and assembly of the various components which make up the arm. Table 24 gives a reference to the CAD drawings given in the appendix.

Drawing Number	Drawing Name	Description of Job	Material	Quantity
1	Arm Joint 1	5 Axis CNC	Aluminium	**3**
2	Arm Joint 2	5 Axis CNC	Aluminium	**1**
3	Arm Joint 3	5 Axis CNC	Aluminium	**1**
4	Arm Joint 4	5 Axis CNC	Aluminium	**1**
5	Arm Shaft	5 Axis CNC	Steel	**3**
6	Arm Tube	Various	Carbon Fibre	**2**
7	Arm Washer 2mm	Various	Steel	**6**
8	Arm Washer 7mm	Various	Steel	**6**
9	Potentiometer Back plate	Laser cut	0.9 mm Stainless Steel	**3**
10	Arm Internal Gear	5 AXIS CNC	Hardened Steel	**1**
11	**Arm Gear**	**Broaching**	**Brass**	**3**

Table 24 - List of parts

5.16.1. Arm Base

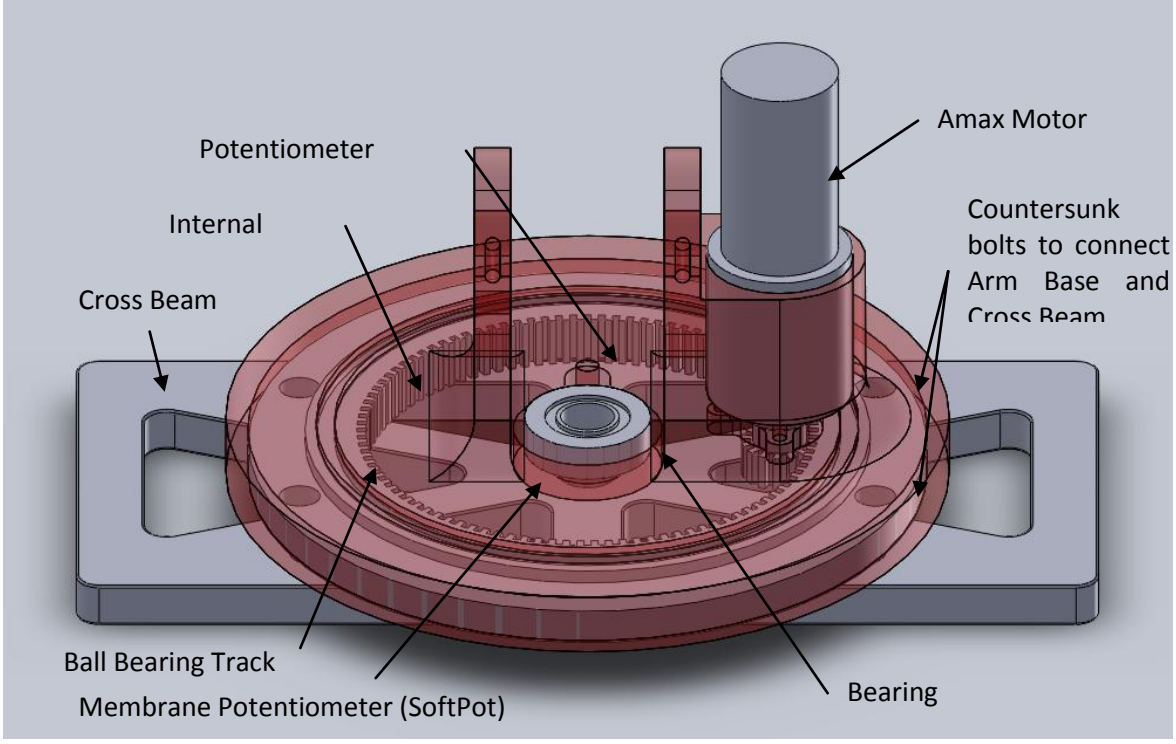

Figure 109 - Arm base

5.16.2. Joint Shaft

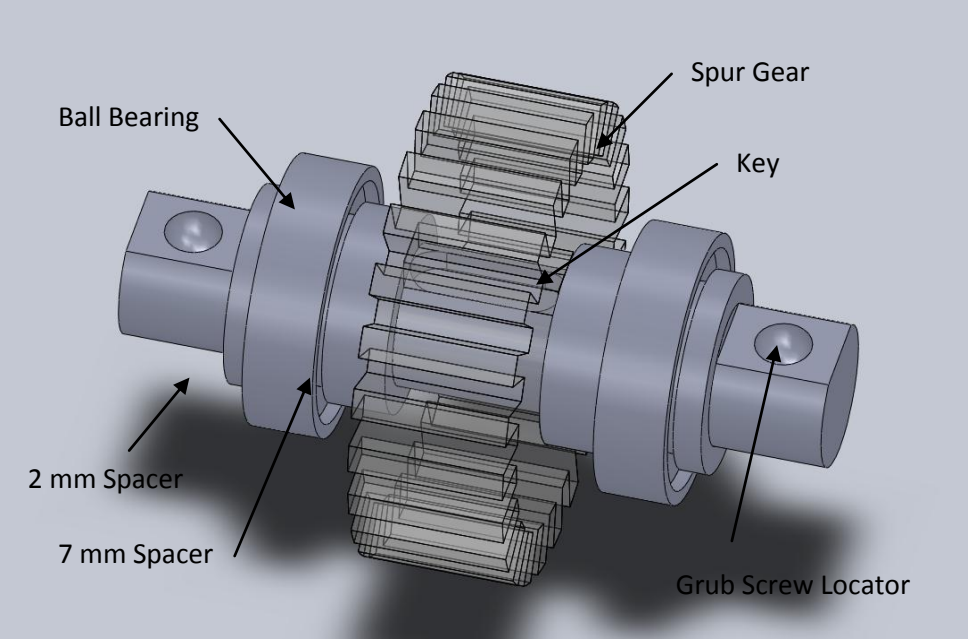

Figure 110 - Joint shaft

5.16.3. Arm Joint Inside

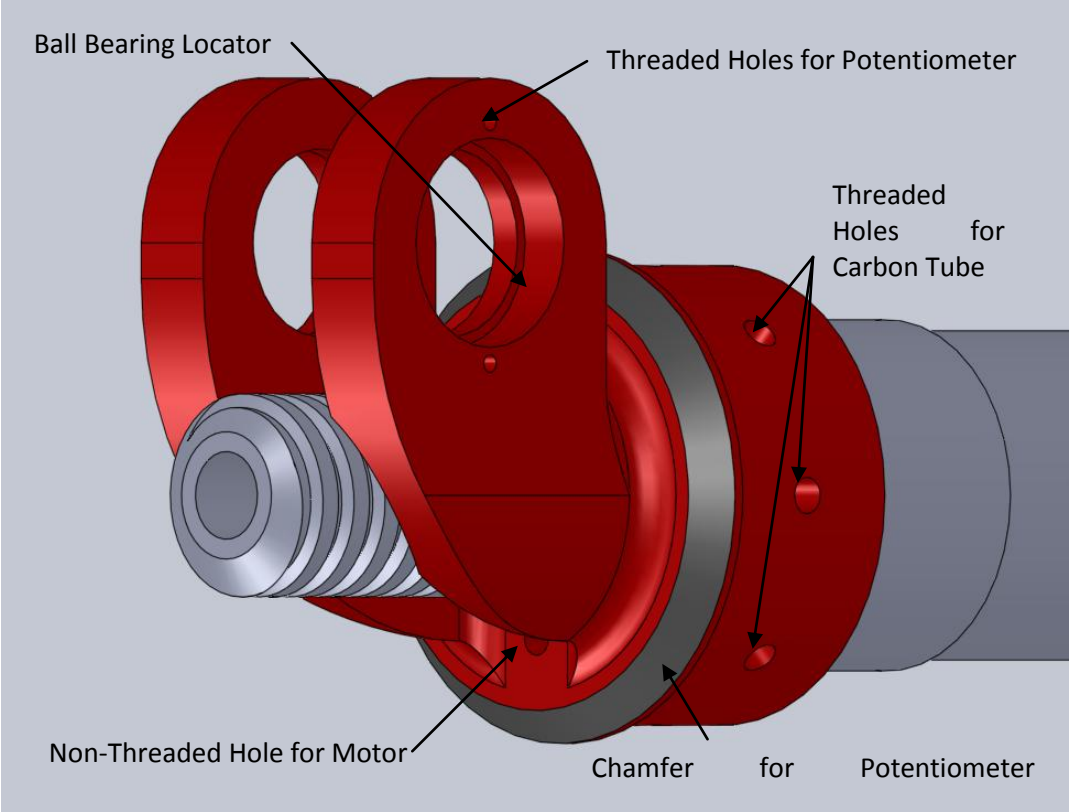

Figure 111 - Arm Joint Inside

5.16.4. Arm Joint Outside

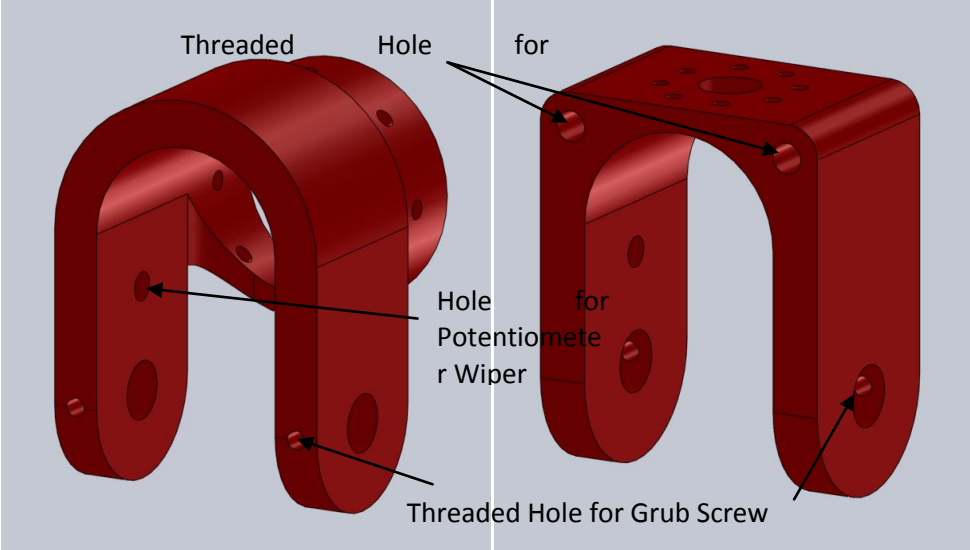

Figure 112 - Arm Joint Outside

5.17. Software

Last year's arm design had four Degrees of Freedom. A 2D representation of the arm in the GUI was used to show the current position and orientation. This proved very useful last year and it was decided that a similar concept should be incorporated this year. The new arm has five Degrees of Freedom, which makes it difficult to clearly show the full position and orientation of the arm in 2D. It was therefore decided to develop a 3D representation of the robot in the GUI. Figure 113 shows the final 3D representation. A low resolution 3D model of the robot was designed in Metasequoia (shown in Figure 114). This program is similar to a CAD package, except aimed at creating 3D models for computer games. The code for updating the 3D model was written in Java 3D. This programming language was chosen because it must seamlessly fit into the existing Java GUI. The coding of the 3D arm proved very difficult because Java is not built for developing 3D applications.

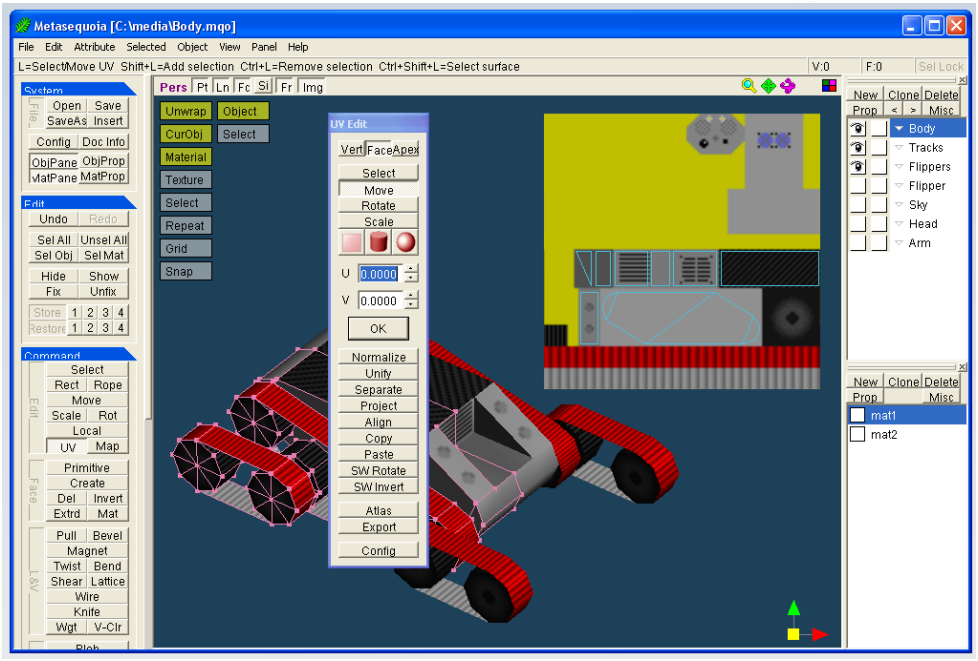

Figure 113 - Low resolution version of the robot

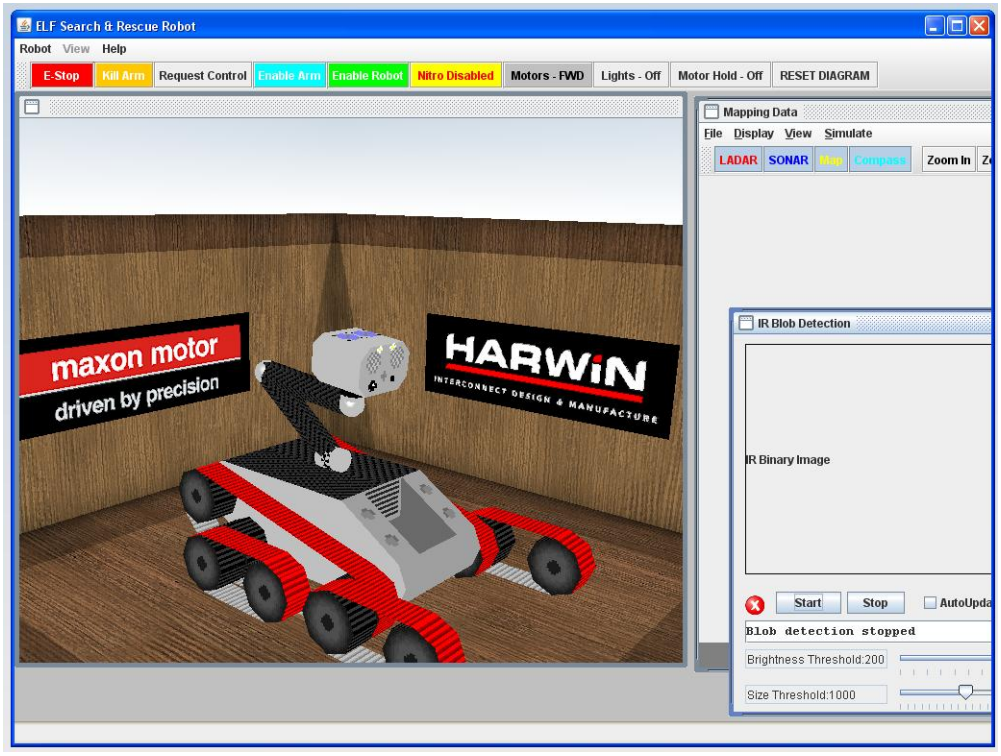

Figure 114 - Graphical user interface for the arm

6. Analysis and Testing

6.1. Tele-operated

6.1.1. Drive systems

6.1.2. Chassis

When testing the new chassis, the team discovered that there was larger-than-expected bending in the panels. This had a number of consequences. Firstly, the bending in the panels had negative implications for the alignment of holes. In an attempt to ensure rigidity, there were a large number of fixation points where two laser cut holes needed to correctly align. When modelled in *Solidworks* 2009, since bending is not accounted for, the alignment was perfect. The bending in the chassis therefore made it difficult to assemble the chassis panels. This was addressed in two ways. Firstly, a number of braces were used to increase the chassis rigidity and reduce bending. Secondly, where possible, the size of the aligning chassis holes was increased (by post process filing or drilling) to alleviate the difficulties experienced.

The second consequence of the chassis panels bending was that the drive motor had a large range of movement. In order to address this, a clamp was made to fix the two motors to one another and therefore, since when this phenomenon occurred the motor were moving in opposing directions (one down, one up), prevent this unwanted movement. It was later decided that this clamp was surplus to requirements as the robot became sufficiently rigid when fully assembled.

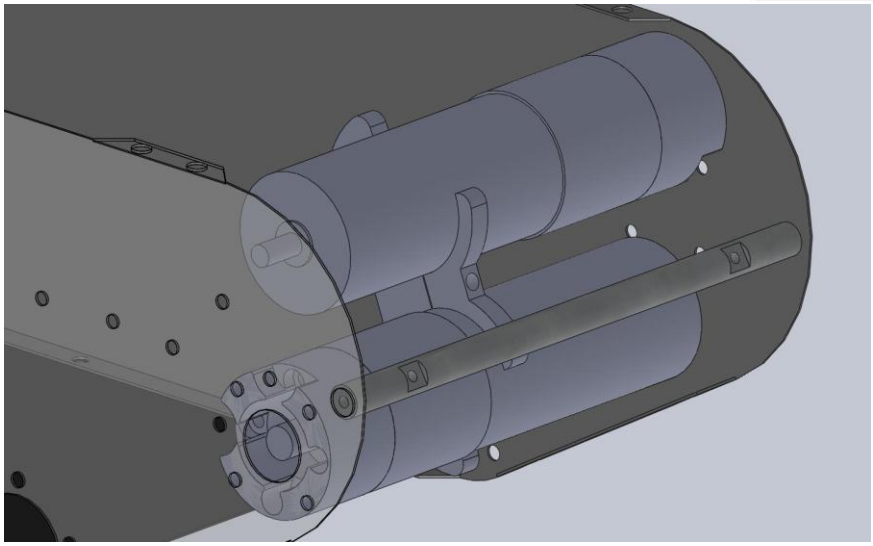

Figure 115 - Drive Motor Clamp as Modelled in *Solidworks 2009*

During the testing phase, one of the lithium polymer batteries was rendered unusable when it was over-discharged. The team had difficulty finding an exact replacement and so had to use a battery with different dimensions to the damaged one. As a result, the new, longer batteries no longer fitted satisfactorily in the battery packs and so the battery packs were redesigned with larger dimensions to accommodate them.

6.1.3. Flipper Motor Mounts

The flipper motor mounts were incredibly difficult to position correctly in order to achieve the required chain tension. Subsequently, the positioning of the mounting holes in the side panels was redesigned a number of times. When testing the chain tension, it was discovered that even minute changes in the positioning had a large effect. For example, if certain mounting bolts were left partially untightened, a desirable level of chain tensioning could be achieved. Since it was not acceptable to leave any bolts untightened, due to the difficult terrain the robot would be experiencing, the team decided to position anti-shake washers on the relevant bolts to accomplish the required chain tension.

6.1.4. Robot arm

Testing of the arm started two weeks prior to the Robocup European Open. Figure 116 shows the most basic form of testing; the motor was connected to a single cell battery. This was the safest form of testing as there was no danger of driving the arm into itself. The next stage of testing was connecting

the motors to the motor control boards. These were then run from the computer using Roborun (software provided by Roboteq). This required a true reading from the potentiometer. Great care had to be taken when using this method as an error in the wiring, the potentiometer reading or the software could cause serious damage to the arm. The next stage involved running the motors from the client software. The final stage involved running the arm through the inverse kinematics and joystick. In these last stages it was important to be sure that the code was correct. As a last resort, there was always someone on the emergency stop button to cut the power to the arm.

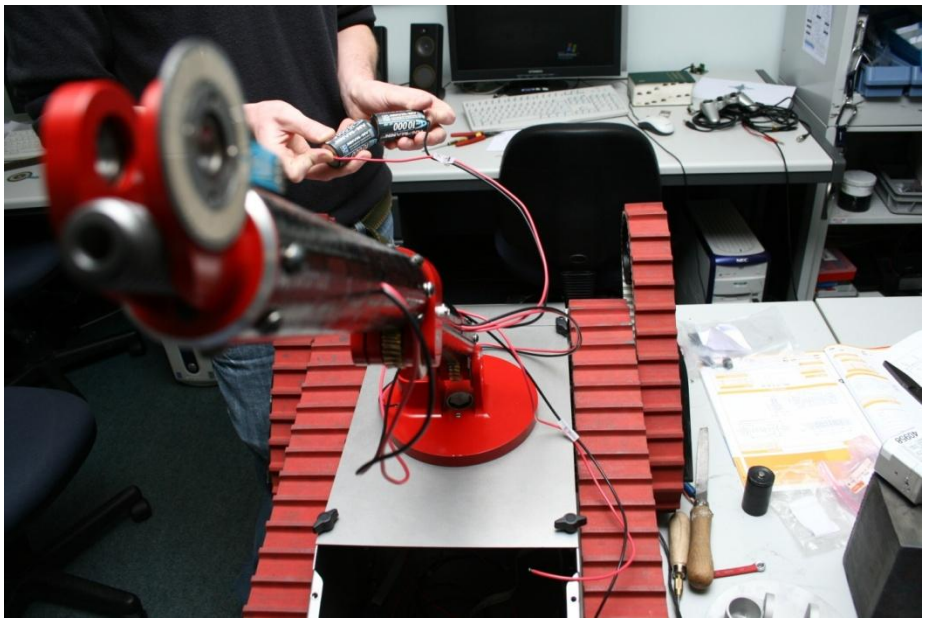

Figure 116 - Testing the arm

6.2. Autonomous

6.2.1. Chassis

Once the first chassis had been laser cut, it was assembled for mechanical integrity testing. The main concern was that the chassis would not be stiff enough because of the thin sheet steel. A central plate across the chassis substantially increased the stiffness and created a division between the motor section and the electronics section. The first version of this divider plate was solid; however, it was decided that ventilation was important so a new plate was made with holes to increase air flow and also allow for easier wiring.

Rivnuts were used on tabs to secure the lid of the chassis. When the bolts were not done up, the chassis was very flexible however, when all bolts were tightened the stiffness of the chassis increased. Despite this, there were still some concerns over the torsional stiffness of the chassis. It was discussed whether cylindrical braces similar to the ones used in the teleoperated robot should be implemented in the autonomous design. It was decided that these would not be required for now, but could be added at a later stage if found necessary after further testing.

6.2.2. Lid

The lid was primarily designed in two sections: one that hinges up over the motors at the back and a second, larger lid, which covers the front (electronics) section. They met at the divider and were secured together into the Rivnuts. This produced a stiff chassis with relatively quick internal access when required. For the front section, patterned cooling holes were positioned over the top and fixing holes located for the Lidar (without gimble).

It was later realised that more sensors were required to be attached to the lid of the autonomous robot. The IR and webcam needed to be attached somehow with the ability to locate victims at various height positions. It was decided by the team to design a simple arm that would be fixed to the lid of the robot. A 'head' on a high-torque gimble (similar to that used for the Lidar) would be attached to the top of this arm to allow for tilt and pan of the head. The lid was subsequently redesigned with the extra holes required for these additions. The original cooling holes were made larger to increase air flow and a fan vent was created to help draw air out of the main section of the robot.

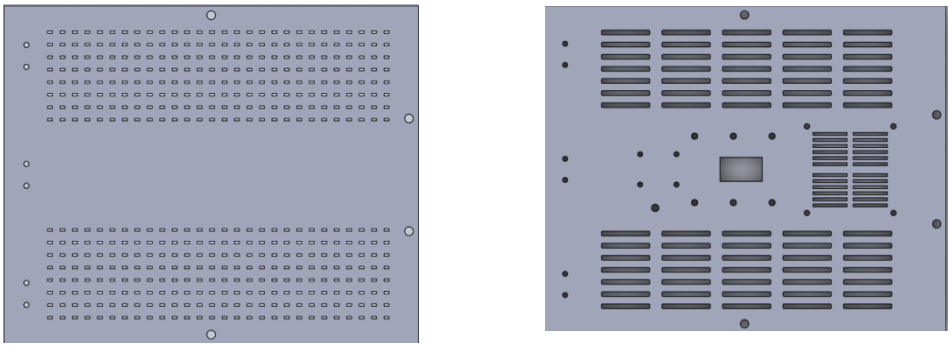

Figure 117 - Autonomous lid development

6.2.3. Drive systems

Once a full chassis was constructed and assembled, one side of the motors, shafts and pulleys were installed to test the power-train system. Slots were designed for the front pulley positioning to allow variable tension on the belts. When the pulleys and belts were first installed it was found that even with the pulleys as far forwards as possible, the belt was too slack. External power was supplied to the motor and the system drove well but more tension on the belts was required to prevent the chance of slipping.

The first option considered to tighten the belts was to add a nylon shaft at some point on the underside of the belt in order to increase the tension. A possible design was produced and is shown below. This solution, however, would be time consuming and also require modifications to the side panels of the chassis. Upon further inspection of the slots that locate the front stub-shaft it was noticed that there was 3-4mm room into which the slots could be expanded. The decision was made to attempt to extend the slots to see if this was enough to increase the tension to an appropriate level. In the event that this was unsuccessful the nylon tensioning device would be manufactured. A Dremel tool was used to extend the grooves and this proved sufficient to increase the tension. Nylock bolts were used to ensure that the front stub-shaft would not come loose and slide back.

6.2.3.1. Belt Slip

As the front pulleys of the robot did not have a middle section to hold the belt in place, it was found that the belt had a tendency to slip slightly off the pulleys. There was concern that with high enough lateral forces, the belts might completely come off. To prevent this from happening, nylon parts were designed to fit between the front pulleys (over the anodised spacer). These nylon runners would guide the centre of the tracks back into place if they drifted off.

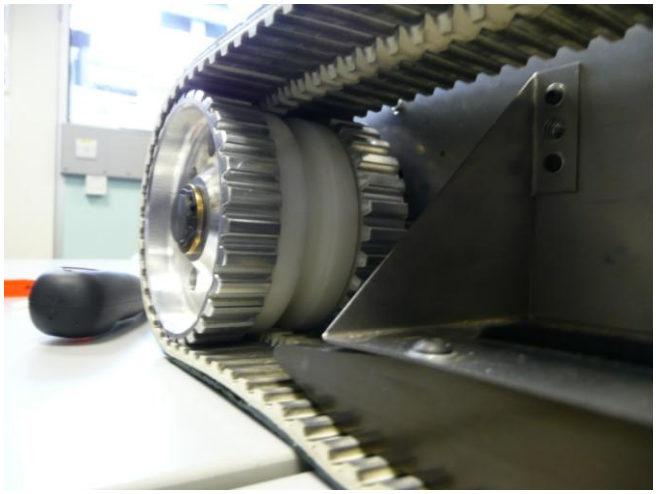

Figure 118 - Nylon belt slip preventer

6.2.4. Arm and Head

The autonomous arm was decided necessary to attach the cameras (thermal and webcam) to the robot in a way that would allow identification of victims in the arena. The arm was fixed centrally to the lid of the front section. Arm movement was not necessary but the computer science team expressed an interest in the ability to pan and tilt the cameras on the head of the robot. To solve this problem a gimble similar to the one used for the Lidar was designed. To cope with the higher load on the servos from the heavier head, high-torque servos were chosen. LEDs were also added to the head to ensure enough light was available to visually identify victims. A mount for the CO2 sensor was also designed into the head.

After all the components for the robot head were manufactured a first test was conducted by assembling it and ensuring all the sensors, circuit boards and wires fit. Next the sensors were powered up one by one to check their functionality. This was particularly important for the front and rear cameras and making sure the viewing angle was suitable for driving the robot. It was also important to ensure that there were no short circuits. After this initial testing phase the head was placed onto the robot arm and it was soon realised that a spacer (Figure 119) would be necessary between the servomotor and arm connection. This is so the head cover did not interfere with the final arm joint surface, as shown in Figure 119.

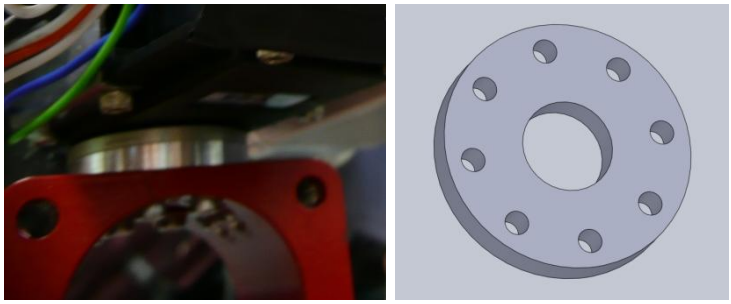

Figure 119 - Head to arm connection (left) and spacer (right)

Having a spacer meant that the head cover had to be modified. A *Dremel* hand drill with a sand paper filing tool was used to widen the notch for the head to arm connection, as shown in Figure 120. This method of cutting is recommended over using a hack-saw, which could crack the head cover. When the head was attached to the arm another problem was identified. Around 20 wires going into the head interfered with the gear of the final arm joint and panning motion of the head was restricted by the wires. To solve this problem another notch was cut-out for the wire connections, as shown in Figure 120.

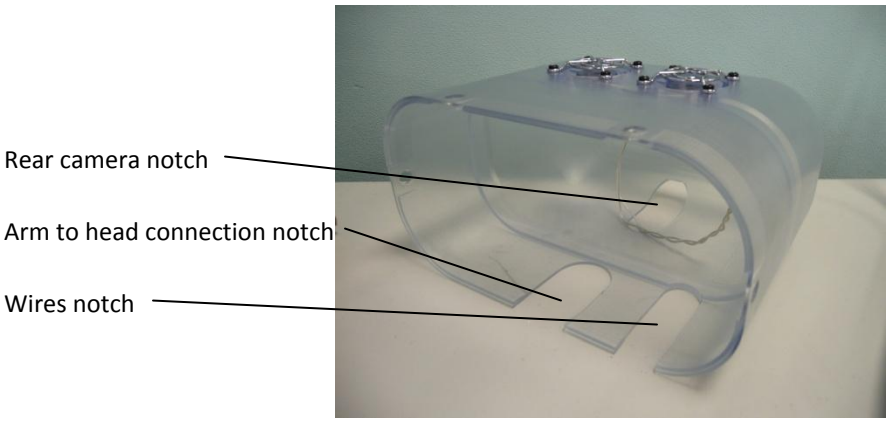

Figure 120 - Widened arm to head connection notch and new wires notch

At the competition no further changes were made to head and no problems encountered with its functionality. It served its purpose of protecting components, the head cover being easily removed making access to sensors simple, and being visually appealing.

6.2.5. Power systems

The battery covers for the robot were designed to protect the Li-Po batteries from damage while the robot was in use. When testing the autonomous robot it was decided that the old NiMh batteries had enough power to drive the robot for normal periods of use. The battery covers were not designed to fit over these old, larger batteries so Velcro was used to secure them to the sides of the robot. This proved a simple solution to ensuring the batteries stayed in place.

6.2.6. Cooling

When running the electronics of the robot for long periods of time on the bench it was felt that quite a lot of heat was coming out of the robot. When the lid was redesigned the cooling holes were made larger and a fan was added to the lid. The fans in the rear section of the robot blew air in over the motors creating positive pressure inside the robot. The air could then flow through the partition into the main section and be drawn up and out of the robot by the front fan. This seemed to work well as no overheating issues were experienced during operation of the robot.

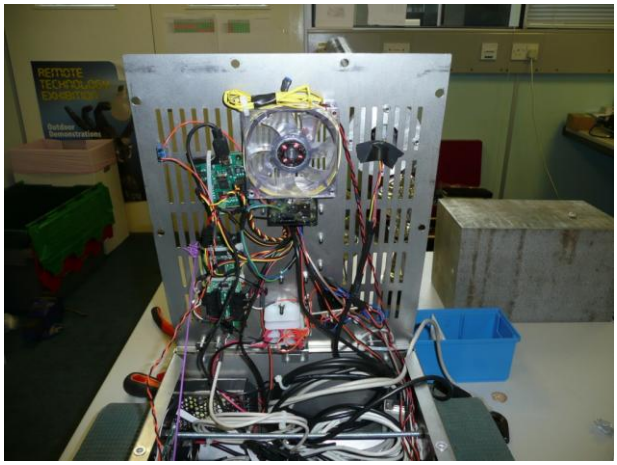

Figure 121 - Cooling fan

6.2.7. Compass and Tilt sensor

The electronic compass was found to be very sensitive to any ferrous materials. The chassis made out of stainless steel, and the large motors caused major interference problems. By manually moving the compass closer and further from the robot it was found that a minimum distance of at least 30cm was required for minimal interference. The compass unit also includes the tilt sensor (used to position the Lidar gimble). It is important that the tilt sensor is held securely for accurate positioning and mapping. To solve these problems a mount was designed. Left-over from the arm of the tele-operated robot was a section of carbon fibre tubing that was stiff and had no metal that would interfere with the compass. An aluminium base to fix the tube to the robot was designed. To attach the unit to the top of the tube a small lid piece was designed. This worked relatively well in holding the compass away from the robot, however the flex in the lid meant that it was not very stable. An additional rivnut was added to each side of the lid to stiffen the lid which proved successful.

Figure 122 - Autonomous robot showing carbon fibre mount

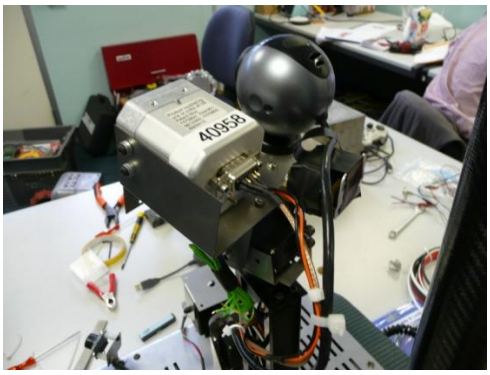

Figure 123- Head

Figure 124 - Arm

6.2.8. Autonomous communications

The old router was to be used in the autonomous robot. When arranging electronics inside the robot an attempt was made to mount the router to the lid using spacers. During this process the router was damaged and a new router had to be ordered. This new router was very large and it was decided safest not to strip it from the case. To fit the router to the robots the best solution was found to be Velcro which was attached to the rear vertical plate of the robot. This would ensure good reception for communications.

6.2.9. Tele-operated testing of robot

To test the mechanical integrity of the fully assembled robot, it was set-up for tele-operation using the controller as for the tele-operated robot. The robot was driven around the flat floor area outside of the lab. Good traction was experience and the robot turned very well with the centre of rotation slightly to the rear of the robot (as expected due to the weight of the motors). The chassis seemed stiff enough with no noticeable bending.

7. Overall design discussion

7.1. Tele-operated robot

Setup day (Day 1):

At this stage the robot was driveable with the main tracks and flippers but did not have use of the arm, CO_2 sensor, IR, LiDAR, gimbal and remote LED control. This enabled testing of the robot in a phase by phase system of implementation. The mobility of the robot was a proven success of last year's design, the new motors however provided more efficient power and increased the longevity of the robot significantly. Most notably was the ease with which the robot was capable of ascending the 45° slope. To ensure the arm, and more specifically the head, was immobile both were mechanically restrained.

Runs 1 (Day 2):

Due to the lack of arm control, the first run of the day required the robot to be lined up with the victims, sometimes using the flippers to gain elevation, to conduct victim identification with the two IP cameras. Following some further testing and development, the thermal imaging camera was available for the second run of the day – therefore being able to score more points per victim. The physical robustness of the chassis was well tested during the day's runs and was showing impressive resilience to the aggressive terrain. The ease of removing the stack was also proven, having managed to remove, modify and replace the stack within two hours in between runs.

Runs 2+3 (Day 3):

With the chassis tested and working well the next stage of development was to gain control of the arm. The first and most simple joint to control was the head pan using the RX64 and the Dynamixel servo controller. This one degree of freedom allowed victim identification when the victim was located alongside the robot. The robot was placed into the arena in advance of the run and straight away communications interference was encountered. The cause of this was unknown; multiple frequencies were tried and even a change of transmission protocol was made. Nothing seemed to improve the reception and the robot was rendered undriveable. This was very disappointing, especially considering the previous day's success. At this point the autonomous robot had ceased to compete so it was decided that the new router on that robot would be included on the teleoperated robot.

The second run of the day was significantly more successful. Withdrawing from the first run of the day meant that by the second run the arm was fully working and the CO_2 sensor was producing good results. The final run of the day proved the capability of the arm and the new sensors, resulting in detection of four victims.

Run 4+5 (Day 4)

The robot demonstrated full functionality, although some problems persisted. The arm joints were still not perfectly rigid, which caused the arm to 'flop' when moved. This made accurate control very difficult for the operator, especially when working through a camera. Additionally, the wireless problems encountered the previous day were, although alleviated with the more powerful router, not completely solved. In fact, during both runs, the connection seemed to drop completely, requiring the run to be halted for however long it took to reconnect.

Before the final run of the day, the flipper control board was irreparably damaged for an unknown reason. Fortunately, the autonomous robot had been taken out of operation, and thus had an unused AX3500. The team were able to replace the board, and reconfigure the control settings and the PID parameters to run the flippers in time for the run.

Despite these problems, the robot performed admirably in both runs, maintaining the average victim detection of the previous days.

Mobility Run

Here, the victim identification was dispensed with, and the robot was placed in the difficult red area where its mobility was tested. This was very successful; the robot easily climbed the 45° slope and stairs, and in fact managed to climb a 30cm pipe step, which was a feat never before achieved in the Robocup league.

The final challenge was the red stepfield, which had not been attempted during the previous runs. Although the progress was slow, the robot had no problems getting through, and there was no visible damage to the chassis afterwards. It was estimated later that the total run was at least 30 minutes long, which is impressive given the terrain that the robot had to navigate.

7.1.1. Drive systems

7.1.2. Chassis

At the RoboCup Rescue League competition the tele-operated robot was almost entirely without mechanical fault. Although there were concerns as the likely level of damage to the relatively thin stainless steel sheet of the chassis there was little to none, even after the most arduous terrain was navigated. This may have been due the the large amount of tension the chassis plates were under.

One aspect which did prove a slight challenge for the operator was the poorly positioned centre of gravity of the robot. Due to the requirement for large amount of space for electronics within the chassis,

both drive motors and one of the two flipper motors and their mounts were positioned at the rear of the robot resulting in the majority of the weight being there. As a result it was difficult for the robot to manoeuvre the competition arena's 30mm tube step forwards. It was, however, completed with little difficulty backwards.

7.1.3. Robot arm

Referring back to the requirements of the arm, it was noted that rigidity was important. Testing highlighted that each of the joints had a small amount of play. This was due to the accumulation of several factors. There was a small amount of play in the joint shafts held in place by grub screws. There was also a significant amount of play between the worm/wheel and the keys holding them in place.

These tolerances were small, however when multiplied by the 1 meter arm they become a serious problem. To fix this problem, the holes for the grub screws were drilled out and the grub screws were replaced with scroll pins.

7.2. Autonomous robot

7.2.1. Drive systems

When driving over the ramps in the arena the robot was found to slam down causing damage to the robot as the centre of gravity was very far to the rear. With the centre of gravity so far rear it also meant turning on slopes was inaccurate. To improve this two, 1.5kg weights were added into the front of the robot. This seemed to help with the turning of the robot but did not improve the slamming over ramps as hoped.

7.2.2. Head

The centre of mass of the head of the robot was further forward than the servo that the head was fixed to. This meant that to hold the head in a level position required the servo to be continuously working against its weight. To correct this a counterbalance was added using brass weights. This moved the centre of gravity back so that the head would hold itself in a level position with no load on the servos.

7.2.3. Chassis

During operation, the autonomous robot landed hard on one of the front pulleys. This bent in the chassis slightly and slackened the belt on that side. The chassis could be bent back out but in order to prevent further damage it was decided a brace of some sort was needed to strengthen the chassis. A long piece of threaded rod was cut to size and inserted through holes on each side of the chassis near the front. Nuts were put on the inside and then tightened to hold the sides of the chassis outwards.

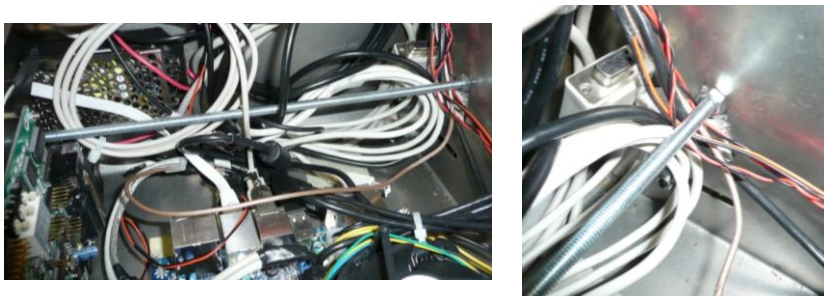

Figure 125 - Torsion bar

7.2.4. Power systems

The battery setup used in the competition proved very effective, with even the oldest set of batteries providing enough power to last more than a run time of 20 minutes. In addition, enough power could be drawn to easily climb the slopes that the competition presented. The fact that the connections were wired in series offered the added benefit of allowing a single LiPo battery to replace the 12V battery packs.

The replacement of the power control board with individual voltage converters had advantages and disadvantages when it came to the competition. On one hand, the system was more versatile and easy to change than with the power board; each converter could power any number of devices on that voltage level, and could be moved anywhere within the chassis. Also, if one device failed, it was easy and relatively inexpensive to replace, whereas a power board failure could be very difficult to fix, with the possibility of affecting the entire board. On the other hand, when looking at the teleoperated stack, the power board offers a neat and organised system of connecting components. If the autonomous robot were required to house more components at more voltage levels (for example, the RX-64 servo, which runs on 18V) the existing system may need to be replaced.

7.2.5. Central Computer

The central computer, as discussed in Section 3, was purchased with the focus on performance, rather than cost. It was felt that a high-performance computer would eliminate any potential problems with the robot's speed of operation, and would justify itself by remaining useful for the next year's team. Indeed, the cost of the PC turned out to be insignificant compared to some of the other components, such as the battery sets or the motors.

During testing, the speed of the computer did not become an issue. The fragility of the software and the sensor meant that the robot was run at very slow speeds anyway, in an attempt to perfect the navigation and mapping, rather than get around the arena quickly.

From the physical perspective, the computer was a good choice. It had more than enough ports to interface all the required sensors, and had a small footprint, which was useful for mounting on the base of the autonomous chassis. Cooling, additionally, was not an issue, as the processor fan on the PC was sufficient to keep the temperature of the PC at around 36°C.

7.2.6. Compass and Tilt Sensor

The OS5000 was problematic throughout the project. The tilt data was extremely accurate, and allowed the gimbal to keep almost perfectly horizontal. However, when attempting to use the compass to estimate turning angles, the interference from various sources made an accurate measurement extremely difficult. In the initial design, the compass was supposed to be mounted on the chassis along the horizontal. When testing this, the data returned was virtually unusable. It is believed that the motors caused most of the interference, because of the strong moving magnetic fields they produced during running.

Mounting Distance (inches)	Error (heading degrees)
2	90
5	10
9	1.6
11	0.2

Table 25 - Compass Magnetic Interference

The enormous decrease in interference with distance prompted a change in the design – the compass was mounted on a carbon-fibre tube to keep as far away from the motors as possible. This, when

combined with the scan-matching technique, returned angles with generally acceptable accuracy (perhaps +/- 4°).

7.2.7. Autonomous control

In the competition, the autonomous robot suffered many problems, some of which were outside of the team's control, which ultimately stopped the robot from successfully mapping or identifying victims.

The most significant problem was to do with the slopes in the arena. The starting position for each run was not on a flat section, as expected, but facing the wall on a slope. The robot was unsuitable for handling this, compared to other competition robots, for several reasons:

- The tracks did not have enough traction to move up the slope without slipping.
- With the differential turning, the point of rotation was not the centre of the robot, which meant that a long turn (with slippage) would cause the robot to drift significantly.
- The robot was much heavier towards the back, due to the motors – when going over a ramp forwards, the robot would drive into the air, before slamming down on the other side, causing the robot to slip even more.
- The gimbal and servo configuration could not be tuned correctly:
    - If the movement was set to be as fast and responsive as possible, the LiDAR suffered from vibration effects.
    - If the movement was damped to remove vibrations, the gimbal was not fast enough (for example, when coming down over a slope, the LiDAR would be pointing at the floor for a short time, which would cause the obstacle-detection to stop movement.)

In addition to the slopes, there were problems with victim identification. The lack of familiarity with the competition's setup, and the inability to do enough testing beforehand, meant that the team was underprepared in this area. Specifically, some of the problems were:

- The face detection algorithms were extremely difficult to implement, since the victims were located inside small holes in the walls, and their faces were not visible in most cases.
- The arm on the robot was at the right height for the mid-level victim holes, but was fixed and made identifying victims in the lower and upper holes much more difficult.
- The infrared blob detection algorithm, which had been successfully tested on still images, would not successfully identify victims once at the competition. No reason for this could be established while there, and it proved too difficult to fix in the timeframe.

In summary, the autonomous robot suffered many problems which were insurmountable in the week of the competition. All of the problems can be attributed to the fact that the team was largely

unfamiliar with the setup at the competition, and was unable to test the autonomous software properly before the competition.

7.2.8. Software Portability

This was largely untested, due to the limitations of what could be achieved in the time frame. The software written for the autonomous robot was never moved to the teleoperated, due to the problems that were encountered and the continuous developments that had to be made in the run-up to the competition.

One of the most important aspects of the code that can be transferred to the tele-operated robot is LiDAR mapping. It would be an enormous advantage in the competition if the robot could be driven throughout the arena with victims manually identified along the way, while the software uses continual LiDAR scans and the compass data to map the area explored, with pinpointed victims. Theoretically, there is no reason why this should not be a feasible goal, and should be considered by next year's team.

8. Future work

8.1. Head

Future work needs to focus on making the head even more compact. This is only possible in conjunction with using smaller sensors. Smaller sensors also mean less weight which would in turn minimise the wobble of the head during driving. A compact rear-facing camera would also mean the length of the head could be significantly reduced. The large size of the tilted rear-facing camera and Ethernet cable coming out of it were the limiting factors in making the current head design more compact. The rear camera notch could be made smaller as the 45 degree incline was sufficient for driving and was never changed during the competition. If the head were to be commercialised sealing rings and enhanced protection of components would have to be looked into.

8.2. Electronic systems

Although impressive, the teleoperated robot is still not perfect. There are a number of key electronic improvements that would be of benefit in the future.

Two LiPo batteries this year were undervolted and as a consequence expanded rendering the batteries unsafe for use and had to be decommissioned. This not only is a safety concern – severely undervolted batteries have been know to explode, but also a waste of resources; especially considering the batteries that were undervolted cost in the region of £250 each. It is proposed that battery protection circuitry is developed to avoid this in the future. It is expected that the circuit would be based on a power MOSFET with a specific reference voltage against which the voltage of the batteries could be checked. Once they reached a low enough level the circuitry would cut the supply to the robot, thereby protecting the batteries from further discharge.

An LCD display would be useful on the robot. This could be mounted on the lid and would display simple status information, such as internal temperature, battery voltage, e-stop state. This LCD display could also be used to display simple error messages to aid with faultfinding, thus possibly reducing the requirement for more intrusive faultfinding.

Two USB ports and a VGA/DVI ports on the lid would be extremely useful, again to avoid the need to gain access to the stack just to plug a keyboard, mouse and monitor into it. Although most changes to the robot software or the OS can be made remotely, there are some changes that are easiest made when looking at the GUI and are often fastest.

The IR camera capture script used at the competition, although effective, was slow to act – taking about 20 seconds to deliver an image back to the driver. When finding four or possibly five victims this can constitute up to 10% of the time in the arena; time that is effectively wasted. A fast and efficient thermal image capture system, possibly even a live feed of the images would be a large asset.

The last and most difficult improvement to the robot would be to furnish it with a mapping capability. This presents a large challenge due to the varied and aggressive terrain the platform navigates. Problems with LiDAR overshoot, skidding, difficulties measuring turning to name but a few. Investigations this year into LiDAR stabilisation using a tilt sensor and gimbal were very promising and did give good results on the autonomous robot. More work however would be required as it is likely that hardware stabilisation alone would not be enough to give quality scan data. With two robots producing maps investigations into the possibility of map sharing between the two could significantly improve the speed and performance of both. One robot could locate the victims on the map but not investigate them and the second could follow the map to fully identify the victims.

Throughout the project there have been stability issues with the software. It would be extremely useful to create a stable framework from the software which would allow future years to build onto. This would be time consuming but should be considered paramount.

9. Conclusions

- Warwick Mobile Robotics has achieved 1st place overall and best in class for mobility at the RoboCup European Open 2010.
- The robot chassis has been redesigned giving a weight saving of 9kg compared the 08/09 robot, giving an improved power to weight ratio.
- The overall weight reduction, after the addition of the arm, was 3kg.
- The autonomous robot has been designed and completed successfully.
- The autonomous robot achieved mapping as well as navigation capabilities.
- The software for the tele-operated robot has been improved, with the addition of 3D arm control and interfacing with the new sensors.
- The tele-operated robot and arm run on Maxon motors, giving reliable and efficient operation.
- A new battery compartment, designed for ease of use and speed, has successfully been implemented.
- A new arm with five Degrees of Freedom has been developed and tested successfully.
- A new head with extended sensory feedback has been developed and tested successfully.
- The cooling system for the robot has been improved with the implementation of a new electronics stack and one large fan.
- New Harwin connectors have been incorporated, providing reliable and quick connections.
- Substantial funding has been raised for the project with the following sponsors: Warwick University School of Engineering, WMG, IMRC, ITCM, Harwin Interconnect and Maxon Motors.

- Carbon fibre panels have been hand crafted and can be utilised in future projects.

- For publicity, WMR newsletters, an appearance on BBC South Today and various news articles have been achieved.

- Continued publicity with Newspaper articles, BBC news coverage, radio stations, quarterly newsletters to sponsors, presentations and website updates.

- Increased profile and exposure of WMR, Warwick University, WMG and other sponsors through winning the competition.